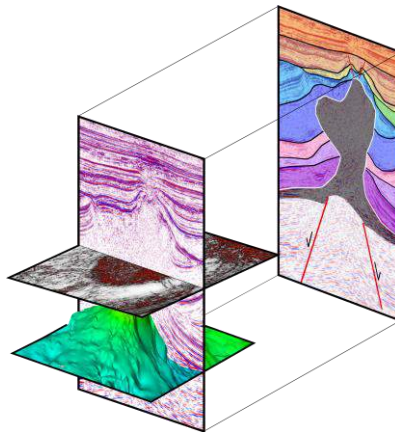


# Salt Tectonics in the northern Dutch offshore

A study into Zechstein halokinesis in the Dutch Central Graben and Step Graben

Matthijs van Winden<sup>1</sup>



MSc. Thesis – April 2015

**Supervisors:**

Prof. Jan de Jager<sup>1</sup>

Drs. Bastiaan Jaarsma<sup>2</sup>

Dr. Renaud Bouroullec<sup>3</sup>

**<sup>1</sup>Utrecht University**

Heidelberglaan 8, 3584 CS Utrecht, The Netherlands

**<sup>2</sup>EBN B.V.**

Daalsesingel 1, 3511 SV Utrecht, The Netherlands

**<sup>3</sup>TNO**

Princetonlaan 6, 3584 CB Utrecht, The Netherlands

© Copyright by EBN, TNO and Utrecht University

Without written permission of the promoters and the authors it is forbidden to reproduce or adapt in any form or by any means any part of this publication. Requests for obtaining the right to reproduce or utilize parts of this publication should be addressed to:

EBN B.V., Daalsesingel 1, 3511 SV Utrecht, The Netherlands, Telephone: +31 (0)30 2339001

# Table of Contents

<b>o. Abstract .....</b>	<b>6</b>
<b>1. Introduction .....</b>	<b>7</b>
1.1. Exploration .....	7
1.2. Objectives .....	7
<b>2. Geological Setting .....</b>	<b>9</b>
2.1. Assembly of Pangea .....	9
2.2. Break-up of Pangea .....	10
2.3. Alpine Inversion .....	11
2.4. Structural Elements .....	13
2.4.1. Dutch Central Graben (DCG) .....	13
2.4.2. Step Graben (SG) .....	13
2.4.3. Elbow Spit Platform (ESP), Elbow Spit High (ESH) and Schill Grund Platform (ESP) .....	13
2.5. Stratigraphy .....	14
2.5.1. Zechstein Group .....	14
2.5.2. Post-Permian Stratigraphy .....	17
<b>3. Mechanisms of Salt Tectonics .....</b>	<b>19</b>
<b>4. Analogue Research .....</b>	<b>23</b>
<b>5. Salt Structures in the northern Dutch offshore: An Inventory .....</b>	<b>26</b>
5.1. Methods and Approach .....	26
5.1.1. Salt Structure Inventory .....	27
5.1.2. Isopach Maps .....	28
5.2. Results .....	30
5.2.1. Orientations and Dimensions .....	31
5.2.2. Faults .....	33
5.2.3. Associated stratigraphic relationships .....	35
5.2.4. Data and Locations .....	38
5.2.5. Isopach Maps .....	38
5.3. Interpretation and discussion .....	40

5.3.1.	Triassic .....	40
5.3.2.	Jurassic .....	46
5.3.3.	Cretaceous and Tertiary .....	50
5.3.4.	Mechanisms of salt tectonics in the study area.....	53
5.3.5.	Main Uncertainties .....	53
<b>6.</b>	<b>Structural Restoration .....</b>	<b>54</b>
6.1.	Methods: From geology to model .....	54
6.1.1.	Approach .....	54
6.1.2.	Seismic interpretation and depth conversion.....	54
6.1.3.	Restoration model input and workflow.....	56
6.2.	Results .....	60
6.2.1.	Seismic interpretation and stratigraphy.....	60
6.2.2.	Structural restoration.....	65
6.3.	Discussion .....	79
6.3.1.	Restoration model considerations .....	79
6.3.2.	Uncertainties and assumptions .....	80
6.3.3.	Alternative models .....	81
6.3.4.	Summary of structural development.....	82
<b>7.</b>	<b>Integration.....</b>	<b>83</b>
<b>8.</b>	<b>Implications for prospectivity &amp; Recommendations.....</b>	<b>86</b>
8.1.	Chalk play .....	86
8.2.	Volpriehausen play .....	93
8.3.	Upper Jurassic plays.....	94
8.4.	Other affected plays.....	95
8.5.	Recommendations .....	98
<b>9.</b>	<b>Conclusion .....</b>	<b>99</b>
	<b>Acknowledgements.....</b>	<b>101</b>
	<b>List of Figures.....</b>	<b>102</b>
	<b>References.....</b>	<b>105</b>
<b>10.</b>	<b>Appendices .....</b>	<b>111</b>

# List of abbreviations

ZE	-	Zechstein Group
RB	-	Lower Germanic Trias Group
RN	-	Upper Germanic Trias Group
AT	-	Altena Group
SL	-	Schieland Group
KN	-	Rijnland Group
CK	-	Chalk Group
NS	-	North Sea Group
MMU	-	Middle Miocene Unconformity
B(ZE)	-	Base (Zechstein)
T(ZE)	-	Top (Zechstein)
(D)CG	-	(Dutch) Central Graben
SG	-	Step Graben
ESP	-	Elbow Spit Platform
ESH	-	Elbow Spit High
SGP	-	Schill Grund Platform
TWT	-	Two Way Travel Time
TVD	-	True Vertical Depth
TVT	-	True Vertical Thickness
TST	-	True Stratigraphic Thickness
DEFAB	-	Dutch offshore blocks A, B, D, E, F
EBN	-	Energie Beheer Nederland B.V.
TNO	-	Nederlandse Organisatie voor toegepast-natuurwetenschappelijk onderzoek (The Netherlands institute for applied natural science)
NLOG	-	Nederlands Olie en Gas Portaal (the Netherlands Oil and Gas portal)

## o. Abstract

Until recently, the northern Dutch offshore was a relatively under-explored area. Newly acquired 3D seismic data provides new opportunities for exploration and allows re-evaluation of existing play concepts. The presence and movement of Upper Permian Zechstein evaporates in this area has had a major effect on the geological development of this area. The timing of this halokinesis affects depositional patterns, structural development, hydrocarbon migration, trap formation and other aspects of plays in the DEFAB area of the Dutch offshore. This is the first study to look specifically into salt tectonics in this area of the Dutch offshore.

This study analyses a range of salt structures in the Step Graben, Dutch Central Graben and adjacent platform areas. Salt structures are described and characterized in a salt structure inventory. Assessment of timing of salt structure growth and its effect on depositional patterns shows initiation of salt movement in the Triassic, salt tectonic climax in the Jurassic and renewed salt movement in the Cretaceous. However, salt movement is not always consistent throughout the study area. A correlation can be seen between the location of salt structures within the structural elements, the way salt structures developed and the timing of salt movement. For example, isolated salt diapirs almost exclusively occur within the Dutch Central Graben, while in the Step Graben and towards platform areas, salt walls and elongated salt pillows occur above major basement faults.

To be able to assess salt tectonic evolution within a structural context, a 2D structural restoration of the Step Graben and Dutch Central Graben was performed. Results provide a conceptual model, constraining periods tectonism, deposition, erosion and salt movement in these graben systems. With this model, salt tectonic development of the study area can be viewed in a structural framework. It becomes evident that observations in depositional patterns, distributions of salt structure types and timing of salt movement have to be regarded as the consequence of an interplay of salt movement and structural development of the Step Graben and Dutch Central Graben.

**Keywords:** *Salt tectonics, northern Dutch offshore, Dutch Central Graben, DEFAB, Structural restoration, Exploration*

*If you are interested in the main results and impacts on exploration see chapters 7, 8 and 9.*

# 1. Introduction

## 1.1. Exploration

The northern Dutch offshore is relatively under-explored and most exploration so far focused on the Mesozoic and Tertiary plays. Gas and oil have been discovered and are being produced from Tertiary, Chalk and Jurassic reservoirs in a handful of fields. Exploration activities have increased recently, focusing again mostly on the Chalk and Jurassic plays. The discovery of oil in block F17 is a clear example of the hydrocarbon potential still to be tested. A package of hundreds of meters of Upper Permian Zechstein salt was deposited in the northern Dutch offshore. This salt has played a large role on the geological development of the area, impacting many aspects of the petroleum systems and plays. The formation of salt diapirs, salt walls and salt pillows is associated with the formation of a range of trap types, has impact on source rock burial depths and maturity, affects hydrocarbon migration paths and controlled intra-reservoir facies distributions and fracturing. Therefore, it is crucial to understand the timing of episodes of salt movement and the mechanisms associated with this halokinesis. Despite several studies in the Dutch offshore and adjacent offshore areas, salt tectonics and its control on deposition is still not fully understood in this area. New 3D seismic data (2012, courtesy of Fugro) allows for a more detailed study of this subject and may provide new insights about of salt movement in the Dutch offshore.

## 1.2. Objectives

The main aim of this study is to obtain better constraints on how salt movement in the this area initiated, when salt movement occurred and how salt structures developed. In order to fully understand the role of salt movement in this area, it will be investigated what underlying mechanisms might be responsible for salt movements and how episodes of salt movement can be placed in the context of regional tectonics. In order to do this, a good understanding of the structural development of the main structural elements is needed (Dutch Central Graben, Step Graben and adjacent platforms).

This study will consists of 1). A salt structure inventory of the DEFAB offshore area 2). A structural restoration of a 2D seismic section, within the study area 3). Geological interpretation and integration of 1) and 2).

By restoring the structural development in a cross-section, the role of Zechstein salt in the different stages deformation can be tested and visualized. A combination of a regional assessment of Zechstein salt structures and this structural restoration provides an insight in salt in its static, present day configuration and its dynamic role throughout the geological history of the North Sea basin. This study can be considered an initial framework for the analysis of salt tectonics in the northern Dutch offshore in the context of 1). Hydrocarbon exploration and play development 2). The structural evolution of the wider North Sea. Since this study is the first study to look

specifically into salt tectonics in this area, with availability of the DEF 3D seismic survey, it can be regarded as a starting point for future discussion and research on impact of salt tectonics in this area.

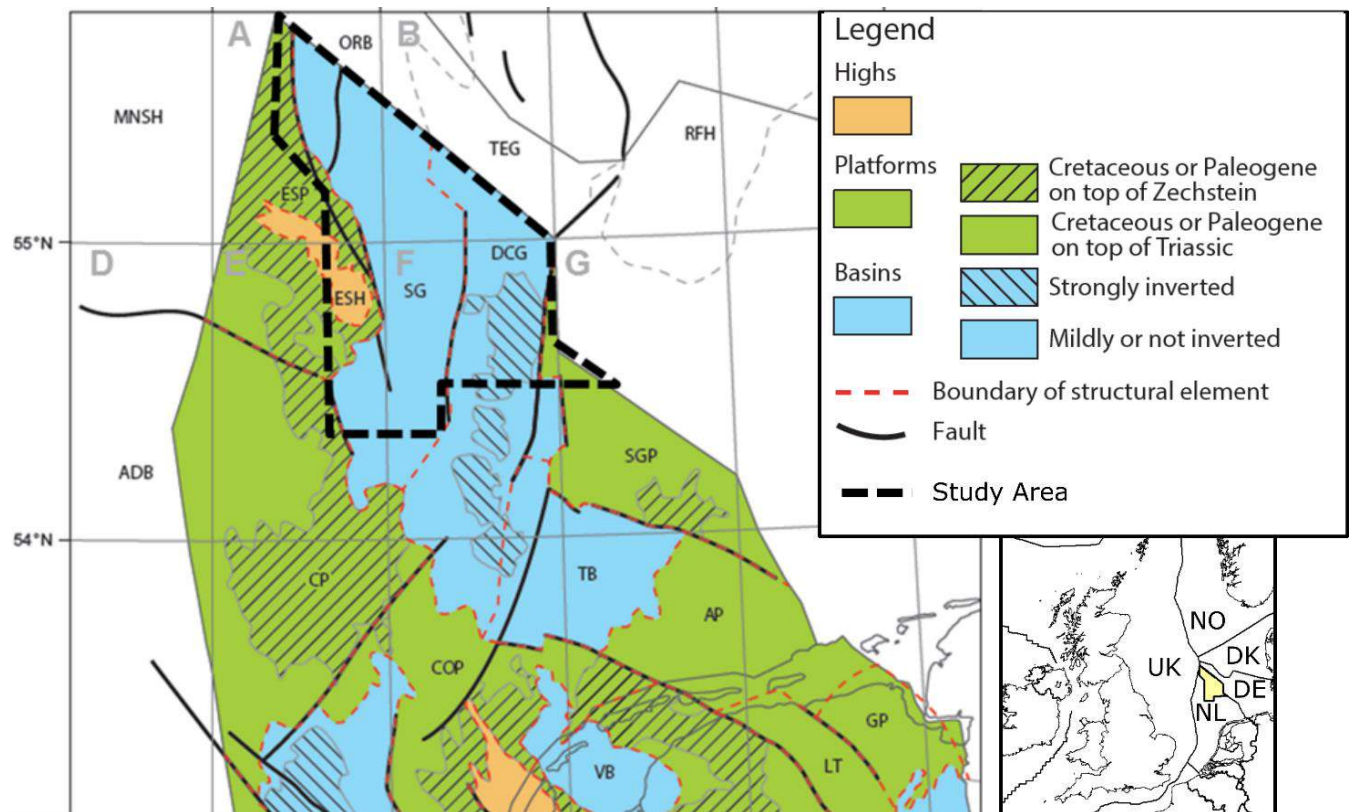


Figure 1: Location of the study area (black outline) indicated on a map showing the main structural elements in the northern Dutch offshore (after Kombrink et al. 2012)



## 2. Geological Setting

The study area is located in the southern part of the intra-cratonic North Sea basin (**Figure 1**). The wider North Sea area has been subjected to a wide range of tectonic events, which resulted in highly complex and laterally variable geology. Generally the development of the wider North Sea area can be placed in the context of 3 major periods of plate tectonics: 1). Assembly of the Pangea supercontinent 2). Break-up of the Pangea supercontinent 3). Distal inversion effects of the Alpine orogeny (after De Jager, 2007).

### 2.1. Assembly of Pangea

The assembly of Pangea is characterized by two major collisional events, resulting in the Caledonian and Variscan fold and thrust belts. The Caledonian collision occurred in the Early/Middle Palaeozoic between the continents Laurentia and Baltica and resulted in the closing of the Tornquist sea along the NW-SE running Tornquist suture zone. The micro-continent of Avalonia collided from the South, which closed the Iapetus ocean along the SE-NW to N-S running Iapetus suture. This created a triple junction of plate boundaries just to the NW of the study area (Ziegler 1978, 1990; de Jager, 2007), generally this junction is linked to the location of Mesozoic basins, which show a similar configuration (Ziegler, 1990). The only direct evidence of Caledonian basement in the Dutch subsurface is altered biotite monzonite overlain by Devonian Old Red Sandstone, encountered in well A17-1 on the Elbow Spit High (Frost et al., 1981; Pharaoh et al., 1995; de Jager, 2007). Some studies suggest the development of graben structures in the area of the Dutch Central graben as early as the Devonian (Wong et al. 2007; Ziegler, 1990), where back-arc extension induced the development of the Rheno-Hercynian basin. This structural grain is considered an early indication for a proto-Central Graben system, although this is still very much a topic of debate.

Collision of the resulting continent Laurussia with the Gondwana continent resulted in the development of the Variscan orogeny (**Figure 3**). The Variscan thrust front moved northwards throughout the Carboniferous, with its final position running E-W through present day Belgium and to the NE into Germany (Ziegler, 1990). A Late-Variscan tectonic pulse induced widespread erosion in the Late Carboniferous (Geluk, 2005).

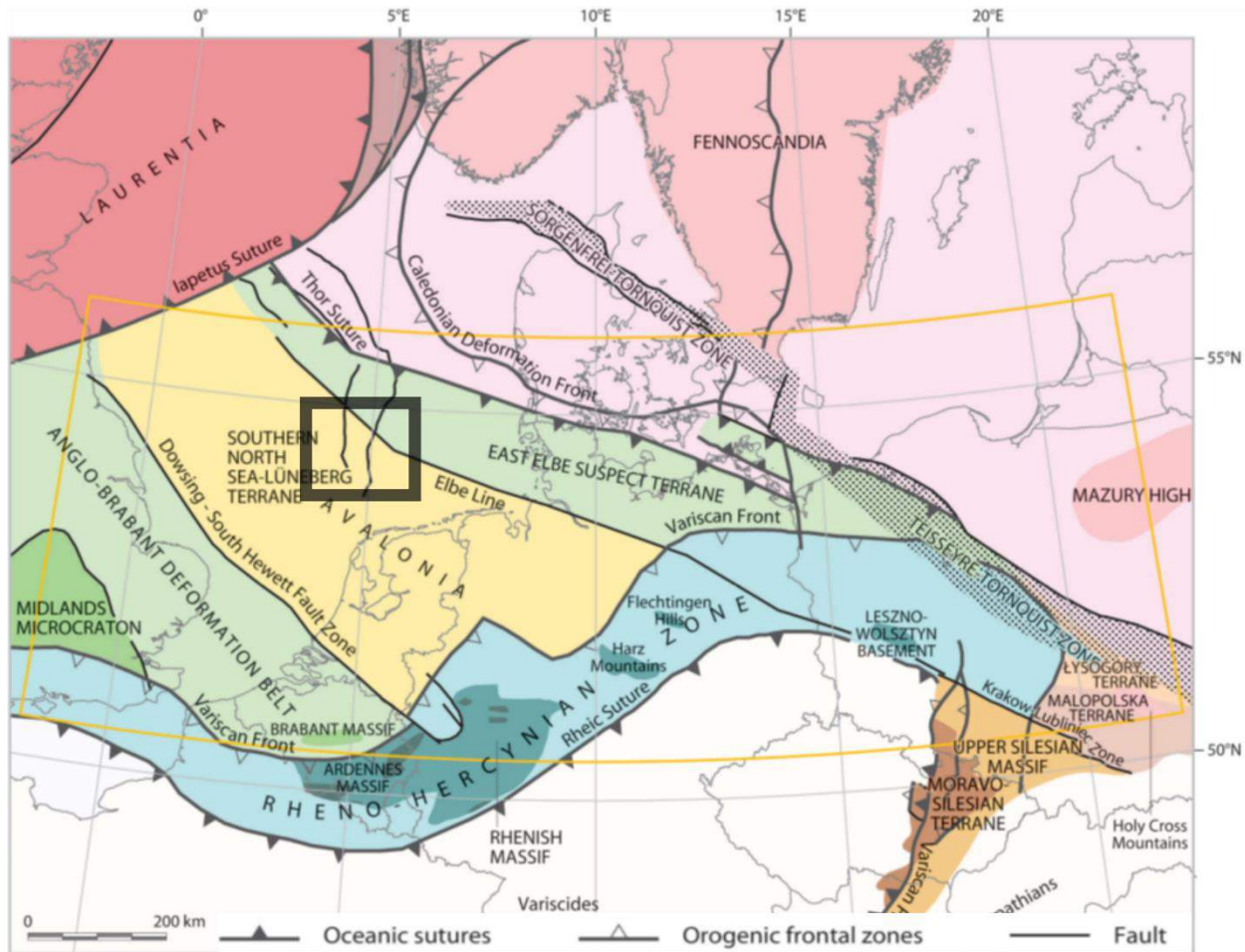


Figure 2: Structural configuration in Northern Europe during the Carboniferous. Main suture zones are shown, where terranes amalgamate, forming the continent of Laurussia (Doornenbal et al., after Pharaoh et al., 2006). The study area of this study is indicated with the black box, where a 'proto-Dutch Central graben' is suggested.

## 2.2. Break-up of Pangea

A phase of dextral translation of Northern Africa relative to Europe indicated the onset of a phase of basin formation in NW-Europe, which resulted in the start of orogenic collapse of the Variscan orogeny in the Late Carboniferous to Early Permian (Ziegler, 1990; Geluk, 2005). An arid, desert-like area developed North of the Variscan front (**Figure 3**), where Lower Permian Rotliegend sediments were allowed to accumulate. Rotliegend isopach maps show an early structuration in the underlying basement, where several separate basins can be distinguished in Northern Europe (Geluk, 2005). Again, indications for a proto-Central Graben are observed in these maps (Ziegler, 1991). Regional subsidence in the Early Permian resulted in the development of the large E-W running Northern and Southern Permian Basins. As subsidence progressed, the southern North Sea was incorporated in the Southern Permian basin. This induced flooding, which initiated the cyclic deposition of the Zechstein Group (Geluk, 2005).

During the Early Triassic, rifting commenced in the Northern Atlantic domain, from where a rift arm reached into the North Sea area, inducing several phases of extension from the Triassic to Early Cretaceous. No continental break-up occurred along this rift arm. Several NNW-SSE graben structures in Northern Europe developed and continued to subside rapidly during the Triassic, among which the Central Graben, Glückstadt Graben and Horn Graben. In these basins, underlying Zechstein salt deposits already were an important factor in Triassic depositional patterns. Thermal subsidence was interrupted by periods of active faulting during the deposition of the Buntsandstein formation and Keuper formation in these basins (Geluk, 2005). These Triassic rifting phases presumably induced early, widespread activation of Zechstein salt movement (De Jager, 2012).

Development of a Mid North Sea dome during the Middle Jurassic presumably induced deep erosion of Jurassic and Triassic sediments on platform and marginal areas, while deposition was limited to the basins, like the Central Graben, where a full Jurassic sequence can be found, since subsidence continued there (Ziegler, 1991). Generally, widespread rifting is inferred during the Late Jurassic to Early Cretaceous, due to accelerated extension in the North-Atlantic/Arctic domain. Generally a regional E-W orientation of extension is assumed, although some basins clearly follow a persistent NW-SE fault trend, possibly due to older, reactivated basement fault trends (Ziegler, 1991).

Active rifting stops in the Early Cretaceous and rift basins are filled up with Lower Cretaceous sediments. The DCG was incorporated in the marine Southern North Sea basin. The sediments deposited here can be seen thickening from the north of the Dutch Central Graben towards the south (Doornenbal et al., 2010).

### 2.3. Alpine Inversion

In the Mid-Cretaceous, continental break-up occurred in the Mid-Atlantic domain, which caused extensional stresses to focus towards the arctic and extension in the southern North Sea to quickly die down (Ziegler 1990). Regional subsidence persisted in most of the southern North Sea area. The closing of the Tethys Ocean was initiated in the Late Cretaceous, due to collision of the African, Indian and Kimmerian plates from the South with the Eurasian continent in the North (**Figure 3**). The Alpine orogeny developed from the Late Cretaceous and throughout the Early Cenozoic. Distal effects of this event significantly affected the southern North Sea area, where inversion of some Mesozoic basins occurred, among which the Dutch Central Graben and the Broad Fourteens Basin (De Jager, 2003, 2007). This inversion induced differential depositional patterns, uplift and truncation of older Mesozoic sediments. Several pulses of inversion occurred throughout the Late Cretaceous and Tertiary, which was accompanied by reactivated Zechstein salt movement and internal truncation of Late Cretaceous and Tertiary deposits, e.g. Chalk Group and North Sea Supergroup. Most significant inversion pulses affecting the Dutch Central Graben occurred during the Campanian, Paleocene and Eocene (De Jager, 2003, 2007). While these inversions typically induced uplift of the basin centers of affected basins, most platform areas subsided.

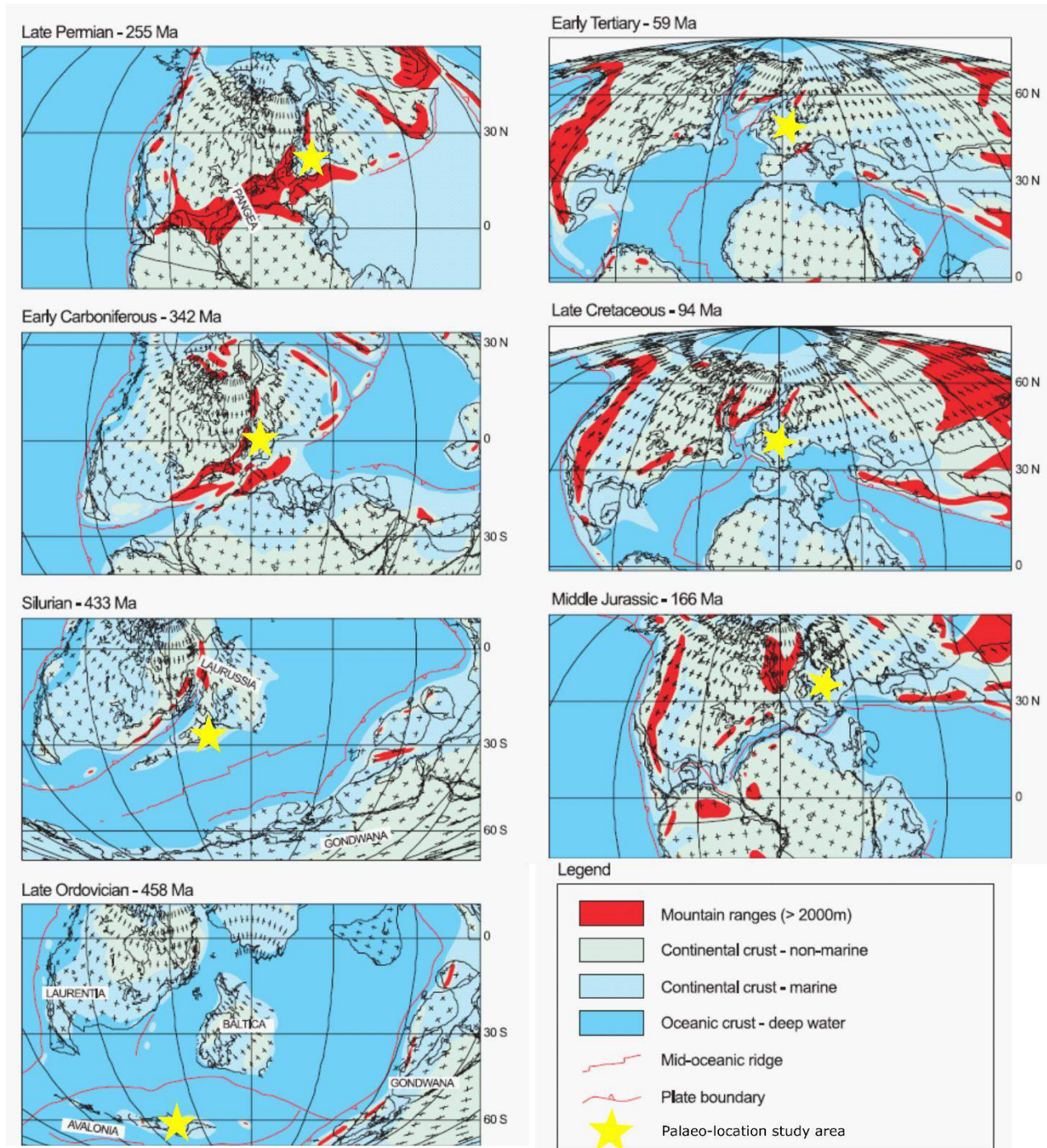


Figure 3: Palaeogeographic maps, showing the plate configurations from the Late Ordovician to Early Tertiary. The position of the study area is indicated with the yellow star. (after De Jager, 2007)



## 2.4. Structural Elements

The main structural elements within the study area are the Dutch Central Graben, Step Graben, Elbow Spit High, Elbow Spit Platform and Schill Grund Platform (as is shown in **Figure 1**). **Figure 4** shows a regional overview of the structural elements, which shows how the Central Graben and Step Graben continue to the North in the German and Danish offshore sectors.

### 2.4.1. Dutch Central Graben (DCG)

The Dutch Central Graben is generally considered to be a mainly Late Jurassic to Early Cretaceous graben structure. There are, however, strong indications for excessive subsidence and active fault movement from the Early Triassic onwards (Geluk, 2005; this study). The presence of a proto-Central Graben is often inferred already in Devonian and Carboniferous times. The final structuration of the DCG is thought to have occurred in the Mid- and Late-Kimerian rifting phases. The DCG was affected by Cretaceous and Tertiary inversion, although the effects of inversion appear to decrease rapidly towards the North. The DCG is bounded by the Step Graben in the West and the Schill Grund Platform in the East. The DCG-system continues as the German Central Graben (N-S) and the Tail End Graben (NW-SE) towards the North (**Figure 4**). Large isolated salt diapirs can be found within the basin and elongated salt structures occur along the N-S running boundary faults of the DCG (Wride, 1995; this study).

### 2.4.2. Step Graben (SG)

The Step Graben forms a terrace-like basinal structure, bounded by the DCG in the East and the Elbow Spit Platform and Cleaver Bank Platform in the West. It is structured internally by deep faults, creating highs and lows within the SG (**Figure 4**). Typically Cretaceous sediments can be found overlying Triassic deposits, although patches of Late Jurassic sediments can be observed locally. Zechstein salt typically forms large elongated salt structures above basin faults within the SG and along its boundary faults.

### 2.4.3. Elbow Spit Platform (ESP), Elbow Spit High (ESH) and Schill Grund Platform (ESP)

The Elbow Spit Platform is characterized by Cretaceous deposits overlying Permian and towards the South-East, Triassic rocks. It was part of the Mid-North Sea High, which extended towards the NW. The ESP is bounded by the Step Graben in the East and the Elbow Spit Platform in the North (Kombrink et al., 2012).

The Elbow Spit High is an area where Cretaceous deposits can be seen overlying Devonian and Carboniferous rocks. This area was part of the southernmost part of the Mid-Jurassic North Sea Thermal Dome. This resulted in the erosion of the entire Triassic and Jurassic succession (Kombrink et al., 2012). The buoyant nature of the ESH is possibly explained by the presence of an Early Devonian magmatic body (Donato et al., 1983).

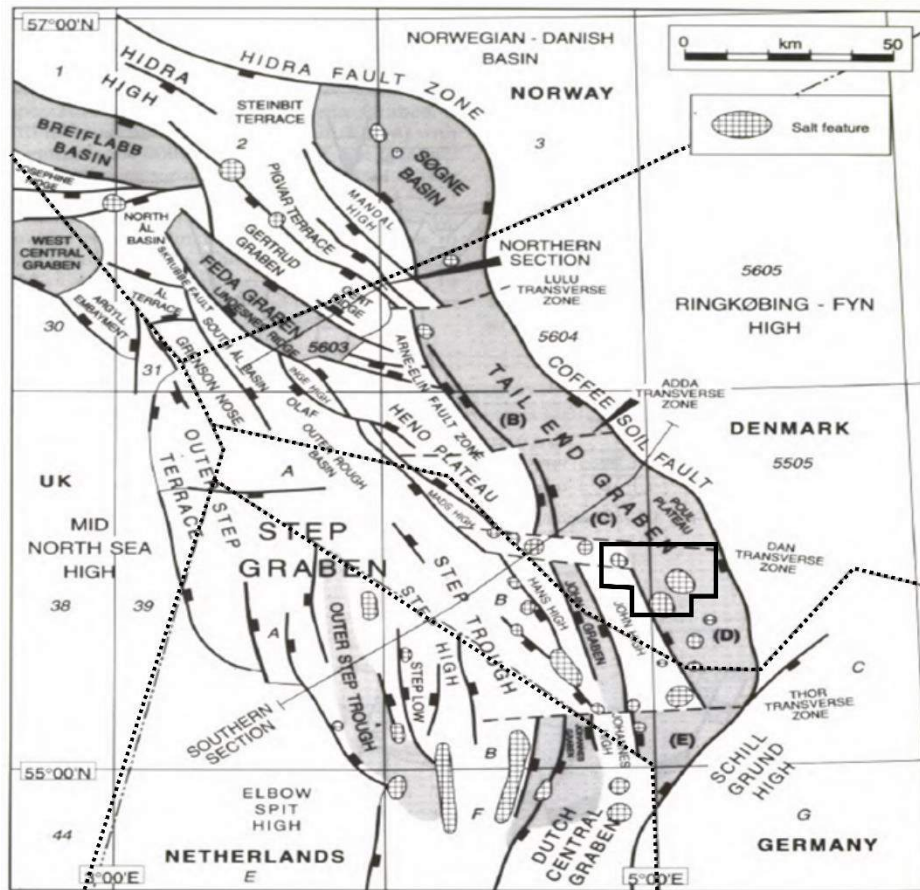


Figure 4: Structural configuration of the southern North Sea. The study area is located in the Dutch sector and continues to the South. The study area of the analogue study of Rank-Friend and Elders (2004) is indicated with a black box. (after Wride, 1995)

## 2.5. Stratigraphy

### 2.5.1. Zechstein Group

The stratigraphy in the study area is characterized by a post-Variscan sequence of sediments on top of a faulted pre-Permian basement. Lower-Permian Rotliegend sandstones are overlain by the evaporitic Zechstein Group. The Zechstein Group was deposited in the Southern Permian Basin and is dominated by evaporitic deposits (mainly halite, NaCl), which attained an original depositional thickness of up to 1500-2000m in the deepest parts of the basin (Ziegler 1990). The permanent flooding of the subsiding Southern Permian Basin is marked by the Kupferschiefer (copper shale), at the base of the Zechstein Group. In the study area the Zechstein depositional cycles defined as Z<sub>1</sub>-Z<sub>5</sub> can be found (Figure 6), where the Z<sub>2</sub> and Z<sub>3</sub> members typically contain the thickest Halite intervals (in the order of 600m and 300m; Ten Veen et al., 2012). It should be noted here that later erosion and dissolution of these evaporites are cause for large uncertainties

in the estimation of the initial distributions and thicknesses, although they were likely linked to the locations of deposition within the basin. Within the Zechstein Group carbonates can be found, which are subdivided in a shelf, slope and basin facies. Shelf facies consist of shallow water deposits with occasional karst features (Scholle et al., 1993). Basin facies were deposited in water depths up to 200 m and can have high Total Organic Carbon contents (Geluk, 2000). The thickest carbonate intervals are found in the slope facies. Occurrences of the slope-facies carbonates in the Zechstein Group are an indication of the location of the margins of the Southern Permian Basin and the extent of Z<sub>2</sub> and Z<sub>3</sub> halite deposition (**Figure 5**). Occurrences of Zechstein slope carbonates within the DEFAB area were described in detail (Tolsma, 2014; Geluk, 2000). Occurrence of these Zechstein carbonates was inferred along the western and eastern margins of the Elbow Spit High and possibly in the area around the Step High, within the Step graben. Slope facies were previously interpreted to have been absent in this area, although geologically it might have been expected, since the presence of Zechstein platform carbonates is often controlled by palaeogeography and typically occurs on structural highs. Based on these observations and observations in the German offshore area (Arfai et al., 2014) a modified distribution map for Zechstein palaeogeography was created and a modified depositional margin of the salt basin can be proposed for the Southern Permian Basin. **Figure 5** shows a map by Geluk (1999, after Lokhorst 1998; Taylor, 1998) with the modified salt basin margin within the study area.

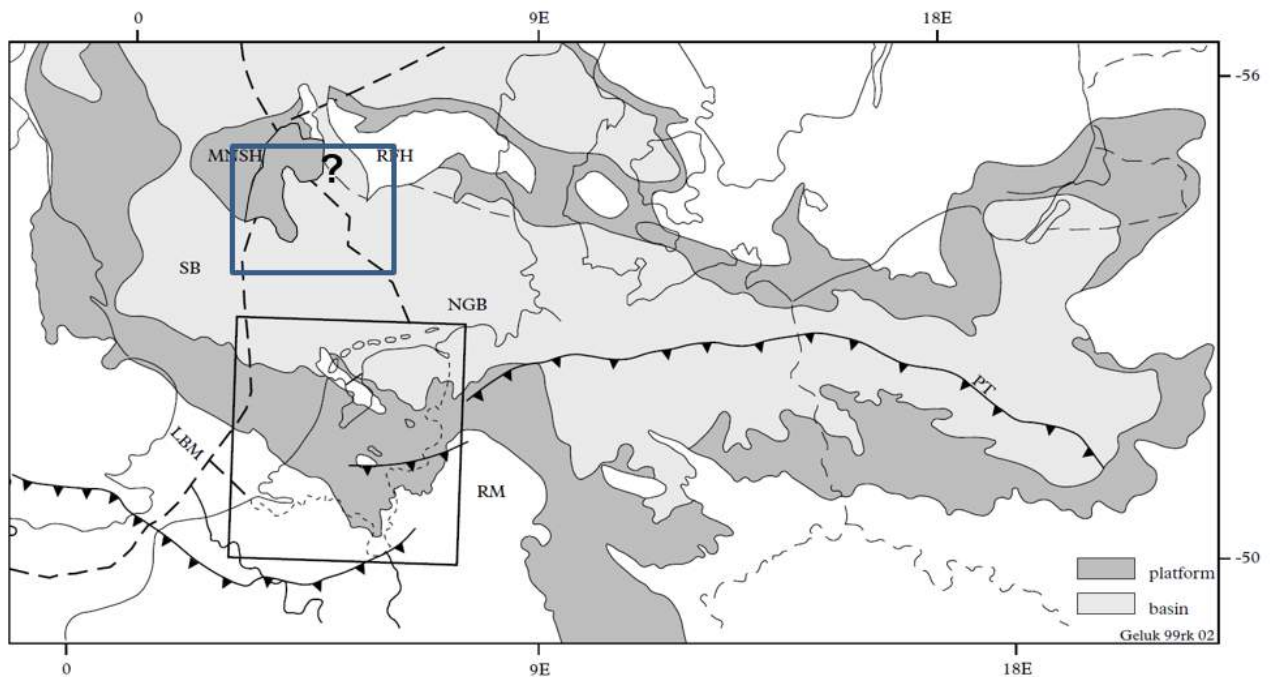


Figure 5: The Late-Permian Southern Permian Basin (Modified after Geluk 1999); Note: Within the study area (blue box), the basin margin was modified based on recent EBN study of Zechstein carbonate platform facies occurrence (Tolsma, 2014). Towards the east, in the German offshore area, the location of the basin margin remains uncertain due to restricted availability of seismic and well data.

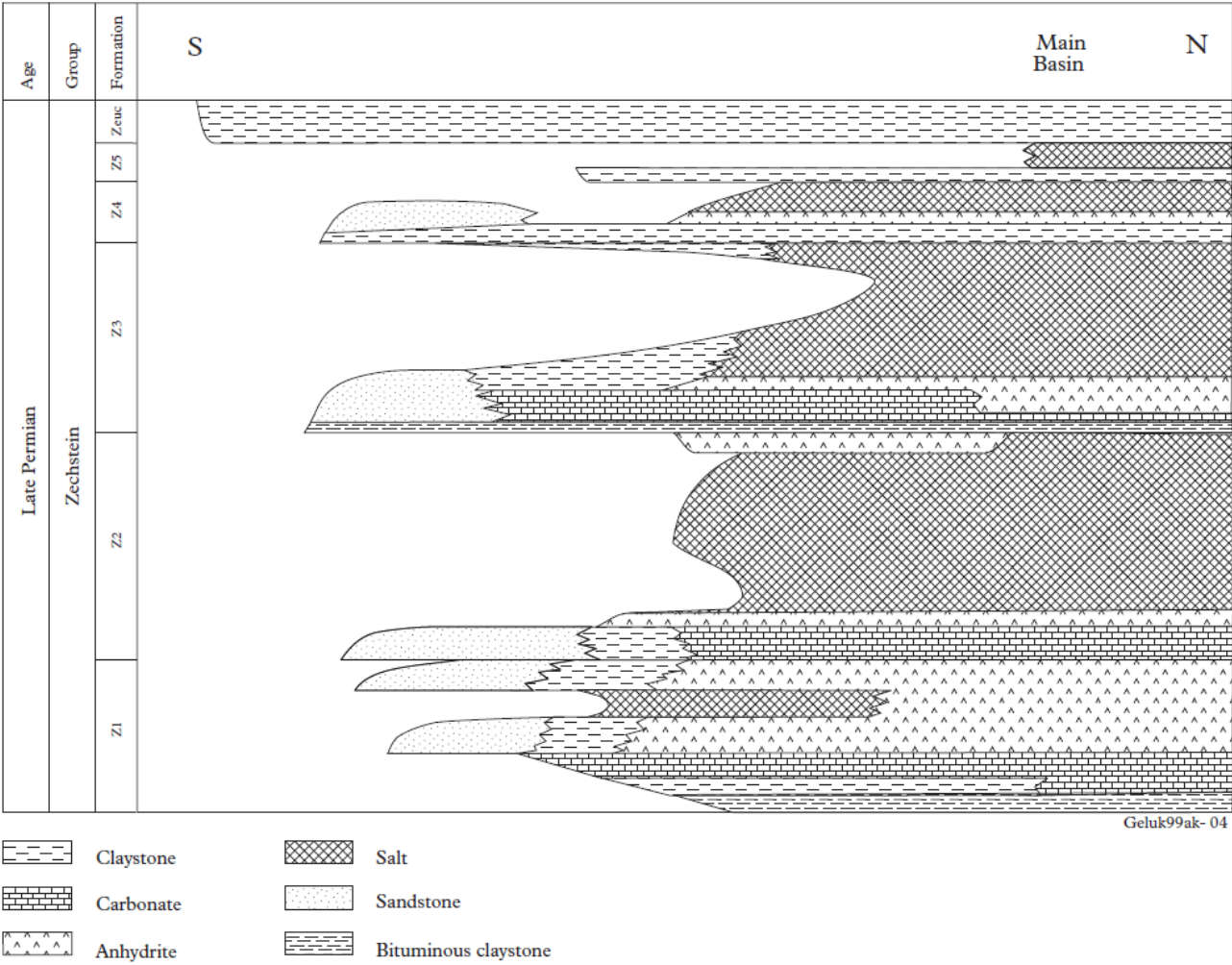


Figure 6: Zechstein Group Z1-Z5 formations: Zechstein Facies in the Netherlands, from South to North (Geluk. 1999)



### 2.5.2. *Post-Permian Stratigraphy*

The post-Permian stratigraphy in the study area will be described according to boundaries and nomenclature as defined in Kombrink et al. (2012; **Figure 7**). 7 Intervals describe the most important stratigraphic intervals present in the study area:

- 1). Lower Germanic Trias Group (**RB**); Early Triassic sediments mainly consisting of red-bed type sandstones, siltstones and claystones.
- 2). Upper Germanic Trias Group (**RN**); Middle to Late Triassic sediments containing silty claystones, carbonates and sandstones. This interval contains evaporitic deposits within the Röt formation.
- 3). Altena Group (**AT**); Early to Middle Jurassic sediments consisting mainly of argillaceous deposits with some calcareous intercalations in the lower part, and alternating calcareous and clastic sediments in the upper part. This group contains the bituminous Posidonia claystone formation, of which occurrence is restricted to the DCG.
- 4). Schieland Group (**SL**); Late Jurassic to Early Cretaceous sediments consisting of grey and variegated claystones, coaly to clayey sandstones, rare coal seams (associated with grey claystones), and locally calcareous intercalations. Within this interval the bituminous Kimmeridge clay formation can be found, of which occurrence is restricted to the CG in most of the study area.
- 5). Rijnland Group (**KN**); Early Cretaceous deposits containing argillaceous (and some marly) formations which may contain sandstone beds at the base and, locally, similar coarse clastic intercalations.
- 6). Chalk Group (**CK**); Late Cretaceous sediments comprising white, buff, cream and light-grey, hard, fine-grained, bioclastic limestones and marly limestones. Locally, marls, calcareous claystones and glauconitic sands occur.
- 7). North Sea Supergroup (**NS**); Tertiary and Quaternary deposits consisting of a range of clays, silts and sands, mainly of marine origin.

(Source: *DinoLoket*, 2015)

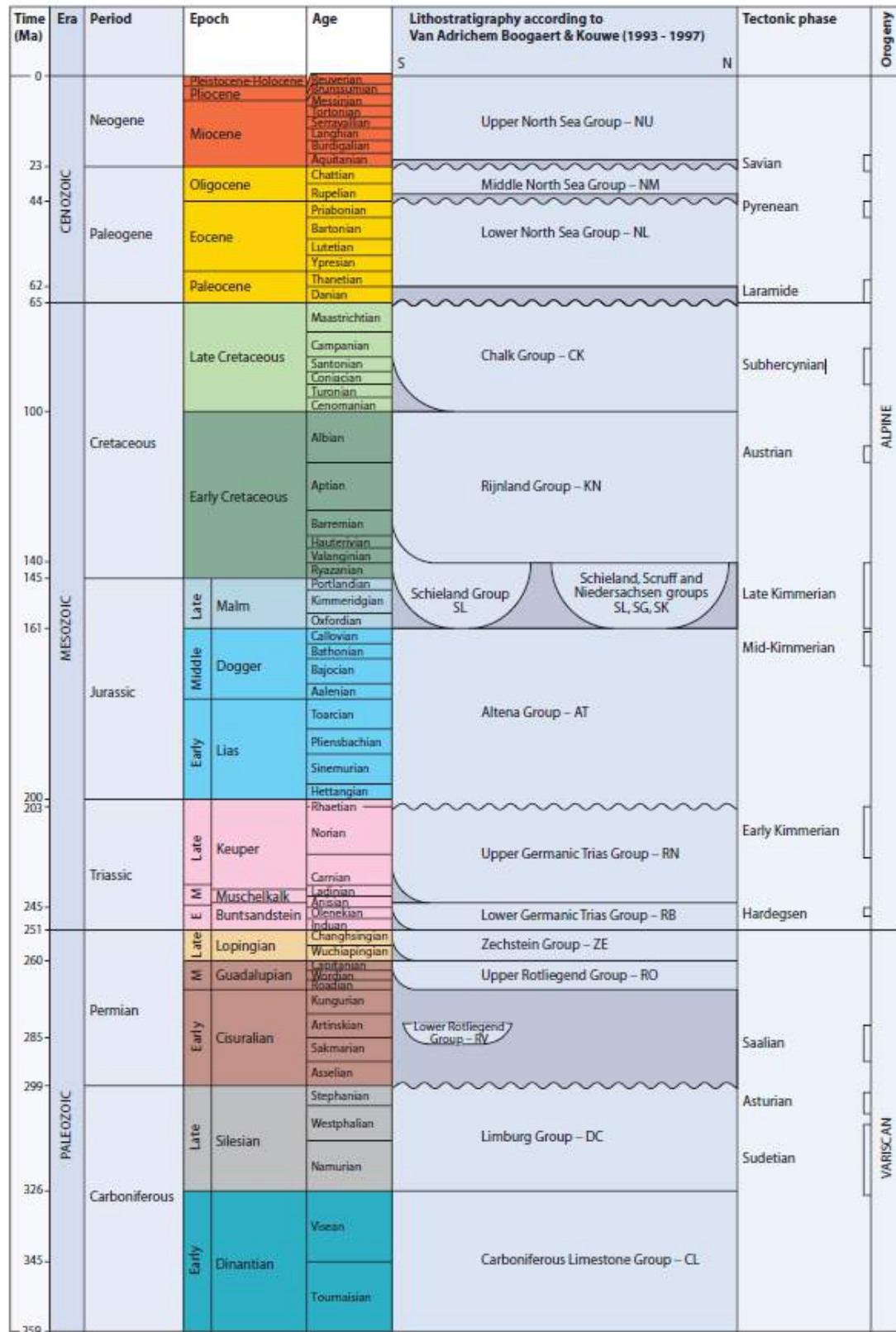


Figure 7: Simplified stratigraphic chart of the Netherlands (Kombrink et al., 2012)

### 3. Mechanisms of Salt Tectonics

Strictly speaking salt is defined as the crystalline aggregate of the mineral Halite (NaCl), however, when referring to salt in this study, a rock primarily containing Halite (but likely also containing other evaporitic, clastic or carbonate rocks) is meant. Basins where salt is present typically behave profoundly different than basins where salt is absent and salt can often be seen impacting a wide range of processes within these basin. This can all be rooted to the fact that salt inherently has different mechanical properties than most clastic and carbonate rocks: while it fractures like other rocks under very high strain rates, over geological time salt behaves visco-elastically (Hudec, 2007). Another important property of salt, which distinguishes it from other rocks, is its incompressibility. This property causes salt, when buried, to become less dense than the overburden, making it buoyant and making the subsurface system unstable. In order for salt to reach the surface by buoyancy alone, a siliciclastic overburden of at least 1600m is required (Baldwin and Butler, 1985).

Although it was long thought that these buoyancy forces were the main driving mechanism of salt tectonics, modern conception is that stress differential loading and roof strength are the main driving forces, especially in salt movement initiation (Hudec, 2007). The important role of active faulting in the formation of accommodation space to allow differential loading has also recently been fully acknowledged (Vendeville and Jackson, 1992; Vendeville, 2002). Current theory for a setting like the North Sea is that salt movement is typically controlled by an interplay of several factors: weakening of the overburden by active faulting, consequent differential loading induced by fault controlled accommodation space generation and buoyant behavior of salt.

The internal geometry of the salt is often ignored, where salt structures are presented without internal structure. In the case of the Zechstein salt, the internal structure consists of complexly folded and faulted strata, where 'stringers' (or 'floaters') represent relatively brittle layers of anhydrite, carbonate and clays (e.g. Z3-stringers; van Gent, 2011). In this study will not go further into detail regarding these internal complexities of Zechstein salt, partly because they are not visible in most of the study area, due to salt migration.

Depositional patterns in salt controlled basins are directly related to salt movement. Around salt structures, deposition patterns are typically controlled by several distinct stages of salt movement (**Figure 8**, after Vendeville, 2002): 1). Layered salt stage (**Figure 8F**): Initial configuration of layered salt. 2). Pillowing stage (**Figure 8E**): Lateral salt movement within the salt layer leads to the development of a primary rim syncline basin (indicated with "I" in **Figure 8**), away from the salt structure. Stratigraphic thinning occurs on top and adjacent to the pillow. 3). Piercing stage (**Figure 8D, C, B**): Salt moves vertically, piercing through younger stratigraphic layers. This stage is typically accompanied by withdrawal of surrounding salt towards the piercing structure, which leads to the development of a secondary rim syncline (indicated with II in **Figure 8**) adjacent to the piercing salt structure. This means sediments were allowed to accumulate here and show a

thickening towards the salt structure. 4). Diapir rejuvenation stage (**Figure 8A**): Reactivation phase of salt structure growth, typically associated with tertiary rim syncline (indicated with III in **Figure 8**) development (after Trusheim, 1960; Vendeville, 2002).

The initial model for salt structure growth as proposed by Trusheim (1960) was based entirely on the buoyant behavior of salt according to Rayleigh-Taylor instabilities. This theory was reinterpreted by, among others, Vendeville and Jackson (1992), Vendeville (2002), Weijermars et al. (1993) to show the importance of regional tectonics on the controls of salt structure growth. Present day conception is that the initially proposed model of Trusheim (1960) by itself is irrelevant and that tectonics and active faulting play a crucial role in salt movement. This aspect is illustrated in **Figure 8** by the extension and compression of the section.

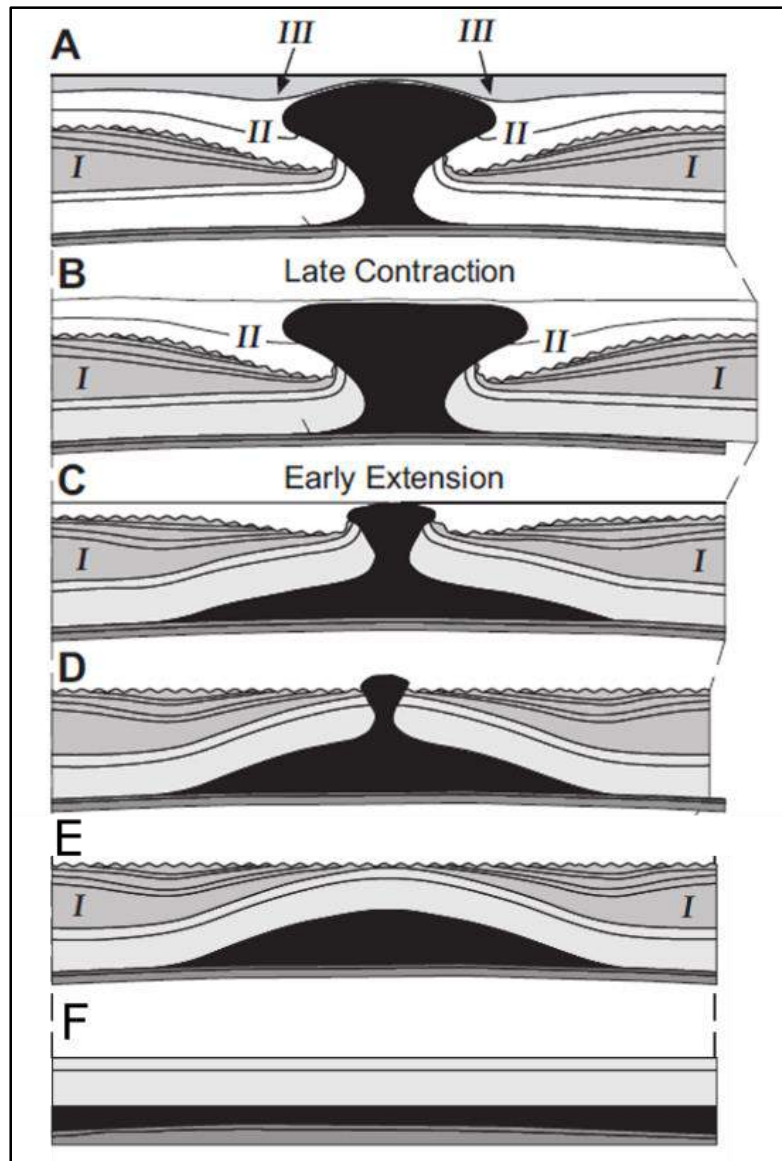


Figure 8: Development of a salt structure. Effects of successive tectonics events on salt structure development and associated cross-section shortening and extension (After Vendeville, 2002).

Faulting associated with a salt cover can be distinguished in 3 main categories: 1). Hard-linked faulting: Faults above and below the salt cover are in direct contact. This typically occurs where the salt cover is relatively thin (referred to as '3' in **Figure 9**). 2). Soft-linked faulting: Faults above and below the salt cover are spatially related, but show lateral offset. This typically occurs where the salt cover is slightly thicker (referred to as '2' in **Figure 9**). 3). Non-linked faulting: Fault below the salt cover are completely decoupled from faulting in the overburden above the salt (referred to as '1' in **Figure 9**). This typically occurs where the salt layer is relatively thick (**Figure 9**; Ten Veen et al., 2012). These modes of faulting show a clear relationship between initial salt thickness and structural style, where thin-skinned (1 in **Figure 9**) or thick-skinned (2 and 3 in **Figure 9**) tectonics occur, depending on salt thickness. Steward (2007) notes that the ratio between basement fault displacements and local salt thickness is crucial in the mechanism of fault linking that is dominant within the North Sea basins. Also for the Dutch offshore, previous studies on salt tectonics (Remmelts, 1996; De Jager, 2003; Ten Veen, 2012) have shown a close relationship between the elements of: depositional salt thickness, structural style, timing of deformation and thickness of the overburden above the salt.

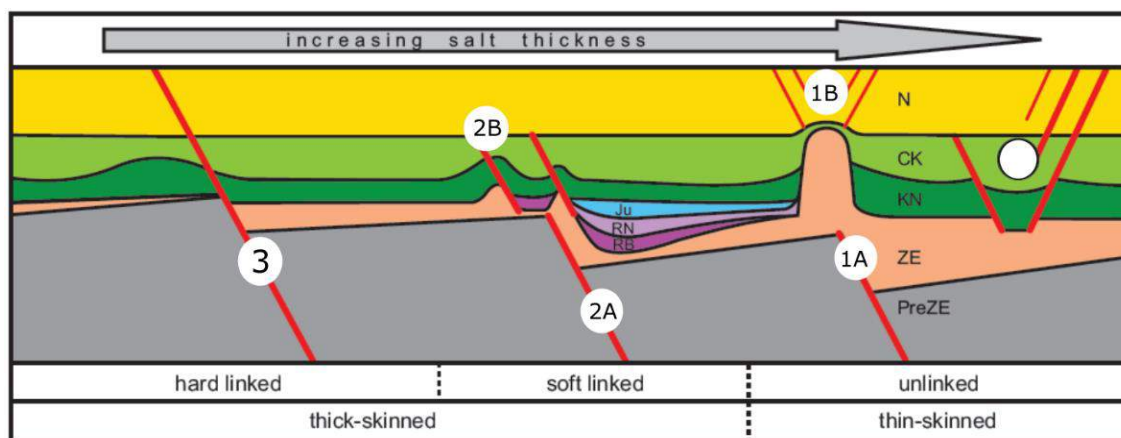


Figure 9: Linking of faults below and above a salt cover (after Ten Veen, 2012; 'Cartoon modified from Stewart (2007) and adapted to the Dutch North Sea'). 1). Non-Linked faulting 2). Soft-linked faulting 3). Hard-linked faulting.

The structural style dominating the initiation of a rift event and the climax of a rift event is also dependent on the thickness of the (pre-rift) salt within a basin (Duffy et al., 2013). Where thick salt is involved, typically an initial stage of salt structuration will involve formation of pillows (or monoclines), where depocenters thicken away from salt structures and are unaffected by basement faults. During rift climax, detachment faults can become active above a salt cover, where large offset faults are able to penetrate the fault cover entirely. Salt structures form on structural highs like fault block tips or fault block dip slopes. Where salt structures pierce, they will partly subside, providing accommodations space for new depocenters, as described as the 'piercing stage' above (Trusheim, 1960; Jackson et al., 2010). Later, where salt supply is exhausted, these structures may collapse, forming a collapse graben in the overburden strata. Due to this crestal collapse, ridge collapses due to dissolution or differential compaction of salt structures, small extensional faults may develop, typically in a radial pattern (**Figure 10**; Steward, 2006, 2007).

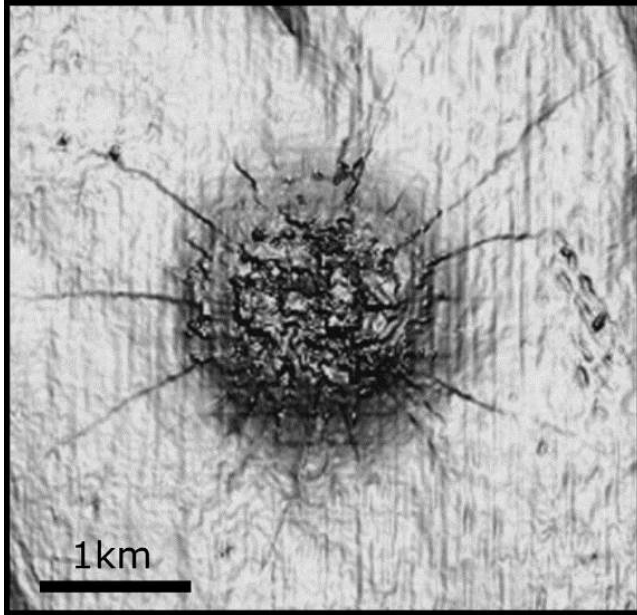


Figure 10: Radial fault pattern in domed sediments above a salt diapir in the North Sea (Steward, 2006)

## 4. Analogue Research

Salt tectonics has been subject of numerous studies by the oil and gas industry as well as academia. Salt provinces are widespread around the globe, and salt almost always plays a crucial role in the geological development of these areas. The Niger delta, the Zagros mountains and the Gulf of Mexico are examples of famous and thoroughly studied salt provinces. However, the specific geological setting largely determines the role of salt in the geological development of an area. Therefore, for this study, some analogue studies will be considered in adjacent or comparable geological settings. Despite being one of the most studied basins in the world, there is still much unknown in the North Sea subsurface, especially about the role of salt tectonics. Most relevant analogue studies concern the offshore areas adjacent to the Dutch offshore sector (UK, Denmark, Germany and Norway offshore areas) and previous studies in the Dutch northern offshore itself. The important role of salt tectonics becomes evident from the wide range of literature in which different aspects and implications of salt tectonics are discussed.

The role of Zechstein salt in the post-Permian structural development of the Northern Dutch offshore has previously been studied as a part of the general geological development of the area (e.g. Wijhe, 1987; Ziegler, 1987, 1990, 1991; De Jager, 2007; Geluk 2005; See chapter 2. *Geological Setting*), but has also been studied in a more specific and applied context.

Fault analysis in the DEF 3D seismic survey, covering part of the study area, was recently done by Wijker (2014, EBN). Thanks to the high resolution 3D seismic, more detailed fault mapping was possible. Relevant conclusions in this study included: 1). Very limited fault activity is observed during the Jurassic in the Dutch Central Graben 2). Large offset ESE-WNW trending Jurassic faults are observed 3). Although sub-Zechstein faults are obscured by overlying salt, these faults may have controlled Jurassic subsidence and consequently smoothed by salt 4). Effects of inversion affect Late Cretaceous and Tertiary inducing a high in the basin center and possible late reactivation of salt structures affecting deposition. An important observation in this study was that (basement) fault relations are often difficult to analyze due poor seismic imaging induced by overlying salt. A link will be made in this study, by assessing if information about Zechstein salt movement can provide better constraints on movements of faults, rather than obscuring them.

The Dutch Central Graben continues towards the N to NW as the German Central Graben (German offshore area) and the Tail End Graben (Danish offshore area). The N-S running DCG changes orientation to a NW-SE orientation in the Tail End Graben (**Figure 4**). Rank-Friend and Elders (2004) performed an integrated analysis of the structural development of salt structures in the Danish salt province, which is located mostly within the Tail-End graben, to the SW of the NW-SE running Coffee Soil fault (study area is indicated in **Figure 4**). Results from time-based interpretations of faults, horizons and thickness maps around salt structures in this area provides a post-Permian, salt tectonic history of the Danish salt province. A recent mapping study in the adjacent German offshore territory ('Entenschnabel') has been done, focusing on the structural

development of the area (e.g. Arfai et al., 2014; See **Figure 4**). These studies are a good reference for the geological continuity towards the North of the study area.

The role of salt tectonics has also been studied extensively in North Sea basins in the UK sector (e.g. Hodgon, 1992; Davison, 2000; Steward, 1995, 1999, 2007) and other analogous basins in Northern Europe. 3D Restoration ('Retro-deformation') on basin scale and restoration of individual salt structures was done in several North German basins, e.g. North-East German Basin (Scheck et al., 2003), Glückstadt Graben (Baykulov et al., 2009) and Ems Graben (Mohr et al., 2005). Although methods vary in these studies, the concept of a structural restoration of a salt controlled basin a commonly used tool and is very much analogous to this study. In all of these studies the central role of Zechstein salt in basin development becomes evident.

A recent study by Harding (2014) investigates the salt tectonic development of diapirs North of the Hantum fault zone (southern Dutch offshore), including a structural restoration of salt configurations through time. The aim here is again very much analogous to this study: obtaining better constraints on the timing of salt movement in the Dutch offshore. The results of Harding (2014) can be a reference for this study, bearing in mind that its study area is located in a different structural setting than this study, outside of the Central Graben system.

All in all, an extensive framework is available, to which observations on (salt) tectonic development in the northern Dutch offshore, and the DCG in particular, can be compared.

Several studies relate salt tectonics to specific play concepts and prospectivity of the area. For example, internal variations in the Late Cretaceous Chalk Group (CK) are often linked to salt movement during its deposition (e.g. Van der Molen, 2005; Huijgen 2014, EBN; Lanting 2013). This has major implications for the potential and behavior of the North Sea Chalk as a reservoir. In the Danish offshore sector, production from Chalk reservoirs is common and here Chalk fields are almost exclusively linked to salt structures. Detailed studies on the relationships between growth of salt structures and the reservoir quality of Chalk include studies on Chalk fracturing mechanisms above salt diapirs (e.g. Carruthers, 2013; Steward, 2006) and the internal variation within the Chalk reservoir (e.g. Back et al., 2011; Van der Molen, 2005; Molenaar, 1996). Effects of late salt tectonic movements on potential reservoirs in younger Tertiary sediments have also been studied (Clausen et al., 2012).

A good example of a study in which the effects of the presence of salt structures on the burial history of source rocks is investigated, is a study on the Mittelplate oilfield in Northern Germany by Grassman et al. (2005). The oilfield, as well as the underlying Posidonia source rock are located on the flanks of a major salt diapir ('Büsum salt dome'; **Figure 12**). A structural and thermal restoration reveals the crucial role of rim syncline development on the burial of the source rock and the role of late salt movement of adjacent diapirs on petroleum generation and maturation during the Cenozoic. Several basin modelling studies performed by TNO (Dutch institute for applied natural sciences; Verweij, 2009; Fattah, 2012) also show the role of salt structures on the thermal gradients in younger sediments and effects on maturation of source rocks. It is shown that high heat flows through salt structures are associated with increased temperatures in sediments close to the top of the salt structure and reduced temperatures in sediments below salt structures (**Figure 11**). This effect is important in the reconstruction of the maturation history of all source rocks adjacent, below or above major salt structures.



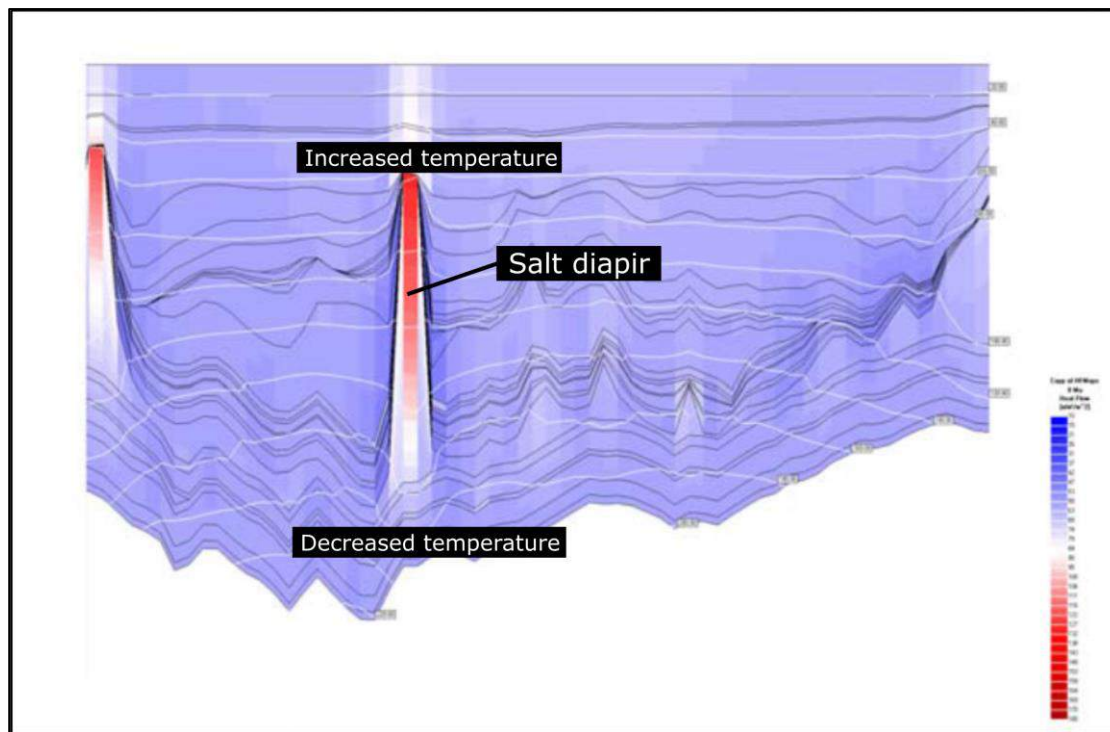


Figure 11: After Verweij 2009: 'Influence of salt structures on present-day temperature and heat flow distribution. High heat flows through salt structures (in red) are associated with increased temperatures in sediments close to the top of the salt structure and reduced temperatures below salt structures.'

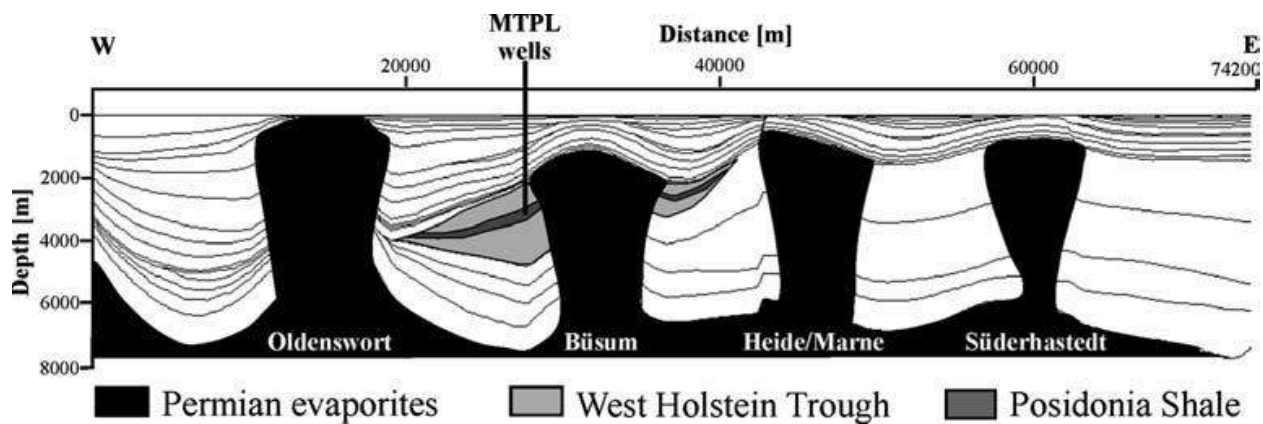


Figure 12: Location of the Mittelplatte oil-field, the largest oilfield in Germany. The cross section shows four major salt structures and is used for a basin modelling study. The source rock here is the Late Jurassic Posidonia Shale (Grassman et al., 2005).

## 5. Salt Structures in the northern Dutch offshore: An Inventory

### 5.1. Methods and Approach

A high degree of coverage of seismic data in the study area is present and this allows for a regional analysis of salt structures. The data that was used for this analysis consisted of a range of 2D and 3D seismic datasets. The 3D seismic datasets that were used are the DEF-survey (2012), the Terracube 1 & 3 merged seismic surveys (2011) and the Z3FUG2002A survey (2002) (Courtesy of Fugro, **Figure 13**). As is visible in **Figure 13**, some areas within the study area are not covered by 3D seismic data, here 2D seismic lines are available from a range of surveys, with varying resolutions and coverage.

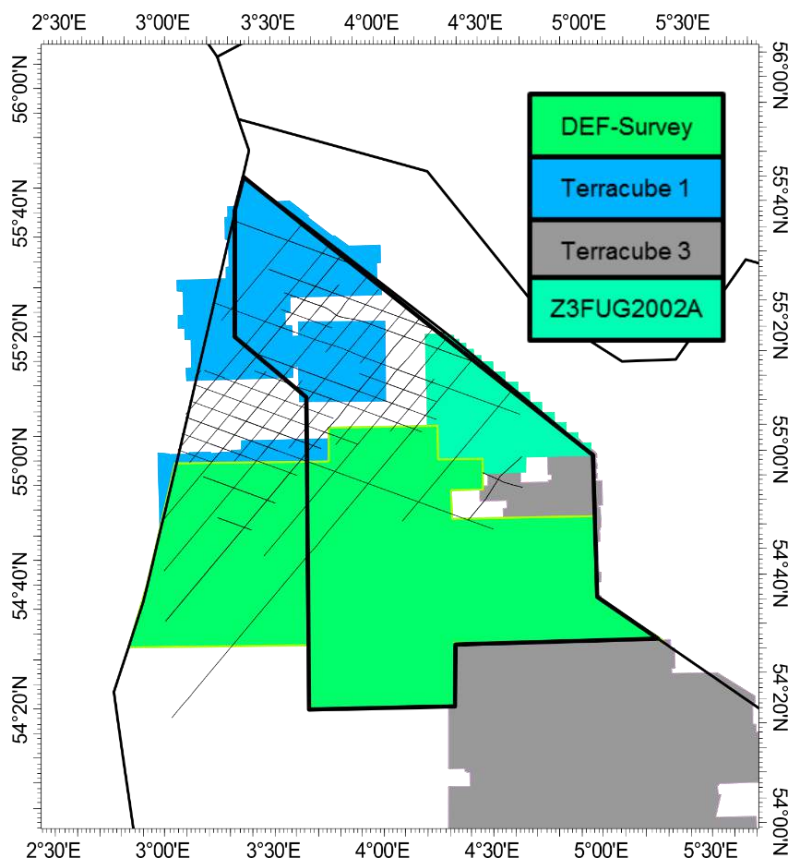


Figure 13: Coverage of 2D and 3D seismic data used in this study; The study area lies within the black outline.

### 5.1.1. Salt Structure Inventory

To get a control on the role of Zechstein salt movement in the northern Dutch offshore it is essential to be aware of the range of different configurations of Zechstein salt that occur in the study area. In order to achieve this, an inventory was made in this study, in which Zechstein salt structures are systematically listed and described according to a set of characteristics (**Appendix 2**). A salt structure in this inventory will be defined as a significant accumulation of remobilized Zechstein salt, affecting overlying younger sediments. It has to be noted here that in defining a single salt structure as such, interpretation and geological setting often play a role, due to the often highly complex structuration of salt, uncertainties in imaging or cut-offs by cultural borders. Since it is not always unambiguously clear why a single structure is defined as it is, this decision is explained in the salt structure inventory, where necessary.

To identify salt structures a combination of 2D/3D seismic data, time-based maps, depth-based maps and thickness maps was used. Analysis of these data was mainly done using Petrel-software (Schlumberger). Throughout the DEFAB area interpreted horizons were available for main post-Permian intervals shown in **Figure 7** (EBN DEFAB regional mapping project, TNO NLOG data). An important map in identifying and analyzing Zechstein salt structures is the regional Top Zechstein TWT map (**Figure 15**). Other interpreted horizons allow for further control on position and extent of salt structures, since overlying intervals are often affected by moving Zechstein salt structures, they help reveal their position. So in order to describe salt structures accurately, not only the Zechstein salt itself is analyzed, but also a range of characteristics of associated younger intervals is described. Depth maps and thickness maps are available in depth (m) for these intervals and are used for regional interpretations (source TNO NLOG). However, more detailed interpretations on seismic sections and horizons are done in TWT, since no depth migrated version of these data is available for this study. Due to relatively straight-forward overburden configurations, away from salt structures, structural analysis in TWT will most likely be reliable for the purpose of this study.

Descriptions of the salt structures in this inventory are listed in 4 different categories: **1**). Orientations and Dimensions **2**). Faults **3**). Associated stratigraphic relationships and **4**). Data and Locations. The inventory lists observations in and around salt structures rather than interpretations. One major aspect to keep in mind here is imaging uncertainty. Since seismic imaging is severely affected by nearby salt, the interpretation around and underneath salt carries an uncertainty. Another factor adding some uncertainty is the lack of detailed interpretations within the DEFAB area, due to poor well control, imaging issues or other factors. A full 3D interpretation for the main stratigraphic horizons in the study area was beyond the scope of this study, however, additional interpretation was done locally, where needed. The inventory lists a range of parameters, relevant to salt tectonic development of the area. Additional parameters can be assessed or more detail can be added to the inventory in the future, since due to the complexity of the structures and the size of the study area, this does not fit within the scope of this study.

### 5.1.2. Isopach Maps

In order to do effective regional interpretation of salt movements, regional thickness trends were assessed using isopach maps for all relevant stratigraphic intervals throughout the study area. thickness maps based on a depth grid (TNO, 2012) were used. Since these maps were initially extracted in true vertical thickness (TVT) for a given interval, these maps were converted to true stratigraphic thickness (TST), in order to correct for thickness anomalies in e.g. steeply dipping horizons. To do this, the dip angle was extracted for every grid. Then a new thickness map was generated with TST values using the formula in

Figure 14.

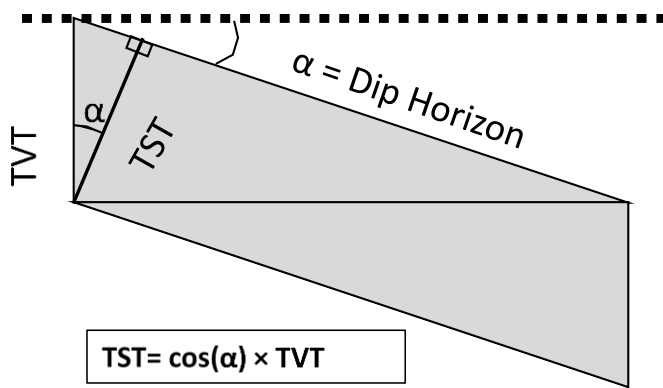


Figure 14: Conversion from true vertical thickness (TVT) to true stratigraphic thickness (TST) of a dipping layer.



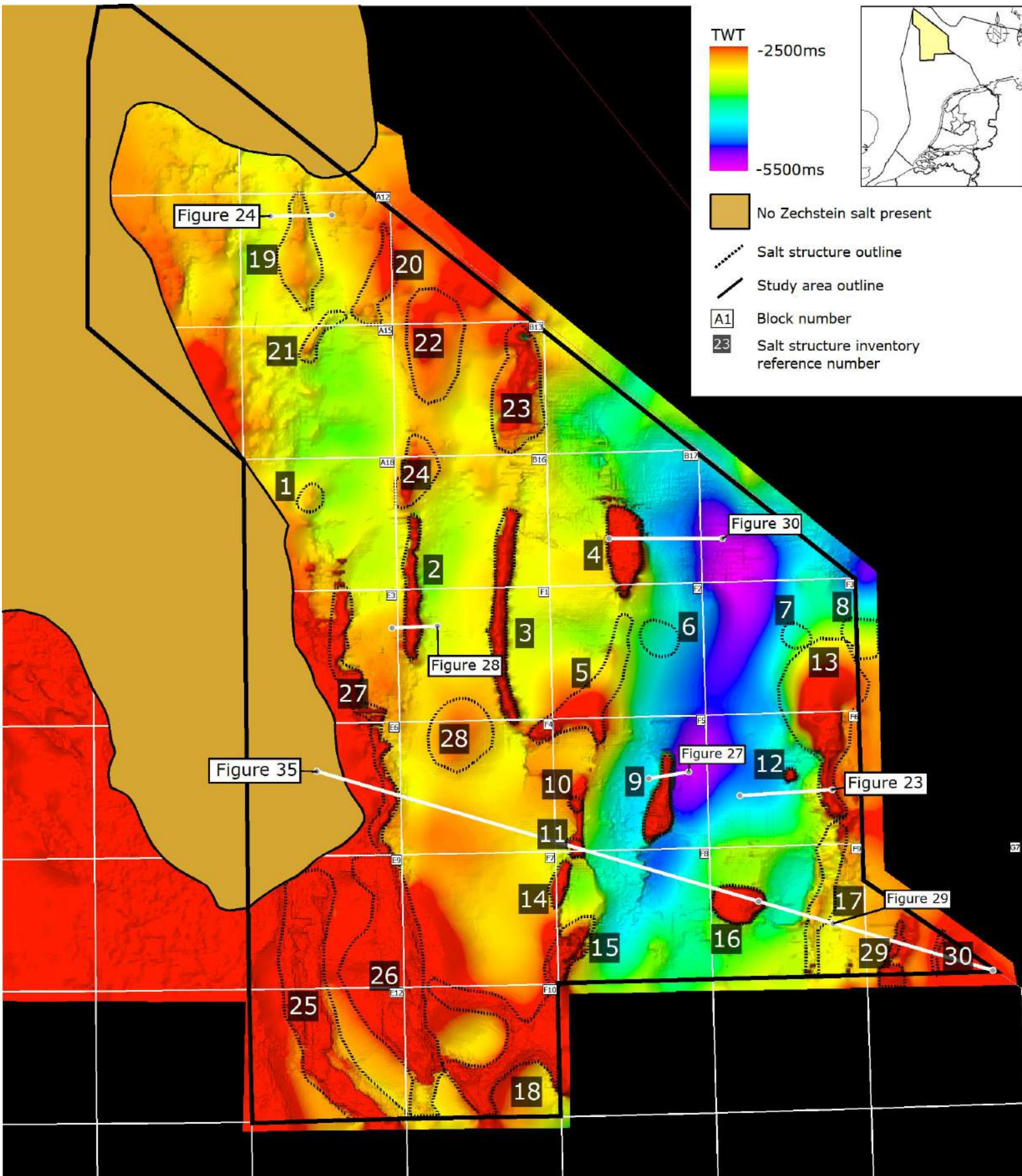


Figure 15: (Previous Page) TWT map of top Zechstein; All 30 salt structures are indicated and numbered with reference to the salt structure inventory (**appendix 2**)

## 5.2. Results

**Figure 15** shows the top Zechstein TWT map with the outlines of all 30 interpreted salt structures within the study area (including reference number). The complete salt structure inventory can be found in **Appendix 2A-H**, which will be referenced to below. **Appendix 1** shows all salt structures with a first order interpretation of top and base Zechstein in a seismic section perpendicular to the strike of the salt structure. In order to effectively interpret observations in **Appendix 2**, spatial distributions of salt structure characteristics have to be assessed and are visualized in distribution maps. Most important results are listed below for every set of characteristics in the salt structure inventory and for salt structure distribution maps and thickness maps of other relevant intervals. **Figure 16** shows some examples of salt structure characteristics.

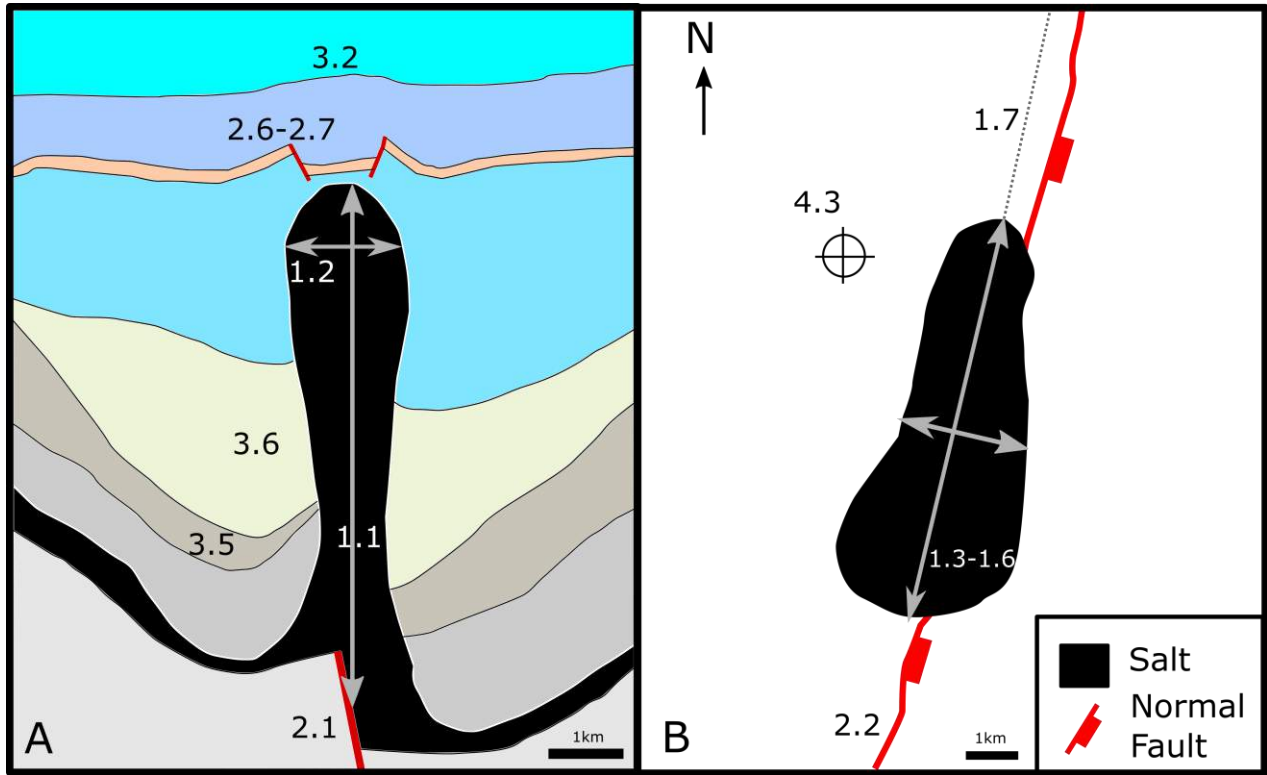


Figure 16: Examples of the salt structure characteristics assessed in the salt structure inventory with numbers referring to the characteristics described in chapters 5.2.1.-5.2.4. A). Section view of a salt structure. B). Map view of the same salt structure.

1.1 = Height from BZE, 1.2 = Maximum width, 2.1 = Sub-salt fault type, 2.6-2.7 = Crestal fault type and geometry, 3.2 = Youngest affected horizons, 3.5 = Interval thinning towards salt structure, 3.6 = interval thickening towards salt structure. 1.3-1.4 = Length and width of salt structure, 1.5 = Elliptical ratio, 1.6 = Shape type, 1.7 = Orientation, 2.2 = Sub-salt fault orientation, 4.3 = Well control.

### 5.2.1. Orientations and Dimensions

For all 30 salt structures in the study area orientations and dimensions were described, as shown in **Appendix 2A**, according to the following characteristics: **1.1**). Height from Base Zechstein (BZE; **Figure 16A**) **1.2**). Maximum width of the salt structure (**Figure 16A**) **1.3**). Length of the salt structure in top view (**Figure 16B**) **1.4**). Width of the salt structure in top view (**Figure 16B**) **1.5**). Elliptical ratio (**Figure 16B**) **1.6**). Shape type (**Figure 16B**) **1.7**). Orientation (**Figure 16B**) **1.8**). Depth of the salt structure crest below sea floor.

The height of the salt structure from BZE was measured vertically in TWT (s). If interpretation of BZE is prevented by overlying salt, the depth of BZE is interpolated from adjacent areas with less overlying salt. Maximum width of a salt structure was measured on a seismic line perpendicular to the orientation of the salt structure on map view. Top view dimensions, the shape types and the orientations were determined by analysis of the Top ZE TWT map and TWT maps of overlying intervals. Salt structure types were defined according to the definition in **Table 1**. The angle of the flanks was estimated from seismic data as the maximum angle top Zechstein makes with a horizontal in a salt structure.

Definition	Angle of flanks (°)	Elliptical Ratio	Piercing
Pillow (subtle)	<30	-	No
Pillow (pronounced)	<75	-	No
Diapir	>75	<4	Yes
Wall	>75	>4	Yes

Table 1: Salt structure types: Definitions

Distribution of these types of salt structures is shown in **Figure 17**. Some important observations here are: 1). No major piercing salt structures occur in the northern SG. 2). Pronounced pillows occur along the western SG boundary fault. 3). Long salt walls (up to 30km) occur along the boundary faults of the DCG and above basement faults within the SG. 4). Isolated, point-sourced diapirs almost exclusively occur within the DCG and above DCG boundary faults. 5). All major salt diapirs are located within the DCG.

**Figure 18** shows all salt structures that have a crest more than 4km above the Base Zechstein level. It becomes evident that all these salt structures are located within the DCG or above one of the DCG boundary faults.

Almost all elongated salt structures show a NNW-SSE to NNE-SSW orientation. Salt structures at the western SG boundary appear to follow underlying faults towards the NNW. Salt structures above the DCG boundary faults are typically elongated N-S, or if circular, are lined up in a N-S direction. Salt structures more towards the basin center of the DCG have developed mostly towards isolated, point-sourced salt structures. Some ENE-WSW to E-W trends can be observed locally in salt structures F10-EAST1 and F02-NORTH1.



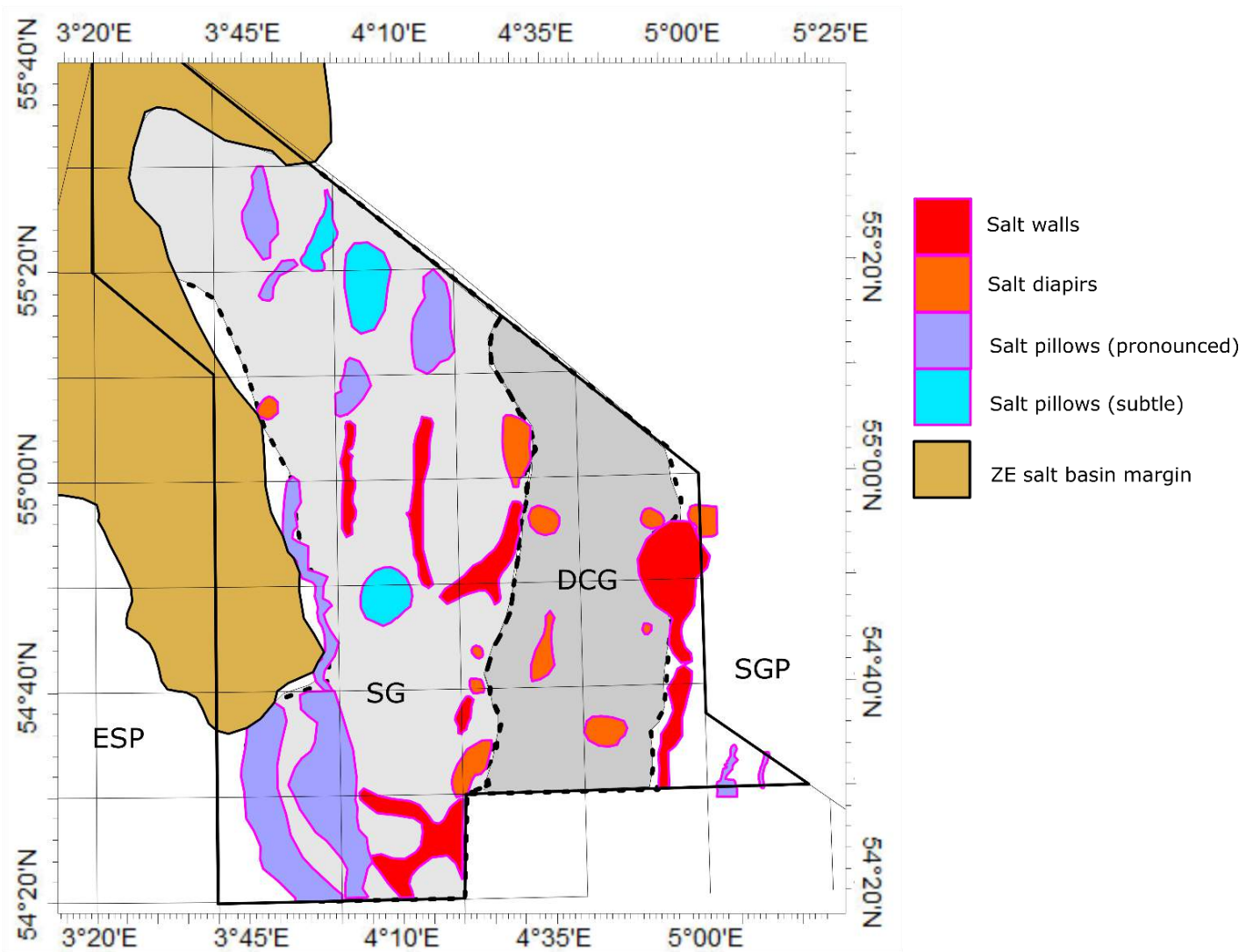


Figure 17: Distribution of salt structure types as defined in Table 1 within the study area.



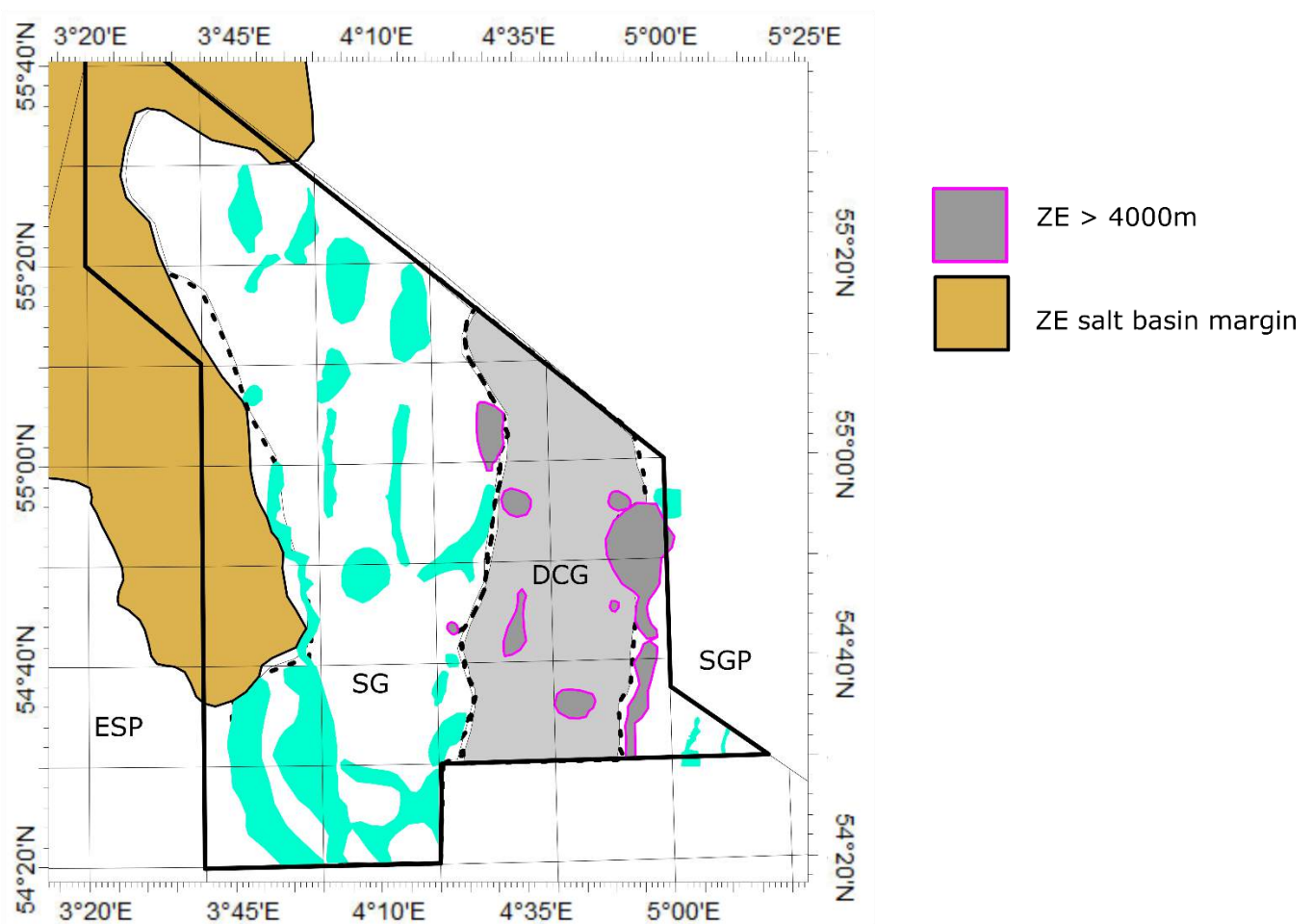


Figure 18: Distribution of salt structures; Salt structures where TZE is more than 4km above BZE are highlighted.

### 5.2.2. Faults

Around salt structures a wide range of associated faults can be found, which can be categorized according to their position and behavior with respect to the salt structure (**Appendix 2B**). Characteristics of these associated faults have been described in the inventory as follows: **2.1**). Sub-salt fault type (**Figure 16A**) **2.2**). Sub-salt fault orientation (**Figure 16B**) **2.3**). Sub-salt fault dip direction **2.4**). Sub-salt fault/ salt structure orientation match **2.5**). Fault linking **2.6**). Crestal fault type (**Figure 16A**) **2.7**). Crestal geometry. (**Figure 16A**)

Where imaging quality allows it, sub-salt faults are described and their orientation and dip direction are plotted. It is also assessed if the observed sub-salt fault orientation coincides with the orientation of the overlying salt structure. Fault linking refers to the dominant style of faulting around the salt structure, where faults are defined as hard-linked, soft-linked or non-linked (see Chapter 3: Mechanisms of salt tectonics, **Figure 9**). Crestal faults are described by their fault sense and by the geometry of associated layers above the crest of the salt structure.

It can be observed that almost all salt structures are associated with basement faults. The orientation of most elongated salt structures matches the orientation of inferred basement faults,

where they can be observed (**appendix 2B**). Distributions of fault linking behavior above and below the salt structure can be seen in **Figure 19**. Important observations are:

- 1). Faults are non-linked below most salt structures in the DCG and along the western DCG boundary fault (e.g. Salt structure Fo9-WEST<sub>1</sub>, **Figure 41**; Fo5-EAST<sub>1</sub>, **Figure 27**).
- 2). The DCG boundary faults can be seen affecting overburden at some locations, which is classified as soft-linked faulting.
- 3). At several locations along the western SG boundary fault and along the southeastern boundary fault of the DCG, faults can be seen directly linking into the overburden, which is classified as hard-linked faulting (see **Figure 35**).
- 4). Most faults associated with salt pillows can be seen affecting the overburden indirectly, which is classified as soft-linked faulting.
- 5). In the north of the SG the dominant faulting style is soft-linked faulting, while further to the south faults below major salt walls within the SG are non-linked.

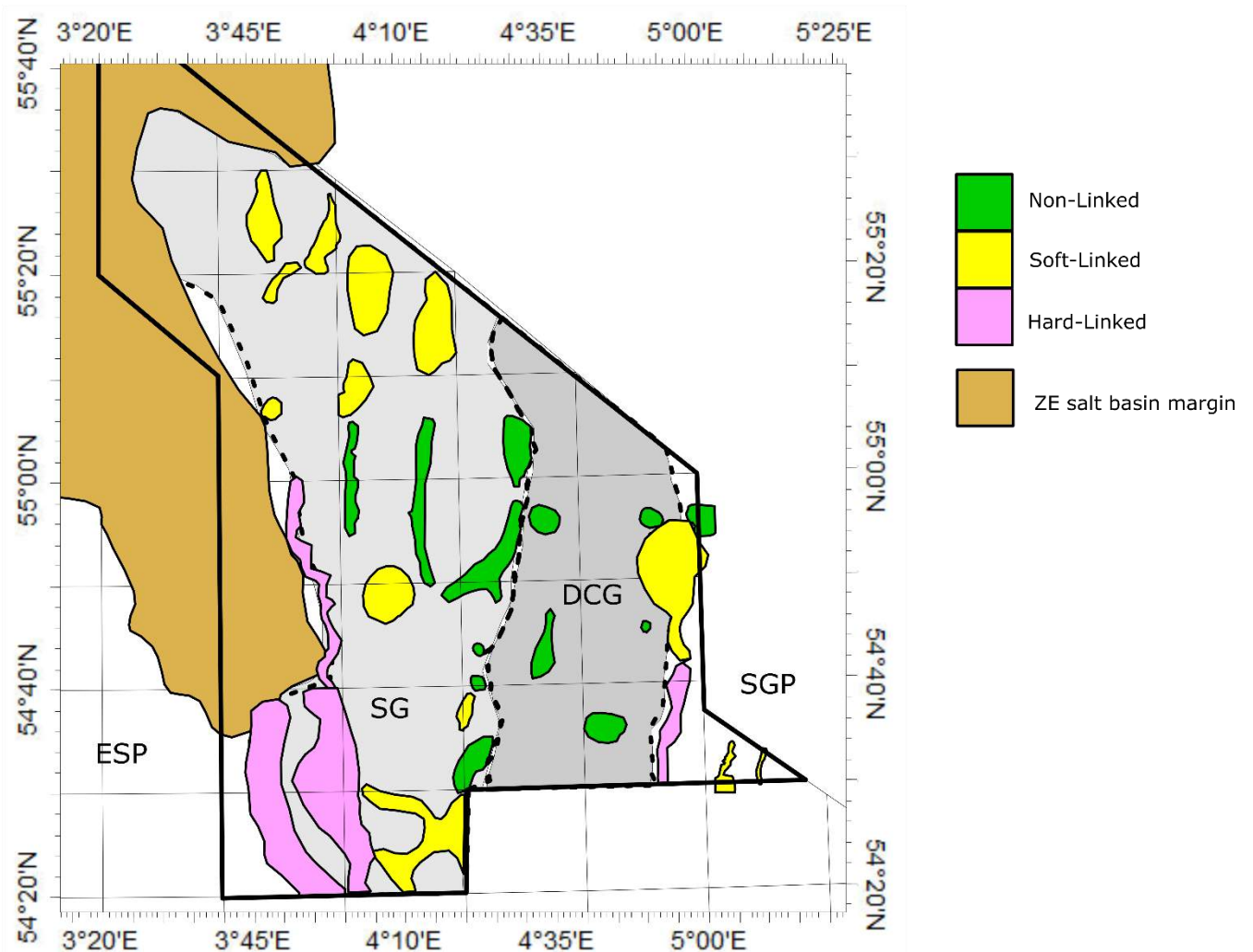


Figure 19: Distribution map of the dominant style of fault linking associated with each salt structure within the study area.

### 5.2.3. Associated stratigraphic relationships

In order to systematically assess periods of movement of salt throughout the study area stratigraphic relationships associated with the salt structures were analyzed. The following characteristics were assessed (**Appendix 2C**): 3.1). Youngest penetrated horizons 3.2). Youngest affected horizons (**Figure 16A**) 3.3). Oldest affected horizons 3.4). Most affected horizons 3.5). Intervals thinning towards salt structure (**Figure 16A**) 3.6). Intervals thickening towards salt structure (**Figure 16A**) 3.7). Occurrence of allochthonous salt wings.

Horizons are considered affected by salt movement, if there are clear indications of deformation or thickness variations around the salt structure present in the concerning interval. Presence of allochthonous salt wings are typically indications of salt expulsion at the surface or post-deposition intrusions in weak zones of the overburden. It has to be noted that allochthonous salt features can occur in a wide range of configurations and are often difficult to interpret directly from seismic data. Intervals are listed as thinning or thickening, when they show clear indications of *stratigraphic* thinning or thickening, towards the salt structure. In some cases intervals will thicken towards the salt structure (e.g. in a rim syncline) but thin over the crest of the salt structure. These nuances in thinning and thickening relationships are important when interpreting the salt structure inventory and are described, if needed, in the salt structure inventory (**appendix 2C**). The distribution of thinning and thickening relationships around salt structures are shown in **Figure 20** and **Figure 21** respectively, for all analyzed post-Permian intervals.

Main observations here are listed for every interval.

- **RB** does not show major thickness variations around salt structures in most of the study area, but shows some thinning towards salt structures in the northern SG and locally along major boundary faults.
- **RN** thins towards most salt structures in the SG and thickens towards the DCG boundary faults. Locally, thickening occurs towards salt pillows within the SG.
- **AT** thins towards structures associated with DCG boundaries and thickens towards salt structures within the DCG.
- **SL** thins towards structures associated with DCG boundaries and thickens towards salt structures within the DCG.
- **KN** shows thinning towards some salt structures within the SG.
- **CK** shows thinning above almost all salt structures and thickens towards salt structures along the DCG boundary faults
- **NS** thins towards most salt structure in the southern part of the study area and thickens towards salt structures associated with the eastern DCG boundary fault.

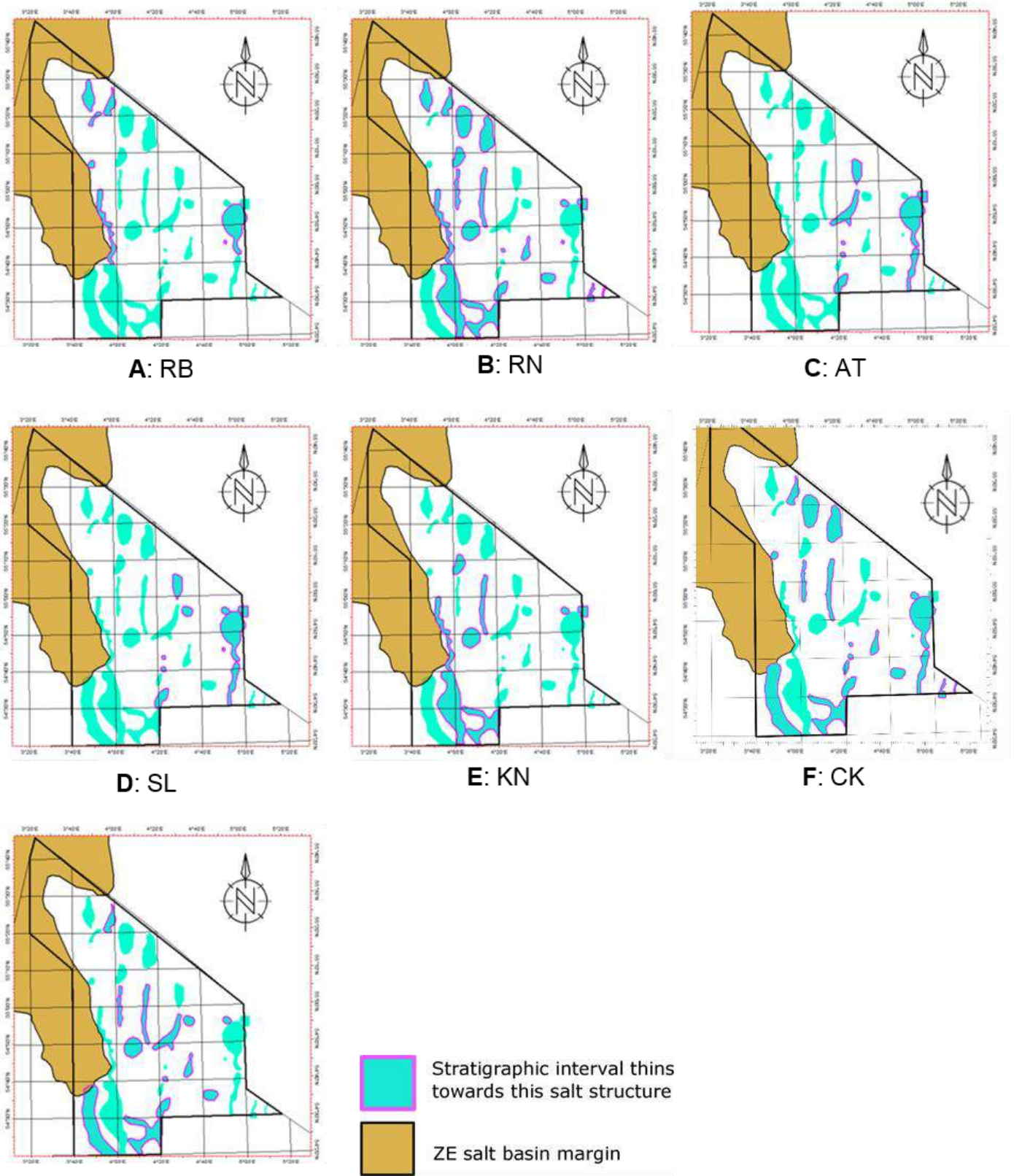


Figure 20: Distribution map of thinning of Stratigraphic intervals towards salt structures within the study area.



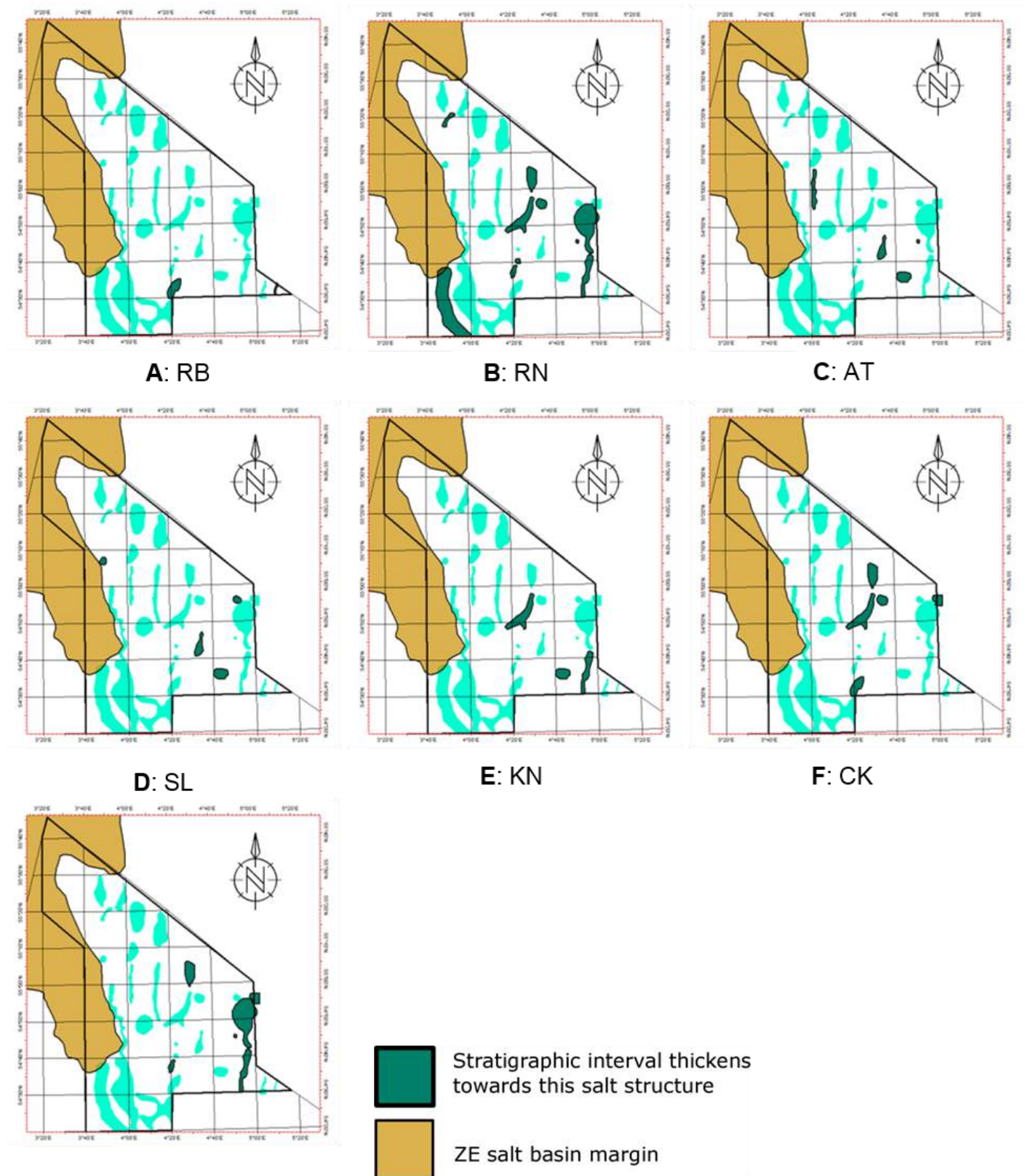


Figure 21: Distribution map of thickening of stratigraphic intervals towards salt structures within the study area.

#### 5.2.4. *Data and Locations*

In order to compare salt structures and effectively analyze their distribution and properties, descriptions of their locations and available data are done (**Appendix 2D**). The following characteristics were assessed: **4.1**). Seismic Imaging uncertainty **4.2**). Seismic data set **4.3**). Well control **4.4**). Associated oil and gas fields **4.5**). Section outline **4.6**). Top structure outline **4.7**). Location in structural element **4.8**). Additional notes.

Since imaging resolution can vary throughout the area, some salt structures will have higher uncertainties in analysis of their characteristics. Although most of the study area is covered by relatively high quality 3D seismic data (**Figure 13**), imaging below salt (especially below larger salt structures) is often poor, resulting in uncertainties in sub-salt interpretations. Assessment of well control is based on the presence of wells in the vicinity of the salt structure. Good well control can potentially reduce uncertainties and constrain interpretations. Well control is poor for some structures, where no wells, or only wells in adjacent areas are available. Around structures where an oil or gas field is present, well control is typically good. Nearby wells and associated oil and gas fields are shown in the inventory for all salt structures.

#### 5.2.5. *Isopach Maps*

Regional isopach maps of the study area were generated and analyzed for 7 intervals (see chapter 2.5: Stratigraphy; **Figure 7**). Resulting maps are shown in **appendix 3** and described below.

##### *Zechstein Group (ZE)*

Thickness distributions of the Zechstein Group within the study area are very much heterogeneous. Zechstein salt is accumulated in structures, where thicknesses up to 7 km are reached. Within the DCG, away from salt diapirs and walls Zechstein salt is very thin (10-100m), because salt withdrawal has occurred. In the SG the contrast between thickness of salt in salt structures and in salt withdrawal areas is less extreme than in the DCG. Thickness of ZE within the SG varies between 50-2500m and accumulated in walls and pillows. On the platform areas (ESP, SGP) ZE is thin or absent and more homogenous.

##### *Lower Germanic Trias Group (RB)*

The RB interval has a relatively homogenous thickness throughout the study area. Locally some thickness variation is observed on seismic. Thickness maps suggest some thicker deposits within the DCG, although this is poorly constraint due to a lack of deep well data in this area.

##### *Upper Germanic Trias Group (RN)*

A general thickening of the RN interval appears to occur towards the DCG, although this area is poorly constraint by well data. Locally thickness variations of RN are observed in seismic data. The most prominent thickening within RN occurs in the SE of the study area, where RN thickens towards the eastern DCG boundary. On the platform areas (ESP, SGP), RN is typically thinner than in the graben structures and is absent entirely on most of the ESP.

*Altena Group (AT)*

AT deposits are mostly restricted to the DCG, with local occurrence within the SG. AT typically thickens towards salt structures within the DCG, where sediments accumulated in local mini-basins. A general thickening of AT occurs towards the center of the DCG.

*Schieland Group (SL)*

A general thickening towards the DCG basin center persists. SL deposits are also mostly restricted to the DCG. In the South of the study area the depocenter appears to shift more to the West of the DCG, where in the North it remains in the East of the DCG.

*Rijnland Group (KN)*

KN is mostly absent along the axis of the DCG and locally absent within the SG. KN can be seen thickening onto the SGP in the SE of the study area, but is mostly absent on the ESP.

*Chalk Group (CK)*

CK thins above the DCG and is mostly absent above its axis. CK can be seen thickening locally towards some salt structures, associated with DCG boundary faults, mostly towards the North of the study area. CK thickens onto the SGP towards the East and remains relatively homogenous towards the West, onto the ESP. Development of secondary rim synclines is observed locally (see **Figure 22**).

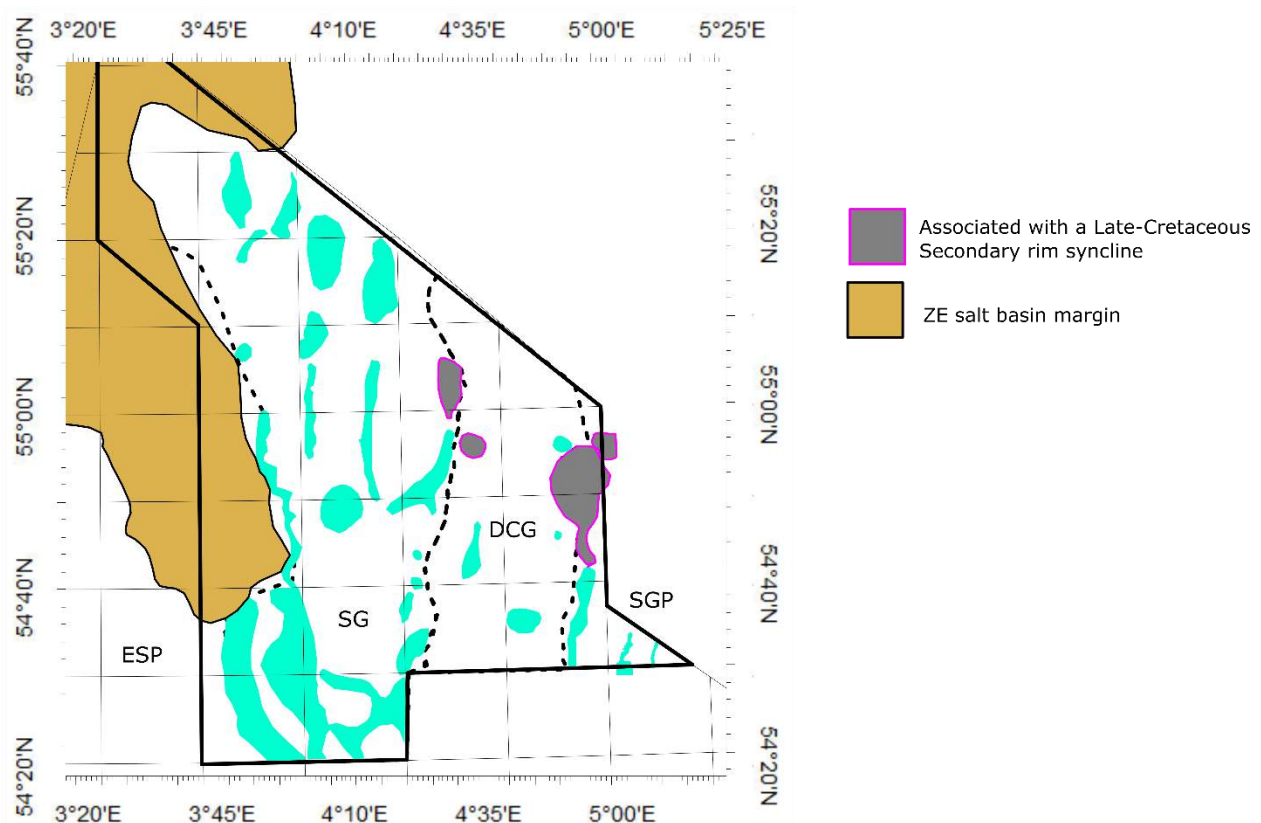


Figure 22: Distribution map of salt structures around which a Late Cretaceous secondary rim syncline is observed.

### 5.3. Interpretation and discussion

Analysis of the salt structure inventory and associated distribution maps, thickness maps and observations from seismic data are integrated in a chronological interpretation below.

#### 5.3.1. *Triassic*

In most of the study area, Early Triassic deposits are unaffected by active syn-depositional tectonic movements. However, thickness relationships suggest an early salt pillowing stage in the North of the SG, where the Lower Germanic Trias Group (RB) thins towards several salt structures (**Figure 20**). Thinning of the RB interval along the western SG boundary and eastern DCG boundary (**Figure 23**) also indicates early, minor pillowing of Zechstein salt and possibly associated fault activity along these faults. The thinning of RB towards salt structures rapidly ceases towards the South. This pillowing might be associated with an early rifting stage, which mainly affected the northern part of the study area. Geluk (2005) describes a rifting stage affecting the Dutch Central Graben area during the Olenekian, which might be responsible for these syn-tectonic relationships. This coincides with observations made by e.g. Dronkert et al. (1989) and Remmelts (1996) of Early Triassic salt movement and observations by Ziegler (1990) of Early Triassic E-W rifting decreasing rapidly towards the South. Slightly thicker RB deposits in the DCG than in the SG (**Appendix 3B**), might suggest an existing pre-Triassic low in the DCG area, while no indications for active, syn-depositional fault movement are observed along the boundary between the DCG and SG.



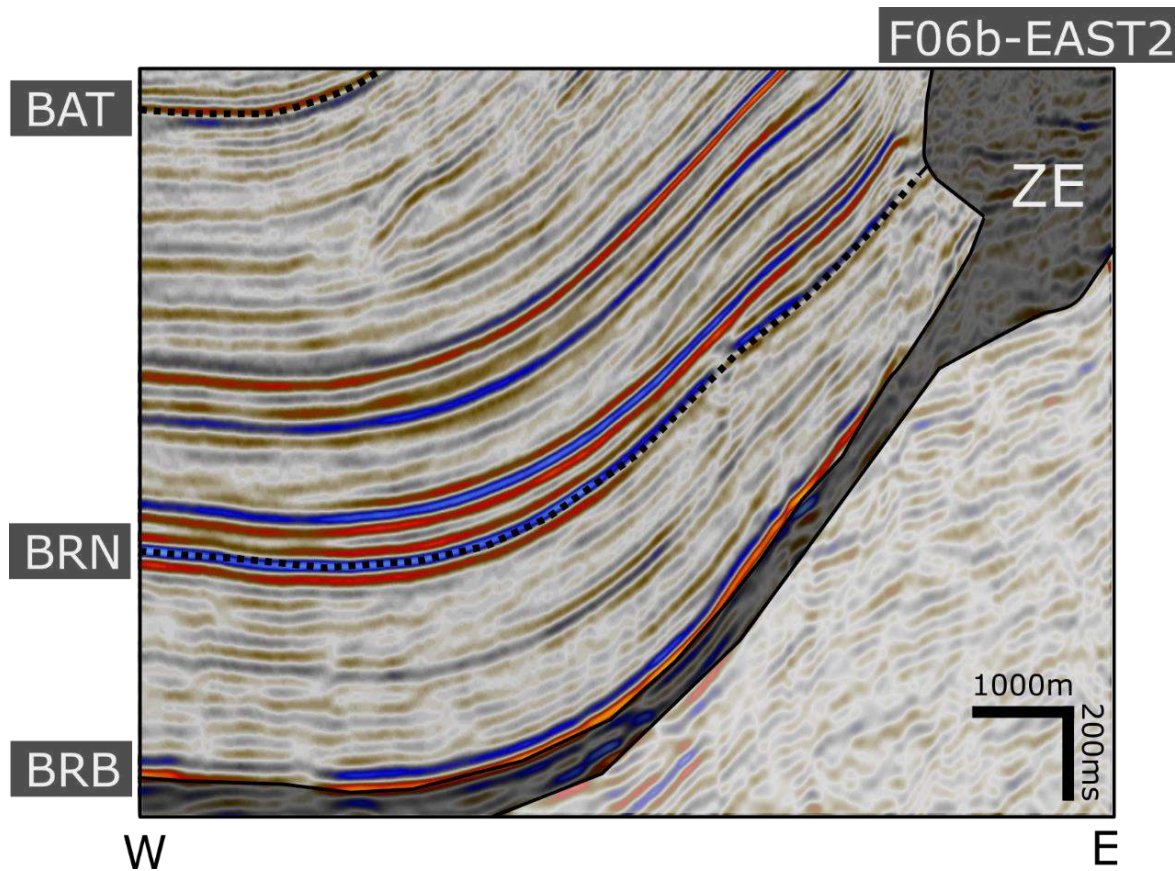


Figure 23: Salt structure Fo6b-EAST2; BRB, BRN and BAT are interpreted. RB interval thins towards the east. (Location of the section is shown in Figure 15; Seismic data courtesy Fugro)

Middle and Late Triassic deposits show large thickness variations throughout the study area. Frequently observed thinning of the RN interval towards salt structures (**Figure 20**) indicates a widespread salt pillowing stage and the first regional onset of salt movements in this area. These salt movements are likely linked to the onset of the Early Kimmerian rifting phase (De Jager, 2007). Thickening of the RN intervals towards salt structures and associated faults are also frequently observed. These varying thickness trends in the RN interval might be explained by a structural style where an interplay of hard-linked, soft-linked and non-linked faults was active. Where sub-salt basement faults failed to penetrate the salt cover, non-linked faulting occurred below the salt cover and presumably reactive salt movement and the formation of salt pillows was the dominant mechanism during the deposition of RN deposits here (**Figure 25A**). Often, however, a wedge-shaped geometry can be observed in RN deposits, where strata shows thickening towards a salt structure. This can be explained by the development of a detachment fault above the salt cover, induced by sub-salt fault movement. This coincides with Triassic salt tectonic mechanisms described in other parts of the North Sea area (de Jager, 2012; Kane et al., 2010; Duffy et al., 2013). This soft-linked faulting would explain the observed depositional thickening of RN, without penetration of sub-Zechstein faults through the Zechstein salt cover occurring (**Figure 25B**).

Salt structure A12-EAST1 is a good example of a geometry where RB is offset and overlying RN deposits thicken towards the salt structure (as becomes evident in **Figure 24**). Since Zechstein salt thickness in the Triassic was likely larger than presently observed (Ten Veen et al., 2012; Remmelts, 1996), it likely occurred in only very few occasions that basement faults succeeded to penetrate the salt cover.

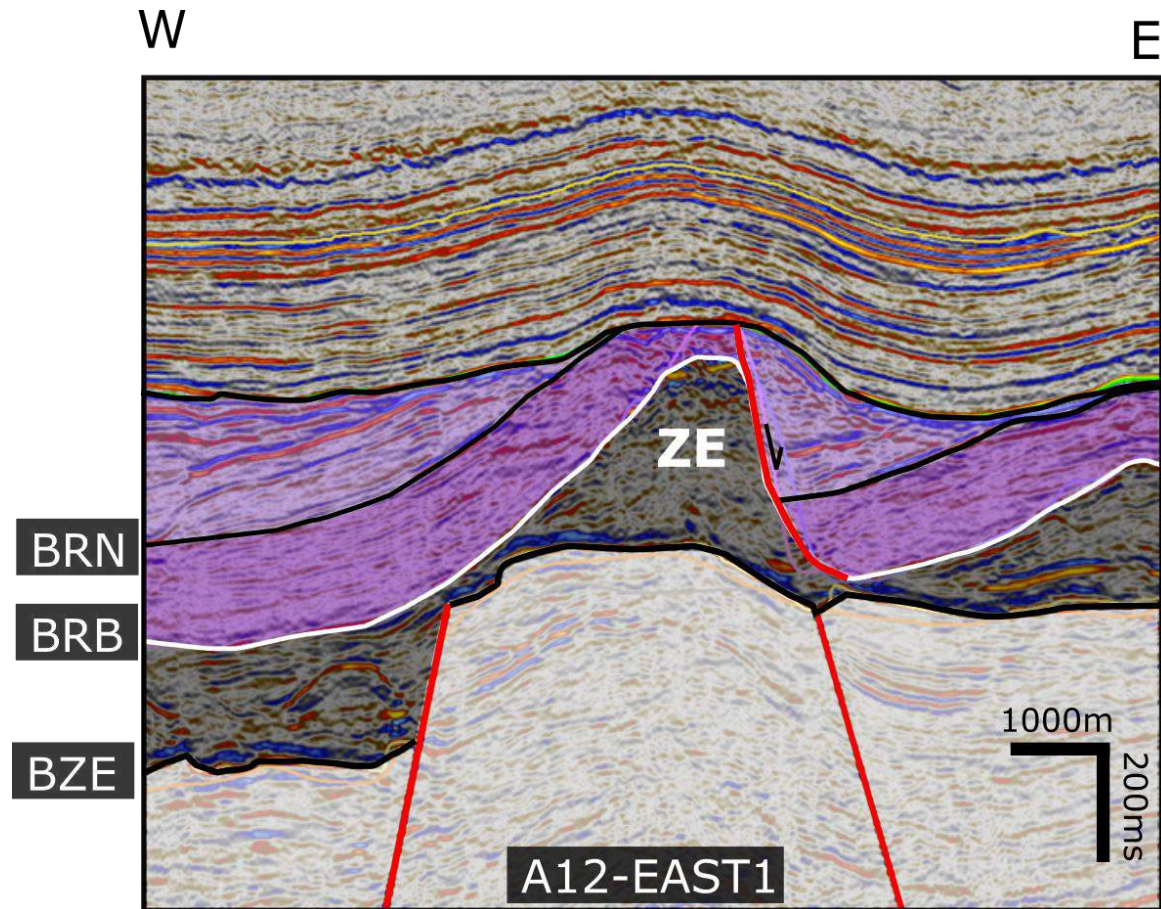


Figure 24: Salt structure A12-EAST1; RB and RN intervals are interpreted above Zechstein salt and a faulted basement. (Section location is shown in **Figure 15**)

At some locations, large offset faults may have succeeded to penetrate the salt cover. Indications for this can be observed at some locations along the DCG boundary faults and within the DCG, where basement faults link directly into Late Triassic strata, offsetting Early Triassic deposits. In this setting significant thickening towards the active hard-linked fault would occur (**Figure 25C**; Kane et al., 2010). This linking, however, may also have occurred during later phase of active faulting, in which reactivation may have occurred. Where in the case of salt controlled deposition, the depositional center would move away from rising salt above a non-linked fault (**Figure 25D**), in the case of fault controlled deposition the depocenter moves towards the fault and associated salt structure (**Figure 25E**). Similar mechanisms are described by Duffy (2013) and Kane et al. (2010) in the Danish and Norwegian part of the Central Graben.

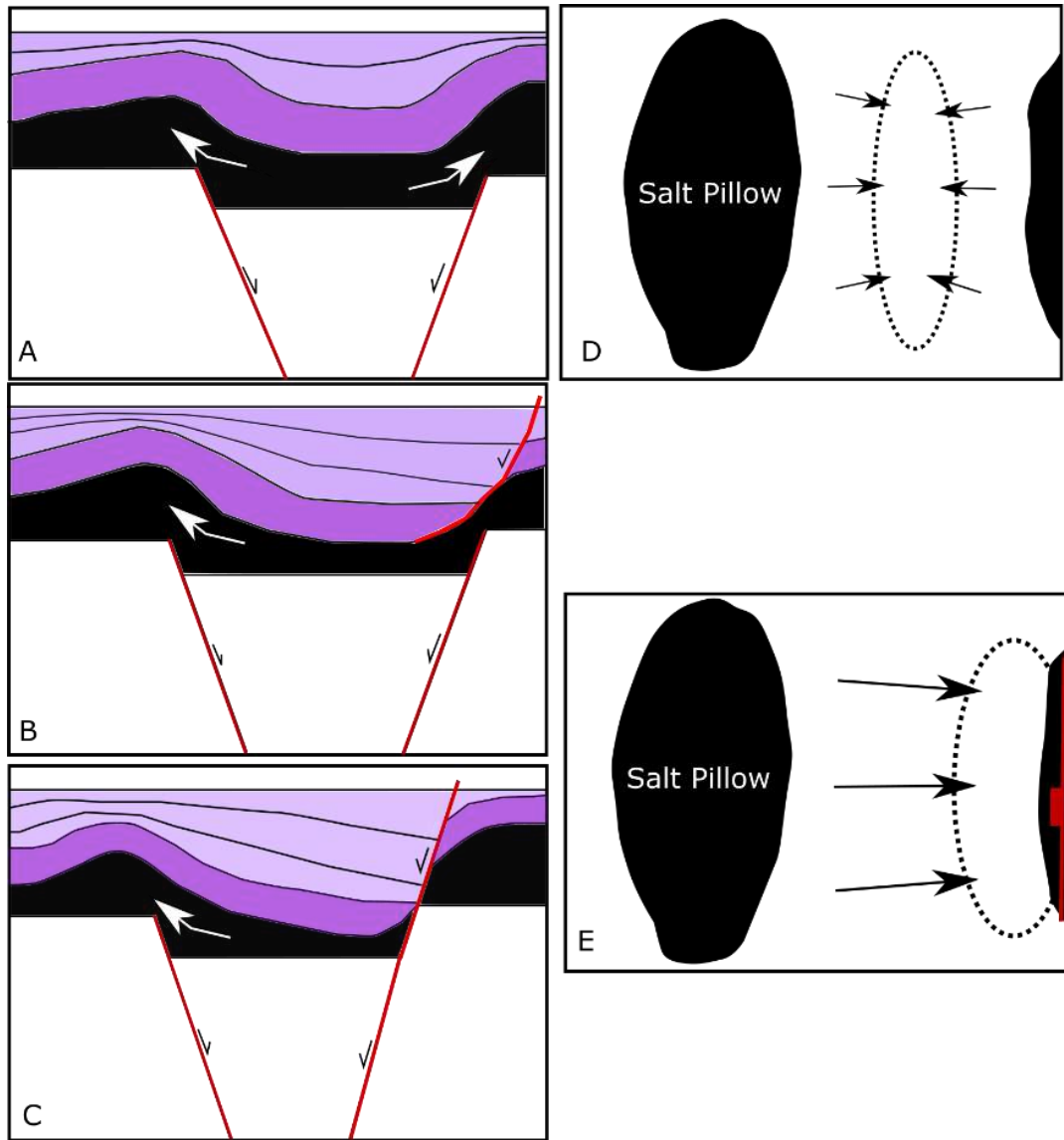


Figure 25: Conceptual drawings showing the relationship between salt geometry and depocenter location: A). Salt-movement controls deposition, deposits thin above salt pillows. B). Thin-skinned faulting induces a thickening of sediments towards the fault, above the salt structure. C). Thick-skinned faulting induces thickening towards the fault. D). Map view: The depocenter moves away from the salt pillow, as shown in A. E). Map view: Depocenter moves towards fault and associated salt pillow, as shown in B and C.



The northern part of the study area contains salt-pillows within the SG (e.g. A12a-EAST<sub>1</sub>, A12-EAST<sub>2</sub>, B13-WEST<sub>1</sub>) that did not develop into piercing salt diapirs or walls. These pillows might be an indication of what salt structures that developed into piercing salt diapirs and walls will have looked like during the Late Triassic. As mentioned by Ten Veen (2012) and Duffy (2013), initial salt thickness is crucial in determining the active structural style in an area. In this case ZE salt thickness in the Triassic will have played a role in the way faulting affected deposition. Although salt thickness is likely to have shown thickening away from the Zechstein salt basin margin (Geluk, 1999; see also **Figure 5**), assumptions about Triassic salt thickness are not straight forward to make, since the SG and DCG have been affected by intense salt migration and the extent of salt erosion and dissolution is unknown here. Despite large uncertainties about salt thickness and imaging uncertainties, it is clear that salt movement during this period has to be seen in the context of the active structural style, rather than an individual process, to account for observed geometries.

Depositional patterns of RN suggest roughly N-S orientated, elongated depocenters, possibly related to active fault movement in combination with the subsequent development of elongated salt pillows. **Figure 26** shows an isopach map of the RN interval, where the elongated shape of the depositional center during this period becomes evident. This depocenter is also visible on a seismic z-line ( $z=-3500\text{ms}$ ) and appears to shift towards the West, moving upwards in the seismic cube. Active rifting during deposition of RN appears to have focused along DCG and SG boundary faults in the South, whereas in the NW of the study area extension appears to have been accommodated over more, smaller offset faults. Especially along the eastern DCG boundary fault, intense thickening of RN strata can be observed. Observations from seismic data combined with the isopach map of the RN interval (**Figure 26**), suggest an elongated depocenter along the eastern DCG boundary fault and a rapid thinning of RN strata towards the West. Shifting of the RN depocenter towards the West might have been caused by an early stage of salt withdrawal during the later part of the Late Triassic. This is also expressed by the local initiation of secondary rim synclines in the upper part of the RN interval. It is often unclear what exactly the balance between salt withdrawal and active faulting was in the creation of accommodation space here, especially within the DCG, where Triassic has been buried below a thick Jurassic sequence (see ).

Although in the DCG, Triassic sediments were deeply buried, in the SG, Triassic sediments remained significantly shallower and have a relatively continuous character away from major faults and salt structures. Aforementioned geometries (**Figure 25**), where thin-skinned tectonics controls depositional patterns, are also observed in Triassic strata within the SG, in the vicinity of major intra-basinal faults and salt structures (e.g. A12-EAST<sub>1</sub>; **Figure 24**). Presumably this structural style was dominant throughout most of the DCG and SG in the Late Triassic. However, due to deep burial and later deformation, present day geometries of Triassic strata within the DCG are different than in the SG.

How Late Triassic faulting affected the platform (ESP, ESH, SGP) areas is uncertain due to widespread erosion and truncation of Triassic sediments, although they are presumed to have been relatively stable. Middle to Late Triassic strata are deeply truncated on the ESP and to a lesser extent on the SGP. Stratigraphic thinning of the RN interval can however be clearly

observed from the DCG onto the SGP, presumably induced by differential movement of the boundary fault during this period.

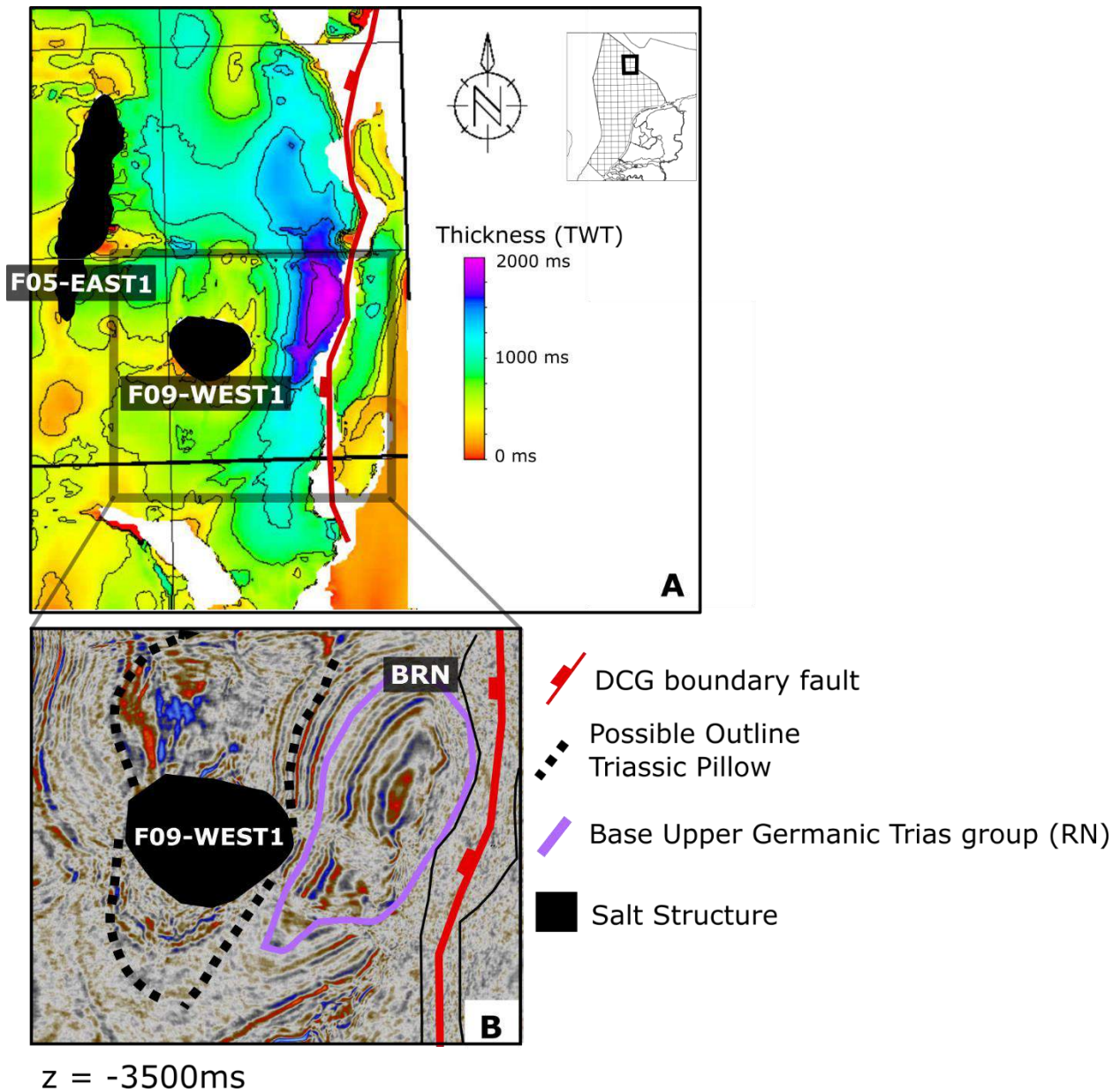


Figure 26: A). Time thickness map of RN (TWT) near the eastern DCG boundary fault and salt structures F05-EAST1 and F09-WEST1.. B). Seismic time-slice at -3333ms from DEF-survey in the same location (F09 block); Seismic data courtesy Fugro.

It is likely that the Zechstein salt was significantly affected by dissolution and erosion, throughout the post-Permian. It is often inferred (e.g. Ten Veen, 2012) that some salt was redeposited during renewed phases of evaporitic deposition (e.g. Röt fm. and Muschelkalk fm.) in the Triassic. Within the Triassic intervals there are indications on seismics of evaporitic bodies within the study area. It is often inconclusive if this is Triassic autochthonous salt or intruded allochthonous Zechstein salt. Poor well control in the study area, prevents further conclusive statements about the origin and composition of these bodies. Rank-Friend and Elders (2004) suggest the role of Triassic salt in Zechstein salt tectonics was mainly providing a weak zone, where Zechstein salt was allowed to intrude. Locally these effects have been seen within the study area (described in appendix 2C). However, the pivotal question if Triassic salt has a generic relationship with underlying Zechstein salt is yet to be answered conclusively, for this area.

### 5.3.2. *Jurassic*

Due to erosion or non-deposition of Jurassic intervals on the Elbow Spit platform and Schill Grund platform and in the Step Graben, not much information is available about the Jurassic development of these areas. In the SG some patches of Jurassic sediments can be observed locally in secondary rim synclines of salt walls (e.g. near salt structures B16F01-WEST1, E09E06E03-EAST1; see Thickness map AT and SL, **Appendix 3D-E**). This is an indication that deposition of Jurassic sediments did occur here and eroded during later times. It is interpreted that there is AT and SL present in these rim synclines, although there is no well data available to back up these observations. **Figure 28** shows salt structure B16F01-EAST1, where Jurassic sediments can be seen in a rim syncline on the eastern flank of the structure and are truncated by the Base of the Lower Cretaceous Rijnland Group (BKN).

The absence of Jurassic sediments on platform areas and in most of the SG also complicates analysis of timing of salt movement. Typically, piercing salt structures in the SG appear to have pierced the overburden after the Triassic, but before the deposition of the Late Cretaceous Chalk Group. Aforementioned secondary rim synclines with Jurassic sediments occurring locally in the SG are an indication for Jurassic piercing of the associated salt structures. Salt structures within the DCG typically became piercing in the Late Triassic to Early Jurassic, whereas structures associated with boundary faults often pierced the overburden in the Late Jurassic or Cretaceous (see **Figure 20** and **Figure 21**).

In the Dutch Central Graben a complete Jurassic succession can be found, where truncation only occurs in the basin center along the post-Jurassic inversion axis (as can be seen in **Figure 35**). Thickness variations of the Jurassic AT and SL intervals in combination with the development of secondary rim synclines adjacent to major salt structures (e.g. F05-EAST1, F09-WEST1; see also **Figure 21**) suggest intense salt withdrawal occurred throughout the Jurassic in the DCG and presumably to a lesser extent in the SG. Jurassic salt presumably migrated towards existing Triassic salt structures. It is likely that the increased sediment loading within the DCG by Jurassic sediments allowed salt withdrawal to occur more intensely than in the SG and platform areas. This was allowed by the continued subsidence of the DCG, which created the accommodation space for these sediments. Development of localized salt withdrawal basins can be seen

throughout the Jurassic in the DCG (for example around salt structures F09-WEST1 and F05-EAST1; shown in **Figure 27**). The location of these local basins were possibly controlled by: 1). Locations of Triassic depocenters and associated salt structures 2). Localized subsidence of fault blocks 3). Local salt withdrawal in throughout Jurassic. The exact balance between these mechanisms is unclear. No clear indications are present in the DCG of active Jurassic E-W rifting in the supra-salt overburden (e.g. Wijker, 2014), so vertical movement of basement fault blocks along faults, was likely decoupled from the overburden and possibly accommodated by the intense movement of Zechstein salt that took place during this period.

Where salt structures in the DCG were most likely more elongated in most of the Triassic (**Figure 26**), in some cases, they developed as point-sourced structures during the Late Triassic to Late Jurassic. The precise mechanism, responsible for this development is unclear. Observations by Wijker (2014, EBN) suggest WNW-ESE running faults were active in the Late Jurassic and have been observed intersecting the dominant N-S fault trend of the DCG near major salt structures. These fault trends are roughly parallel to the Dan (WNW-ESE) and Thor (E-W) transverse zones, which occur further to the North of the study area. Also, a regional thickening of Jurassic sediments has been observed towards the North in the DCG. Differential thickness of Jurassic sediments along a N-S axis and a structuration of the basin by E-W running faults might have contributed to the process of point-sourced salt structure formation, although no other clear indications for a general N-S orientated extensional regime have been observed within the DCG in this study. This would concur with observations by Remmelts (1996) that point-sourced structures preferably form where fault trends interfere. The alternating movements of two fault systems could be the mechanism responsible for this. Additionally, this might explain the presence of elongated salt walls like in the SG, if more homogenous deposition and a more consistent fault trend (NNW-SSE) is assumed there during the Jurassic, since a N-S differential loading would not have occurred. However, the apparent contrast between deposited thicknesses of Jurassic strata in the SG (little to no Jurassic sediments observed in the SG) and DCG and the associated contrast between fault off-sets (which are greater towards the DCG), likely also play an important role in the generation of different types of salt structures (as observed in **Figure 17**). As mentioned, original thickness of Jurassic strata in the SG is highly uncertain. The fact that local Jurassic strata in rim synclines in the SG is thinner than the same intervals in the DCG (**Figure 28**) and observed thinning of Jurassic strata in the DCG towards the West (e.g. **Figure 35**), is reason to suspect a contrast in original thickness of Jurassic sediments between the SG and DCG.

Thickness and distribution of the AT Group, which quickly increases in thickness from the DCG basin margin towards the basin center, suggests strong relative subsidence of the DCG with respect to the SG and surrounding platforms throughout the Jurassic (See AT thickness map, **appendix 3D**). This likely is the result of continued subsidence in the DCG, where surrounding areas experienced doming in the Middle to Late Jurassic (De Jager, 2007), which coincides with observations in burial data (**Figure 39**). **Figure 20** shows stratigraphic thinning occurs in the Jurassic towards the salt structures associated with the DCG boundary faults. There are no conclusive indications however that this thinning is associated primarily with these salt structures, it seems more likely a decrease in accommodation space towards the basin margin was responsible. **Figure 21** shows that Jurassic strata thickens towards salt structures within the DCG. In this case it appears the localization of the depocenter was controlled by salt withdrawal for



most of the Jurassic. Especially during deposition of AT, a strong control on sediment distribution was induced by salt withdrawal. During the deposition of SL, active rifting affecting basement blocks and basin subsidence may have been more important controls. This can be seen in the distribution of sediment thickness of AT and SL. AT deposits are more localized around salt structures, where the thickness distributions of SL suggests a more general thickening of this interval towards the basin center of the DCG (see also thickness maps of AT and SL; **Appendix 3D-E**). Nevertheless it is evident that deposition in localized salt withdrawal basins persisted in the Late Jurassic (as illustrated in **Figure 27**). In the southern part of the study area, the depocenter of the SL intervals shows a marked shift towards the West in the upper part of the SL interval. This shift may be associated with a shift from salt controlled deposition around salt structures, to depositional patterns controlled by active rifting and basement block subsidence.

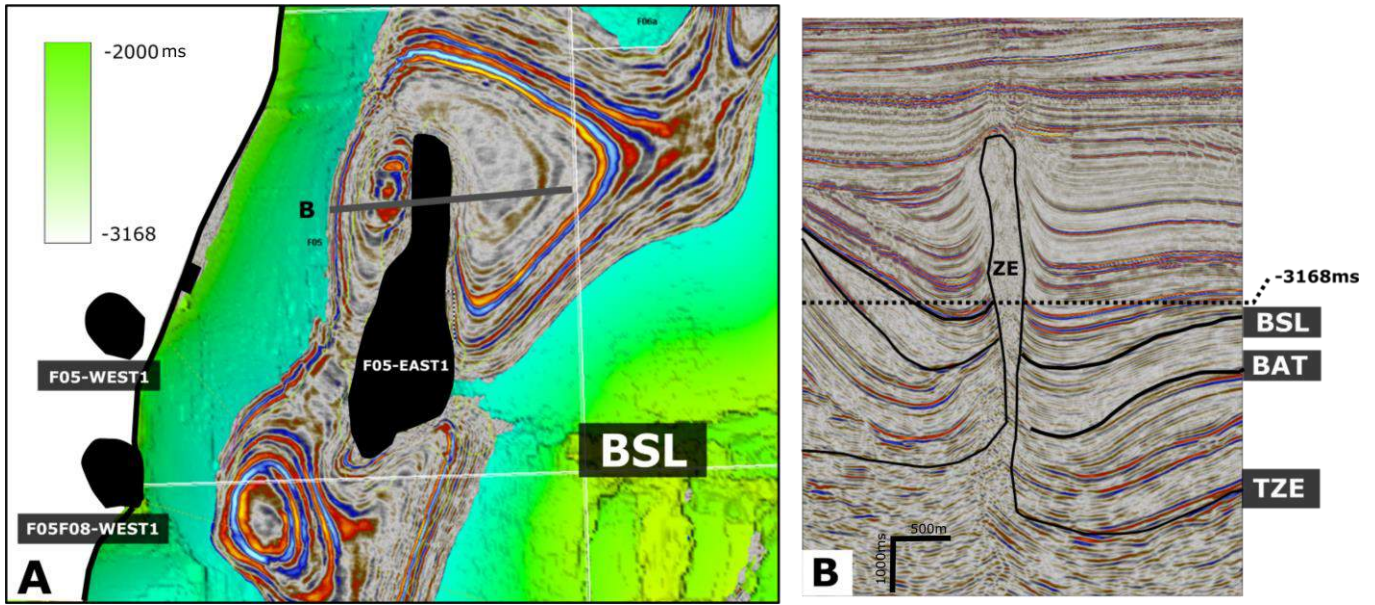


Figure 27: A). Jurassic depocenters around the salt structure F05-EAST1; A seismic Z-line is shown at -3168ms together with the Base Schieland Group (BSL) TWT map; B). Seismic section with relevant intervals indicated; the location of the section (B) is shown in figure A.

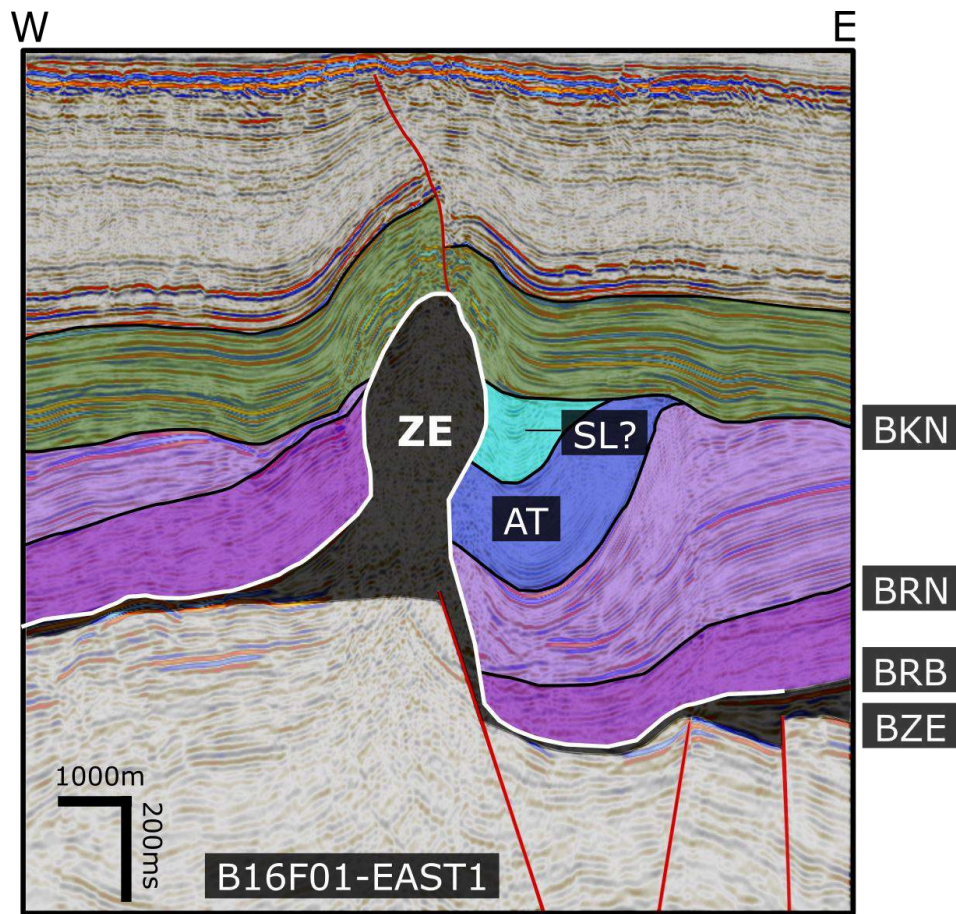


Figure 28: An interpreted seismic section of salt structure B16F01-EAST1 and surrounding strata, above a structured basement; Jurassic sediments can be observed in secondary rim synclines, east of the structure (Location of the section is shown in Figure 15; Seismic data courtesy Fugro)

### 5.3.3. *Cretaceous and Tertiary*

Lower Cretaceous sediments of the Rijnland Group (KN) have been eroded or were not deposited in large parts of the study area (See isopach map of KN, Appendix 3F). Presumably active rifting ceased during this period and KN deposits overlie Jurassic or younger deposits unconformably, indicating a phase of erosion. KN was deposited relatively homogeneously, although it was accompanied by some continued subsidence of Jurassic depocenters. Deposition of the Late Cretaceous Chalk Group was accompanied by a major inversion pulse in the Campanian and ended with a phase of inversion in the Danian (van der Molen, 2005). Subsidence during this period shifted from localized subsidence of graben structures, to more regional subsidence (van Wijhe, 1987). Effects of the Campanian inversion manifest themselves in various ways in the Dutch Central Graben. The presence of Zechstein salt played an important role in the way inversion was accommodated. Presumably the inversion axis runs roughly N-S throughout the DCG. Minor effects of inversion can be observed East of the eastern DCG boundary fault, where reversed faults push up strata within the CK interval. It is likely that these were preexisting faults, inverted during the Late Cretaceous. A major unconformity covers these faults and younger strata seem less affected by the faults. This is an indication that these faults were mostly active before the deposition of the upper part of the Chalk interval. It therefore appears these reversed faults are mainly related to the Campanian pulse of inversion (see also Huijgen, 2014). This becomes evident since, while strata below this unconformity are pushed upwards significantly, younger strata are relatively unaffected. Observations by Huijgen (2014, EBN) suggest that the SG was a high during the Campanian, which explains thin CK deposits. The Campanian unconformity can be seen running close to top CK in this area (**Figure 29**), which is consistent with these observations. Later erosion of post-Campanian CK may have also attributed to a thin CK interval in the SG. The DCG was a low in pre-Campanian times, but due to inversion it became a high from which most of the pre-Campanian CK deposits were eroded (De Jager, 2007). Little to no individual inversion features can be observed within the DCG domain itself. Inversion possibly manifested itself in the DCG by a general uplift of the pre-Campanian strata along a detachment horizon of Zechstein salt (De Jager, 2007), although the exact mechanism is uncertain here. This might also explain the tilting and erosion of Late Jurassic and Early Cretaceous sediments along the inversion axis within the DCG.



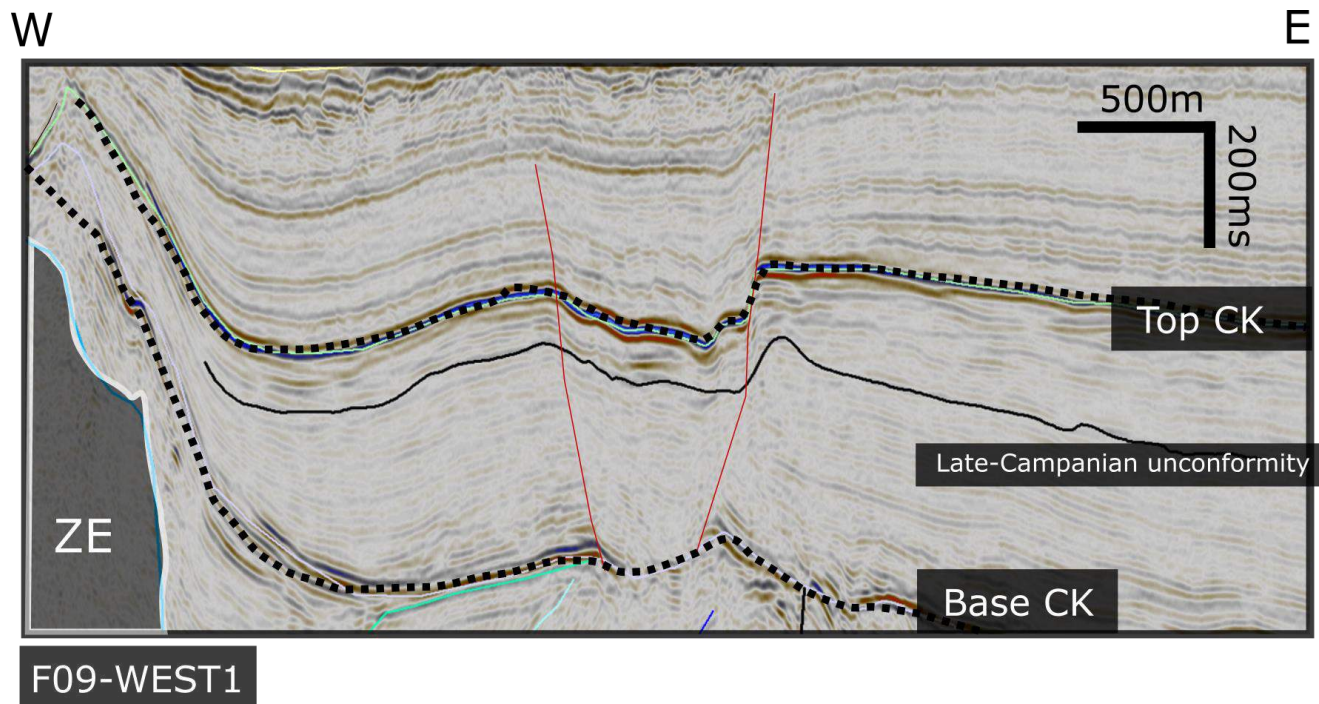


Figure 29: Interpretation of Late-Campanian unconformity East of Fo9-WEST1 (after Huijgen, 2014; Section location is shown in **Figure 15**). Note that the Late-Campanian unconformity runs close to Top CK in this area (Seismic data courtesy Fugro).

Sediments of the Late Cretaceous CK Group show stratigraphic thinning over the crest of most salt diapirs and walls (e.g. **Figure 29**) within the study area. This is indication that these structures continued to grow vertically, or were reactivated during the Late Cretaceous. Presence of secondary rim synclines, which show significant thickening of Late Cretaceous strata is observed around some salt structures (see also **Figure 22**). This is an indication of a renewed phase of salt withdrawal around these structures and in some cases, active piercing of salt (e.g. salt structures B-17-SOUTH<sub>1</sub>, Fo6b-EAST<sub>1</sub>, Fo3-EAST<sub>2</sub> and Fo2-NORTH<sub>2</sub>). This renewed salt movement was likely linked to inversion phases and (re-)activation of the DCG boundary faults, although it is unclear exactly what physical mechanism was responsible.

As an example, in salt structure B17-SOUTH<sub>1</sub> a late piercing stage of the salt diapir is evident (**Figure 30**). Where during the Jurassic a depocenter develops away from the salt structure, in the Cretaceous there is a marked shift of depocenter towards the west and towards the B17-SOUTH<sub>1</sub> salt structure. A secondary rim syncline starts to develop in the Late Cretaceous and this remains the main depocenter throughout most of the Late Cretaceous and Tertiary. This apparent piercing is most likely linked to active inversion within the DCG. **Figure 30** shows that the shift of depocenter can be observed on seismic section as well as on seismic z-lines ( $z = -2792\text{ms}$  and  $z = -3816\text{ms}$ ) and that this shift is seen in thickness distributions of Jurassic and Cretaceous sediments, as expected (**Figure 30D-E**). Note also that the depocenter focusses just north of the section in the Cretaceous (**Figure 30D-E**), where presumably most salt was allowed to migrate.

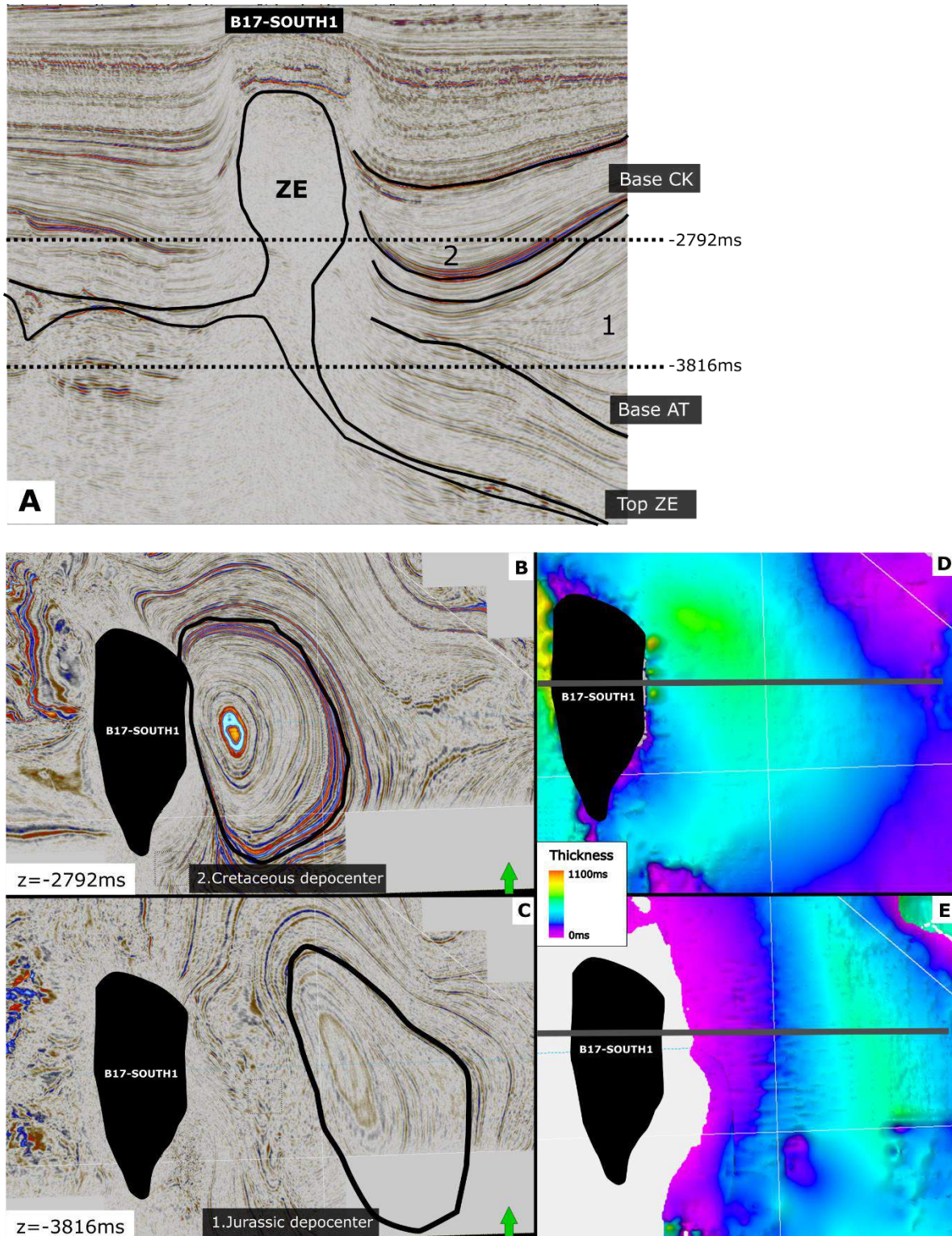


Figure 30: A). Seismic section, with relevant intervals interpreted. 1= Jurassic depocenter 2= Cretaceous depocenter B). Seismic Z-line @ -2792ms; Cretaceous depocenter is indicated (black line) C). Seismic Z-line @ -3816ms; Jurassic depocenter (black line) and shifting depocenter (red arrow) are indicated D). Thickness map in TWT of the Cretaceous Chalk Group (CK) E). Thickness map in TWT of the Jurassic Alتنا Group (AT).



#### 5.3.4. *Mechanisms of salt tectonics in the study area*

Throughout post-Permian times several stages of salt tectonics appear to have occurred in the northern Dutch offshore. These stages overlap on some aspects with the traditional Trusheim (1960) salt structure growth model. A pillowing phase is inferred, which can be subdivided in at least two phases of salt movement. A marked difference with the pillowing stage in the Trusheim model is the role of faulting in the structural and sedimentary development of the area. E.g. detached, thin-skinned faulting was likely a dominant mechanism in determining depocenters during the Late Triassic phase of salt movement (see also Duffy, 2013; De Jager 2012). This mechanism could have been an important control on the location of salt pillows as a reaction on differential accommodation space, generated by aforementioned faults. In turn these detached, Late Triassic faults almost exclusively occur above major basement faults, although sub-salt and supra-salt faults rarely link up. The consequent effects of extensional basement fault movement, detached supra-salt faulting and resulting differential loading were likely the most important controls on the location of initial salt pillows. This process results in accumulation of salt on structural highs adjacent to major faults, as differential sediment loading induces lateral salt movement, away from the structurally controlled depocenter (**Figure 25B, C**). This configuration is observed in the northern Step Graben (**Figure 24**) and indications for similar mechanisms are observed throughout the study area. Although thinning does occur above salt pillows and a depocenter develops away from the salt structures (**Figure 16A, D**), like in the Trusheim model. However, this should be considered as a consequence of the active structural style rather than an isolated process. Analogous to the Trusheim model, a stage of salt piercing occurs in some salt structures in the SG and DCG. This is typically expressed as a shift of depocenter towards major piercing salt structures, forming a secondary rim syncline (**Figure 8**). Late stages of renewed salt movement induce deformation in the younger, overlying strata and cause fracturing. Where salt supply is exhausted, a collapse graben can develop above the structure. During this stage the depocenter moves away from the salt structure again (see also Trusheim, 1960; **Figure 8**).

It can be concluded that the classic stages of salt tectonics (Trusheim, 1960; **Figure 8**) can be recognized throughout the study area, but have to be seen in the context of periods of active tectonism as postulated by Vendeville (2002).

#### 5.3.5. *Main Uncertainties*

In the analysis of salt tectonics in this area, the main uncertainties that have to be taken into account are: 1). Poor seismic imaging locally prevents detailed interpretation of stratigraphic and structural geometries, especially below and adjacent to salt structures and in the deeper parts of the DCG. 2). Large areas of the study area have limited well control, especially in the deeper parts of the DCG. 3). The time-depth conversion model is poorly constrained, as a results of limited well control. 4). Local erosion or non-deposition of stratigraphic intervals, prevents direct interpretation in major parts of the study area. 5). Initial depositional salt thickness and salt thickness throughout the post-Permian intervals is very uncertain, due to intense salt movement and possibly salt dissolution or erosion. 6). Interpretations of horizons and faults in seismic data, are locally poorly constrained or lack detail.



## 6. Structural Restoration

### 6.1. Methods: From geology to model

#### 6.1.1. Approach

In order to gain more insight in the role of salt tectonics in the northern Dutch offshore and implications for its structural development in general, a regional cross section was studied in detail. The main aim of studying this cross section is to be able to perform a structural restoration, illustrating and testing hypotheses for the main stages of deformation in this area. The focus of this restoration will be on the role of movement of Permian Zechstein salt, with the scope of this study in mind. However, such a restoration cannot be done without taking into account the full structural framework and development of the area.

Historically structural restoration has been applied as a powerful tool to gain insights in the geological development of a deformed area. Restoration of salt related deformation was initially attempted in fold-and-thrust belts, where salt typically acts as a basal or intermediate detachment (e.g. Pakistan: Banks and Warburton, 1986; Jura mountains, Bitterli, 1990). However, cross-sections in extensional and diapiric terranes proved more difficult to restore, due to mobility of salt and its changing thickness through time (Rowan and Ratliff, 2012). A paper on the development of normal faults above allochthonous salt in the Gulf of Mexico by Worrall and Snelson (1990) can be considered a pioneering paper in this respect. Vertical simple shear and rigid body rotation was applied for the first time in this context here. Since the 1990s structural restoration involving salt has seen widespread application, for example to quantify process like extension or contraction, salt flow, sediment accumulations (Hossack, 1995), to estimate palaeobathymetry (Rowan, 1996) and produce evolving geometric frameworks for analysis of hydrocarbon migration (McBride et al., 1998).

Rowan and Ratliff (2012) propose some general guidelines for structural restoration, in which salt is involved. They state two important questions which need to be answered, before an effective restoration can be done: 1). What is the purpose of the restoration? 2). Can the desired result be accomplished given the limitations of the restoration in question? In this case it has to be noted that the desired result of this restoration is to give a better idea of the regional structural development of the basin with some quantitative constraints. This is done with the purpose of this restoration in mind: providing a framework for discussion on structural and salt tectonic development in the northern Dutch offshore.

#### 6.1.2. Seismic interpretation and depth conversion

A 2D seismic section was chosen as a starting point for structural restoration (Location shown in **Figure 15**). The section was chosen based on the following criteria: 1). The section transects all the main structural elements in the area, as it transects the Dutch Central Graben (DCG) and Step

Graben (SG), and runs through the Elbow Spit Platform (ESP in the west and the Schill Grund Platform (SGP) in the east. Since the ESP and SGP are assumed to have been relatively stable throughout their geological history, they serve as a structural reference to the movements within the graben structures. 2). The section runs roughly perpendicular to the dominant structural grain of the N-S running DCG and NW-SE running SG and their associated faults. This enables the restoration to include the most important tectonic movements in a 2D section. 3). With the scope of this study in mind, the section was chosen transecting five of the salt structures from the salt structure inventory (**Appendix 2**): Eo9Eo6Eo3-EAST<sub>1</sub>, Fo5Fo8-WEST<sub>1</sub>, Fo9-WEST<sub>1</sub>, Go7-WEST<sub>1</sub> and Go7-EAST<sub>1</sub>. 4). The section was chosen within the extent of the DEF 3D seismic dataset. Although the structural restoration is performed in 2D, this ensures high and consistent data quality and the possibility to constrain observations and interpretations in 3 dimensions in areas adjacent to the 2D section.

In the seismic section, stratigraphic intervals (**Figure 34**) and the most relevant faults are interpreted. Basement faults are an important aspect in the structural restoration and are the main control for tectonic movements in the basin. However, basement faults within the graben structures are poorly imaged, due to their depth and overlying Zechstein salt. In order to better constrain occurrence of basement faults, seismic lines parallel to the section were assessed. Where interpretation of basement faults was difficult due to poor data quality, they were interpreted to fit the restoration model and based on expected geometries in an interior graben system.

Due to decreasing seismic resolution, the uncertainty in horizons and fault interpretation increases with greater depth and in proximity to salt structures. The location of horizons is constrained by available existing interpretations (EBN, TNO), well data and seismic characterization. Especially interpretations of Triassic intervals (RB, RN) and Base Zechstein are difficult to constrain. Well control in this area is poor for the deep parts of the DCG, while most wells that are present only penetrate the shallower parts of the succession (**Figure 31**).

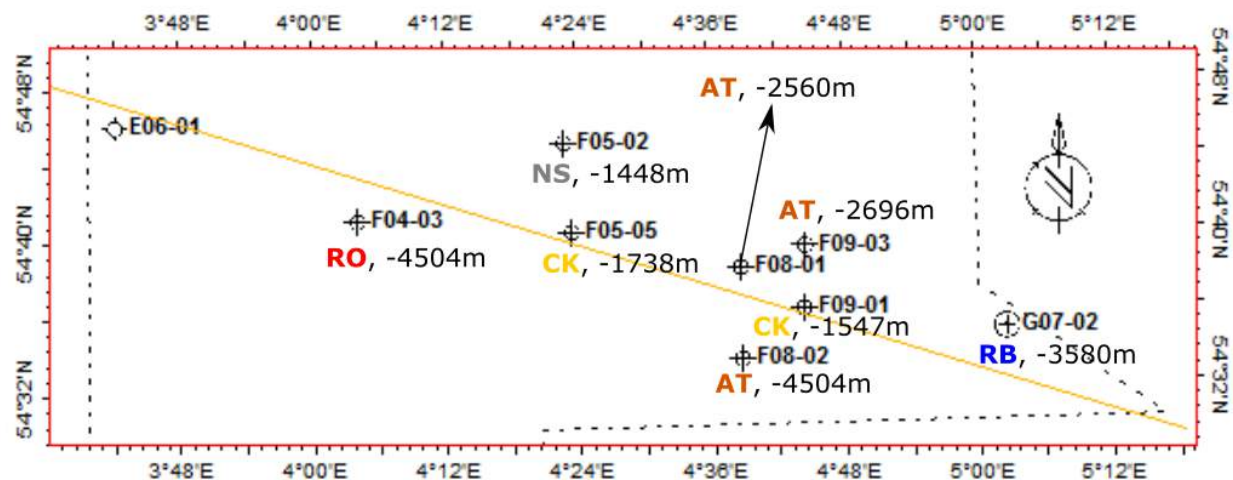


Figure 31: Wells in the vicinity of the restored section; Well name, deepest penetrated stratigraphic interval and final TVD of the well are plotted. NS= North Sea Group, CK= Chalk Group, AT=Altena Group, RB= Lower Germanic Trias Group, RO= Rotliegend Group. Location of this section is shown in **Figure 15**.

Interpretations of horizons and faults were done on time seismic data and were subsequently depth converted. The time-depth conversion was based on a regional time-depth conversion model Velmod (v2.0) made by TNO (Van Dalfsen et al., 2007). For all post-Permian intervals a  $V = V_o * k$  function was applied, where:  $V$  = Velocity,  $V_o$  = Interface velocity,  $k$  = Compaction factor. The  $k$ -values are based on linear regressions using  $V_{int} - Z_{mid}$  method (Robein, 2003; Van Dalfsen et al., 2007).

The  $k$ -values and  $V_o$ -values from this model were assigned to the interpreted intervals in the cross section and the interpreted horizons and faults were subsequently converted to depth. It has been noted that the values used for this time-depth conversion are poorly constrained for the deep parts of the basin, again due to a lack of deep well control. Therefore the  $k$ -values used are likely less appropriate for the deepest parts of the DCG. This could lead to significantly exaggerated depths in the deep part of the DCG.

### 6.1.3. Restoration model input and workflow

The structural restoration has been done using the MOVE© software of Midland Valley Exploration©. A 2D model was created based on the depth-converted interpretations (based on the section shown in **Figure 35**). In order to go from the depth converted interpretations to a restoration model, some adjustments have to be made. All interpreted horizons have to be geometrically consistent, without leaving gaps in the model. Small scale structures and secondary faults are disregarded if they do not have a significant impact or added value for the restoration model. Basement faults are simplified to mostly straight lines.

In order to appropriately model deformation and decompaction of rocks, rock properties were assigned to every interval of the model. For every interval the following properties were defined: 1). Initial porosity 2). Decompaction factor 3). Compaction curve 4). Density. These parameters were based on lithological information from the Terschelling basin, which is to the south of the study area (Verweij, 2009) and Cleaverbank Platform, which is to the Southwest of the study area (Fattah, 2012). Using Petromod© software rock properties were then calculated for all model intervals, using the standardized lithologies defined in **Table 2**.

<b>Lithology</b>	<b>Initial porosity</b>	<b>Decompaction factor (km<sup>-1</sup>)</b>	<b>Density (kg/m<sup>3</sup>)</b>
<i>Sandstone</i>	0.49	0.27	2650
<i>Shale</i>	0.63	0.51	2720
<i>Chalk</i>	0.70	0.71	2200
<i>Salt</i>	0.00	0.00	2200
<i>Marl</i>	0.50	0.50	2700

Table 2: Standardized rock properties for all relevant rock types.

For all post-Permian intervals a Sclater-Christie compaction curve was applied (Sclater and Christie, 1980). Salt is assumed to be incompressible and assigned a decompaction value of 0. A Sclater-Christie decompaction curve assumes that porosity decreases with increasing depth (Compaction) and can be represented by:

$$f = f_o(e^{-cy})$$

Where:

$f$  = Present-day porosity at depth

$f_o$  = Porosity at the surface

$c$  = Porosity-depth coefficient ( $\text{km}^{-1}$ )

$y$  = depth (m)

In the process of restoration, intervals were backstripped, moving from young to older intervals. As a response the underlying rocks decompact and the section is adjusted isostatically. Airy isostasy was applied here, which assumes that an essentially brittle crust is supported and allowed to move on a fluid layer. For this purpose the density of the underlying mantle rocks in the North Sea area was estimated to be  $3200 \text{ kg/m}^3$  (internal information TNO, 2015).

After every backstripping step, the entire section is unfolded to a datum ( $z=0$ ). Palaeo-depositional surfaces that deviate from this datum are not considered in this restoration (e.g. palaeo water depth). Including this would not significantly impact the restoration, considering the large vertical extent of the section. The simple shear algorithm was applied here, with a shear angle of 90 degrees (vertical simple shear). Where relevant, movement along faults were modelled. This was done using the simple shear algorithm, also using a shear angle of 90 degrees (**Figure 32**). Based on basin modelling studies (internal information TNO, 2015) the total post-Permian extension ratio in the DCG area is estimated to be around 1.3. This means that the present day section is extended by 30% compared to its original length in the Early Triassic. The extension and compression of the section throughout the post-Zechstein has been based on proximal well data and relevant literature (e.g. Verweij, 2009; Fattah, 2012). Due to the scale and complexity of the model, realistic values for extension and compression are not obtained by unfolding and fault restoration only. Therefore the section has been adjusted as a whole to match available extension data. Note therefore that this extension and compression of the section mainly serves to indicate phases of extension and compression in the geological history of the model.

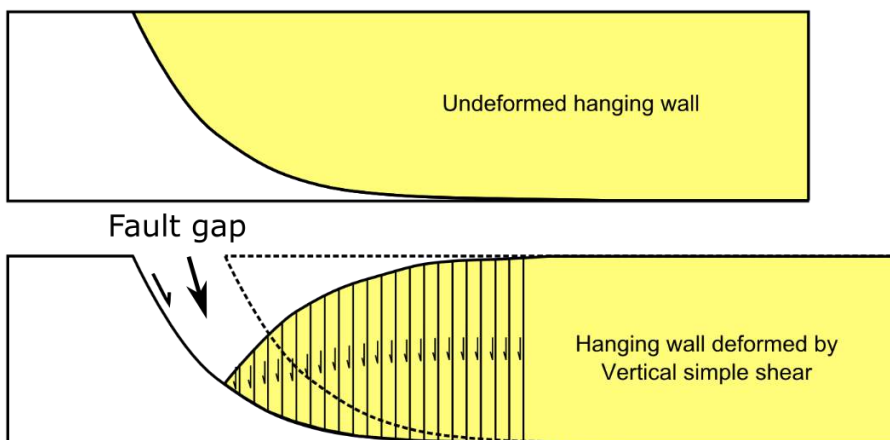


Figure 32: Illustration of vertical simple shear in fault movements (modified from Dula, 1991)

The Zechstein salt layer is treated as an incompressible layer in this model. The software, however, does not take into account the effects of salt flow and lateral redistribution of salt. This aspect of the restoration is left to manual interpretation after every backstripping step. As a result, configurations of Zechstein salt at every restoration step are the result of interpretative restoration of salt flow, following generally accepted principles of salt tectonics (e.g. Vendeville and Jackson, 1992; Vendeville, 2002; Hudec, 2007), constrained by geometries of adjacent stratigraphic intervals. Another reason why the presence of Zechstein salt adds to the uncertainty in the model, is its ability to flow in and out of the 2D section plane. This means the total area of the Zechstein salt layer, as represented in the 2D section, will increase as lateral salt flow is restored to its original position. It is outside of the scope of this study to quantify this out-of-plane redistribution of salt. Ten Veen (2012) performed a quantitative smoothing of the Zechstein salt in the Dutch subsurface, which resulted in **Figure 33**. This smoothing, however, does not take into account the effect of dissolution and erosion of salt. It is likely that additional loss of salt volume occurred due to dissolution and erosion of salt, when salt was at or close to the surface. Although it remains a topic of debate, dissolution of up to 50% of original salt volume is suggested in literature (Hossack, 1995). This would mean salt thickness in **Figure 33** could be multiplied by 2 (which would locally result in 1800m of salt). Occurrence of dissolution and erosion of salt is likely in this area, especially since models from this study suggest salt was at the surface at several locations in different moments in time. Again, in this study the restoration of these volumes of salt is approached qualitatively, and are constrained by stratigraphic and structural geometries within the section, but with observations from previous studies in mind (e.g. Ten Veen, 2012; Hossack, 1995). **Appendix 4** shows the full workflow that was applied in the restoration, within the MOVE software.

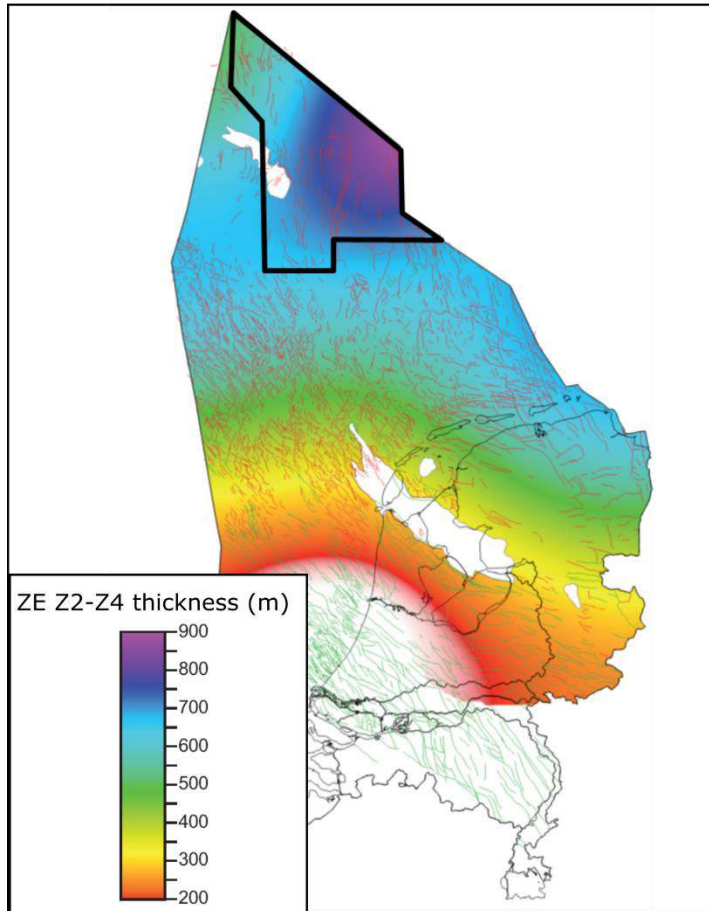


Figure 33: Thickness distribution of original ZE salt thickness ( $Z_2$ ,  $Z_3$  and  $Z_4$  cycles) based on smoothing restoration (Ten Veen, 2012). Note that salt dissolution and erosion, which could be as much as 50% of the original salt volume, is not taken into account here and this map only shows the result of smoothing of existing salt volume.



## 6.2. Results

### 6.2.1. Seismic interpretation and stratigraphy

**Figure 34** shows the twelve (12) Stratigraphic intervals that were interpreted in the seismic section shown in **Figure 35** (see **Figure 15** for the location of the section). Based on the lithologies defined for every interval, a decompaction factor was calculated for these intervals (see **Table 2** for standard values for every lithology). This decompaction factor controls the degree of decompaction that occurs for these intervals when overlying layers are backstripped.

	Horizon	Lithology	Age	Interval	2DMOVE Model Lithology	Decompaction Factor ( $\text{km}^{-1}$ )
Tertiary	Surface		<b>0 Ma</b>			
	MMU	North Sea Supergroup (NS)			50% Sand, 50% Shale	0.39
Cretaceous	BNS		<b>60 Ma</b>			
	CK1	Chalk Group (CK)			100% Chalk	0.71
	BCK		<b>97 Ma</b>			
	BKN	Rijnland Group (KN)			25% Sand, 50% Shale 25% Marl	0.45
Jurassic	SL1	Schieland Group (SL)			50% Sand, 50%Shale	0.39
	BSL		<b>155 Ma</b>			
	BAT	Altena Group (AT)			25% Sand, 50% Shale 25% Marl	0.45
	RN1	Upper Germanic Trias Group (RN)			25% Sand, 50% Shale 25% Marl	0.45
Triassic	BRN		<b>241 Ma</b>			
	BRB	Lower Germanic Trias Group (RB)			70% Sand, 30%Shale	0.34
	BZE	Zechstein Group (ZE)			100% Salt	0.0
Palaeozoic	BZE		<b>258 Ma</b>			
		Pre-Zechstein Basement (BSM)			-	0.0

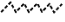

 Local unconformity  
 Regional unconformity

Figure 34: Restoration model stratigraphy including lithologies and decompaction factors:

The pre-Zechstein stratigraphy was not taken into account and is regarded as a rigid, incompressible basement. This is a simplification, since it is known clastics and carbonates are present in the pre-Zechstein succession, which have a higher decompaction factor than 0. In reality, pre-Zechstein sediments will likely decompact significantly when restored to the Triassic configuration in the basin, especially within the DCG and to a lesser extent in the SG and on the platform areas.

In some aspects the post-Permian stratigraphy shown in **Figure 34** deviates from the regional stratigraphy, presented in chapter 2.5 (Stratigraphy). The Upper Germanic Trias Group (RN) is divided in two intervals in this interpretation (**RNo** and **RN1**). The horizon dividing these intervals marks a shift of depocenter and locally represents a downlapping surface (as indicated in **Figure 41**). The Schieland Group (SL) is divided in two intervals (**SLo** and **SL1**). The horizon separating these intervals represents a shift in depocenter within the SL interval. These horizons are based on observations in seismic data and are not constraint by well data. This results in the twelve (12) intervals, which are shown in **Figure 34**.

The intervals interpreted in **Figure 35**, are separated by several unconformities. The base of the Schieland Group (**BSL**) is mostly conformable within the Dutch Central Graben (see also **Figure 35**). This horizon represents the onset of a period of erosion and non-deposition, which induced deep truncation on the platform and marginal areas during the Middle to Early Cretaceous (also mentioned by e.g. Ziegler, 1991). The base of the Lower Cretaceous Rijnland Group (**BKN**) marks the regional Base Cretaceous unconformity and the start of post-rift deposition. During the Late Cretaceous and Tertiary, several pulses of inversion cause unconformities within the Chalk Group (CK). A major pulse of inversion occurred during the Late-Campanian and this inversion is thought to be linked to a major unconformity within the Chalk formation (Huijgen, 2014; van der Molen, 2005). This unconformity can be correlated regionally (Huigen, 2014) and is represented by the '**CK1**' horizon in this study. The Lamaride phase of inversion caused another regional unconformity, marking the base of the North Sea Group (**BNS**). The seismic character of the most important unconformities present in this section are shown in **Table 3**.

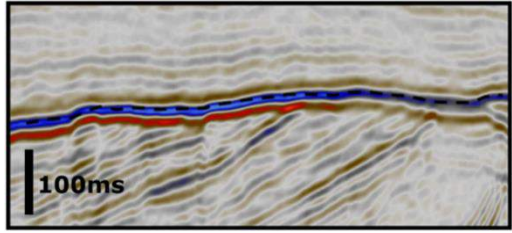
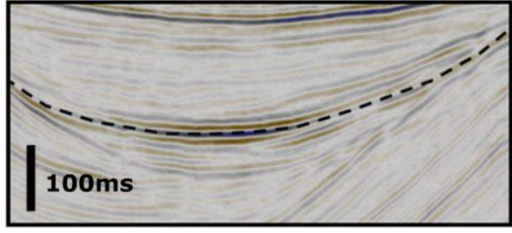
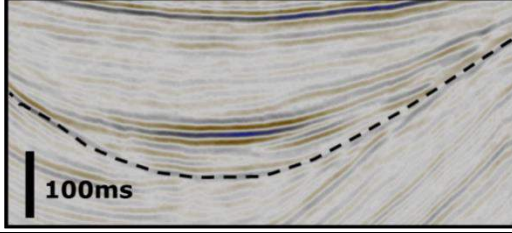
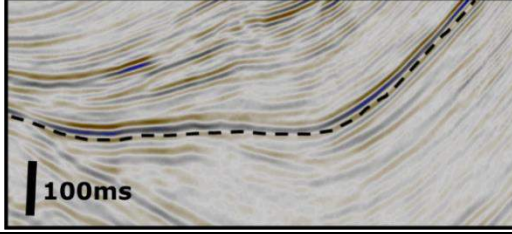
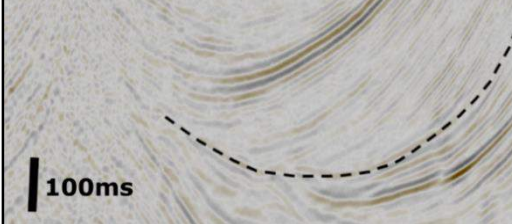
	Unconformity	Characterization
	Base North Sea (BNS)	Strong, continuous reflector. Some distortion around salt structures.
	Middle/Late Campanian (CK1)	Discontinuous reflector near salt structures. Locally characterized by intra-Chalk truncation. Medium reflector strength.
	Base Cretaceous (BKN)	Discontinuous reflector near salt structures and eroded locally. Medium to weak reflector strength.
	Middle Jurassic (BSL)	Continuous reflector within the DCG. Eroded on the platform area, most of the Step graben and above Fo9-WEST1. Strong to medium reflector strength.
	Late Triassic (RN1)	Discontinuous, weak reflector. Local downlapping surface. Appears to be conformable away from the DCG.

Table 3: Seismic characterization of main unconformities

**Figure 35** shows the interpreted section with all intervals interpreted. A description of the most relevant aspects of every interpreted interval is given in **Table 4**. Stratigraphic relationships, geometry and structuration will be discussed in more detail in chapter 6.2.

Interval	Description Figure 35
NS	The North Sea Group (NS) is thickest above the ESP and thins above salt structures, mainly towards salt structure Fo9-WEST <sub>1</sub> .
CK	The Chalk Group (CK) shows a general thinning towards the DCG and is thickest above the SGP. The lower part of the CK interval (CKo) is relatively thick above the SGP, then quickly thins towards the West and is locally absent above the DCG. Above the SGP, CKo directly overlies ZE deposits. The upper part of the CK interval (CK <sub>1</sub> ) is more homogenous, but also thins above the DCG and is locally absent here.
KN	Rijnland Group (KN) is absent in most of the section. Some KN occurs on the SGP, but quickly thins and disappears to the West. Within the DCG, directly East of salt structure Fo5Fo8-WEST <sub>1</sub> , some thin KN deposits occur.
SL	The lower part of the Schieland Group (SLo) shows a thickening towards the basin center and the Fo9-WEST <sub>1</sub> salt structure (SLo). In the upper part of the Schieland Group (SL <sub>1</sub> ) thickening shifts towards the West. All SL deposits are restricted to the DCG in this section.
AT	Altena Group (AT) shows a thickening towards the basin center and the Fo9-WEST <sub>1</sub> salt structure. All AT deposits are restricted to the DCG in this section.
RN	The Upper Germanic Trias Group (RN) clearly shows thickness variations throughout the section, but is mostly absent on the SGP and completely absent on the ESP.
RB	The Lower Germanic Trias Group (RB) has a homogenous thickness throughout most of the section, but is absent on the ESP in the West.
ZE	The Zechstein Group (ZE) has a very heterogeneous thickness and occurs in major salt structures (Eo9Eo6Eo3-EAST <sub>1</sub> , Fo5Fo8-WEST <sub>1</sub> , Fo9-WEST <sub>1</sub> , Go7-WEST <sub>1</sub> and Go7-EAST <sub>1</sub> ), while away from these structures ZE is relatively thin (<500m). This contrast is largest within the DCG.
BSM	Pre-Zechstein basement is structured by major basement faults. The basement structure represents the main structural elements in this area, from West to East: Elbow Spit Platform (ESP), Step Graben (SG), Dutch Central Graben (DCG), Schill Grund Platform (SGP).

Table 4: Description of Figure 35



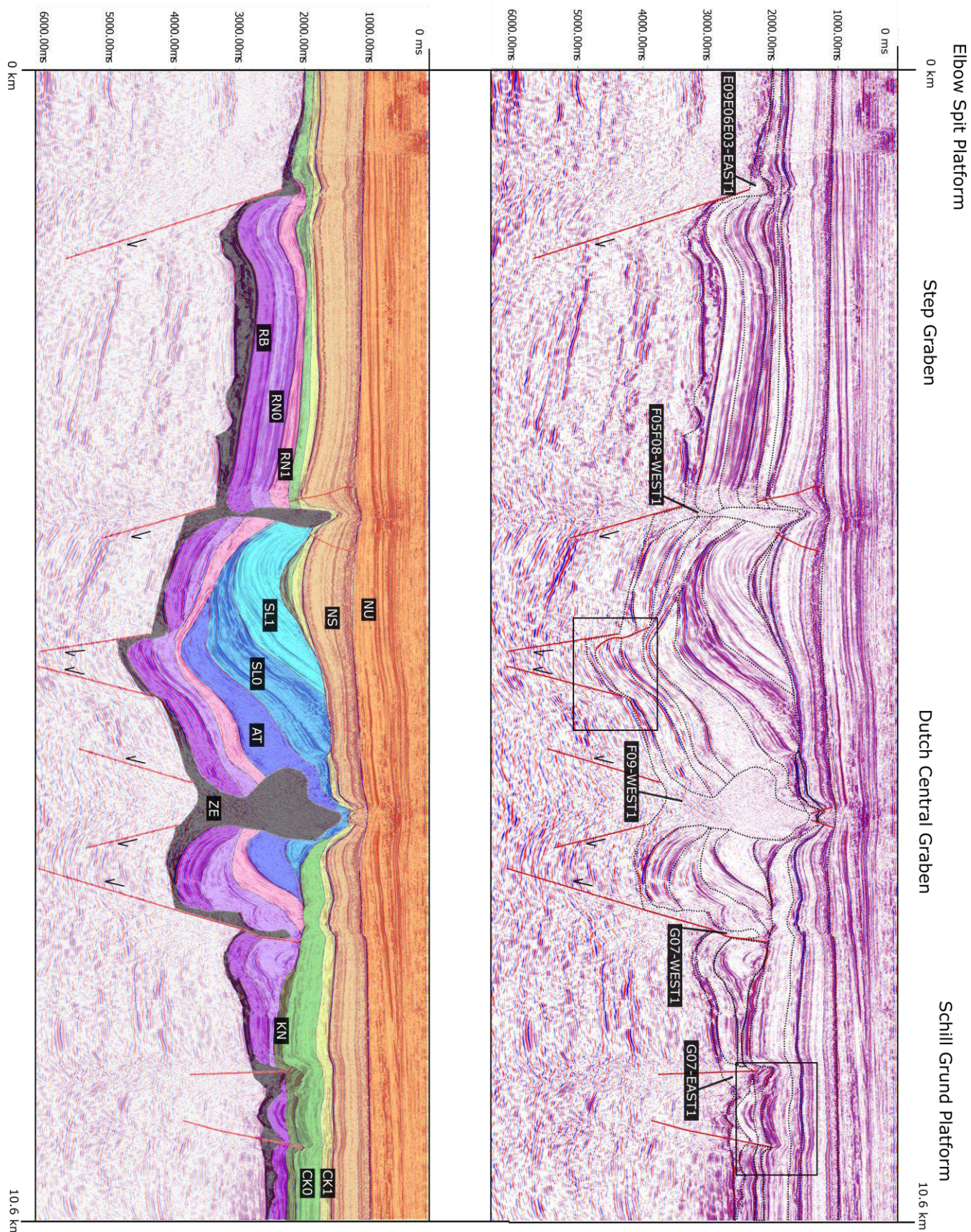




Figure 35: (Previous page) The interpreted seismic section described in Table 4. This interpretation was used for building the restoration model shown in Figure 37. The location of this section is shown in Figure 15; Locations of Figure 36 and Figure 43 are indicated (black boxes; Seismic data courtesy Fugro).

### 6.2.2. Structural restoration

**Figure 38** (A-P) shows the resulting models of a structural restoration of the initial model shown in **Figure 37**, in sixteen (16) restoration steps. In this restoration the section is restored back to its Early Triassic structural configuration. A chronological description of the resulting models is given below. Note that the restoration was performed in reversed chronological order (i.e. modelled backwards in time).

#### *Early Triassic (Figure 38A)*

**Figure 38A** shows the restored model after deposition of the Lower Germanic Trias Group (RB). In the Early Triassic RB was deposited above a layer of Zechstein Group (ZE) evaporites. Although thickness of the ZE interval is highly uncertain at this point in time, it is likely that thinning occurred towards the West, where the interpreted ZE salt basin edge is located, based on the occurrence of slope facies carbonates (Tolsma, 2014). Towards the East salt thickness may have reached up to 1500-2000m. The ZE salt was mostly unstructured at this time and is likely to have had a layered geometry. The RB interval can be seen offset by younger faults at several locations, including the DCG boundary faults, but it appears the RB interval itself was deposited with mostly homogeneous thickness in this area. There are no indications that during the deposition of the RB interval active tectonism occurred in this part of the basin, while further to the North there are indications of active Early Triassic rifting. The model shows some structuration in the pre-Zechstein basement. This interpretation is based on observations of a pre-Zechstein graben structure in the DCG area (See chapter 2. Geological history, Ziegler, 1990).

#### *Late Triassic (Figure 38B-C)*

**Figure 38B** shows the restored model after the deposition of the RNo interval. The Upper Germanic Trias Group (RN) shows clear thickness variation adjacent to major faults and salt structures. At several locations within the DCG, RNo shows stratigraphic thickening towards a fault (**Figure 36**). Considering it was likely that the ZE salt had a significantly greater thickness and was more homogeneously distributed, faults active in the overburden during this period were most likely detached from basement faults. This would also best explain the observed stratigraphic geometries in the RNo interval (e.g. geometries visible in **Figure 41**). The most intense thickening of the RNo interval occurs against the eastern DCG boundary fault. Although presently this boundary fault can be seen directly linking into the basement, in the Late Triassic this fault is interpreted to have been active above a Zechstein salt detachment. This is again based on stratigraphic geometry of the interval (**Figure 41**) and the fact that the Zechstein salt layer likely had a greater thickness at the time of initiation of faulting. The RNo intervals shows clear stratigraphic thinning towards salt structure Fog-WEST<sub>1</sub>. This geometry can be explained with the syn-depositional development of a Zechstein salt pillow, where depocenters are located away from the salt pillow (this concept is illustrated in **Figure 25**). Within the DCG, West of salt structure Fog-WEST<sub>1</sub>, RNo can also be seen thickening into a fault. This geometry is expected to form during detached faulting, where strata thickens into a fault plane on one side of a salt structure and thins towards other side (See **Figure 24** and **Figure 25**). Within the SG, deposition



of the RNo interval appears to have been relatively undisturbed, where reflectors are parallel and continuous (**Figure 35**). Some internal truncation can be observed near the western SG boundary, suggesting some fault activity during the deposition of RNo. On the ESP no Triassic strata is found at present, but it is assumed the interval was deposited homogenously here and eroded at a later stage. From the DCG onto the SGP, RNo shows stratigraphic thinning and is absent further to the East. RNo deposits are restored relatively thin on the stable SGP and thickening rapidly into the DCG towards the West. This can be explained by the differential movement of the DCG with respect to the platform areas.

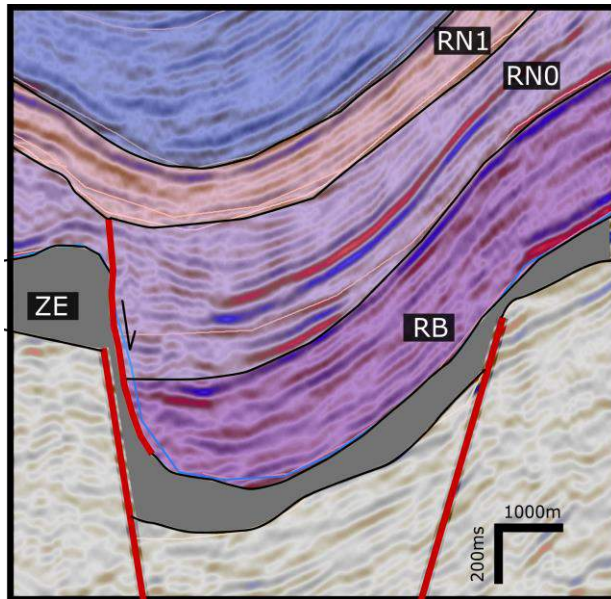


Figure 36: Interpreted seismic section showing ZE, RB, RNo and RN1 intervals. Location is shown on the section in **Figure 35**. (Seismic data courtesy Fugro)

**Figure 38C** shows the restored model after deposition of the RN1 interval. During the deposition of the RN1 interval, a shift of depocenter can be observed at several locations within the DCG. The shift of depocenter is most evident East of salt structure Fo9-WEST1 near the eastern DCG boundary fault. The depocenter shifts here from near the DCG boundary fault in RNo, westwards towards salt structure Fo9-WEST1. Reflectors of the RN1 interval can be seen downlapping onto the top of the RNo interval (**Figure 41**). This indicates the development of an eastward dipping slope during deposition of RN1. **Figure 41** also shows the geometry of the RB, RNo, RN1 and AT intervals below a flattened reflector. Here a clear westward shift of depocenter in the RN1 interval becomes evident. This shift of depocenter and the presence of a tilted depositional surface are indications for local withdrawal of salt towards the West (to salt structure Fo9-WEST1) and possibly the initiation of piercing of the salt. Note that by flattening the seismic data, it is adjusted vertically and the resulting flattened section does not take into account the true stratigraphic thickness (TST, in ms TWT) of a steeply dipping interval. Rather, it will show the true vertical thickness (TVT, in ms TWT) of this interval. This is the reason the RB interval appears to thicken to the West when flattened, while this is not visible in the original seismic data (**Figure 41A**).

In the deepest part of the DCG, between salt structures Fo9-WEST1 and Fo5Fo8-WEST1, the fault that was active during the deposition of RNo is covered by RN1 deposits and the depocenter shifts

eastwards towards structure Fo9-WEST1. Within the SG, the RN1 interval shows some minor stratigraphic thickening towards the western SG boundary fault and towards salt structure Fo5Fo8-WEST1. Away from the graben structures RN1 is mostly absent at present (See **Appendix 3C**), but is interpreted to have been deposited relatively undisturbed and homogenously. Intrusion of Zechstein salt wings occurs in the upper part of RN1, near salt structure Fo5Fo8-WEST1. This could be explained by the fact that salt structure Fo5Fo8-WEST1 was at or near the surface at this time.

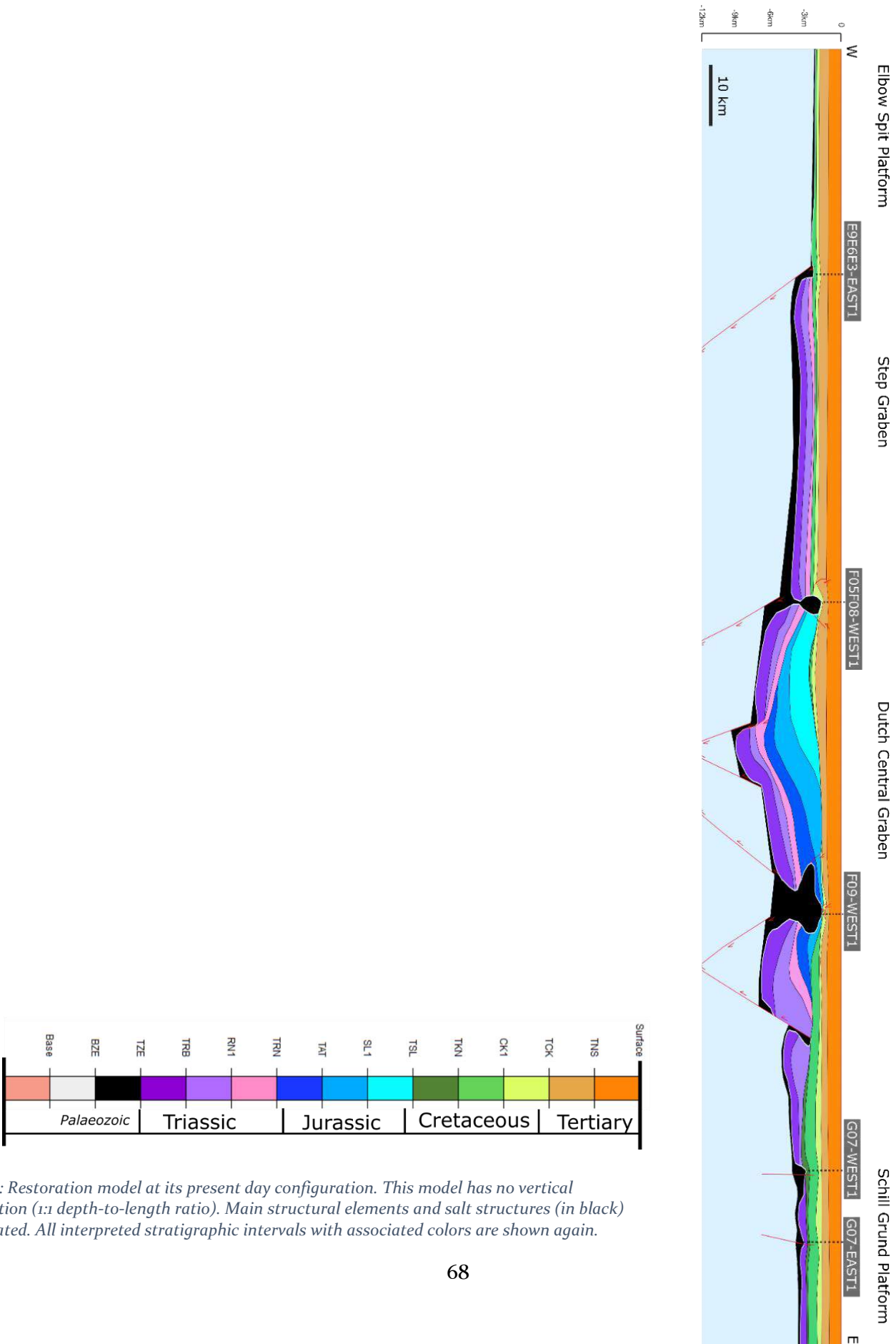
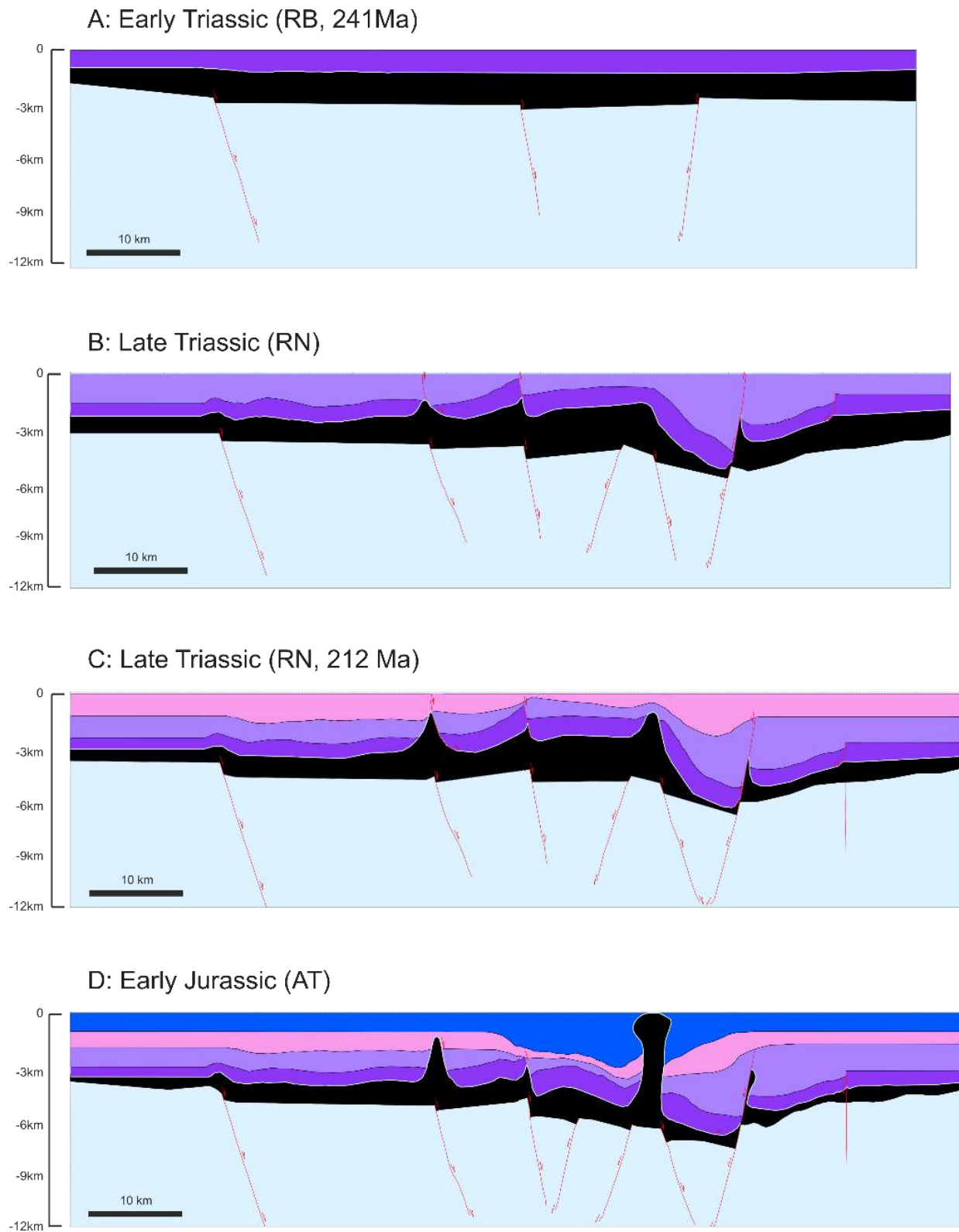
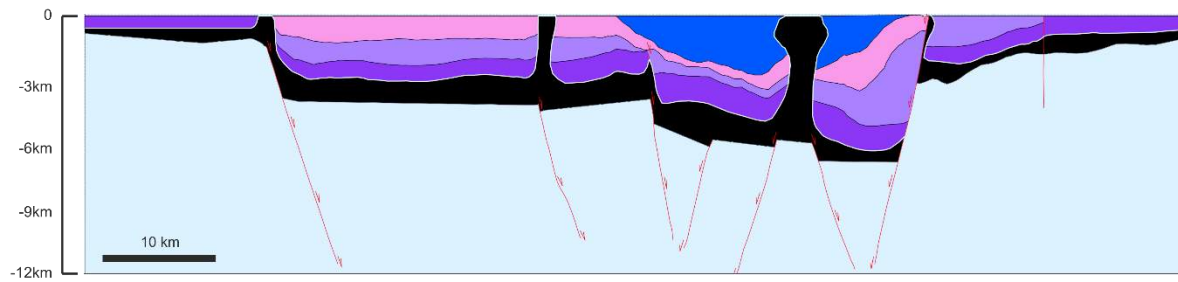


Figure 37: Restoration model at its present day configuration. This model has no vertical exaggeration (1:1 depth-to-length ratio). Main structural elements and salt structures (in black) are indicated. All interpreted stratigraphic intervals with associated colors are shown again.

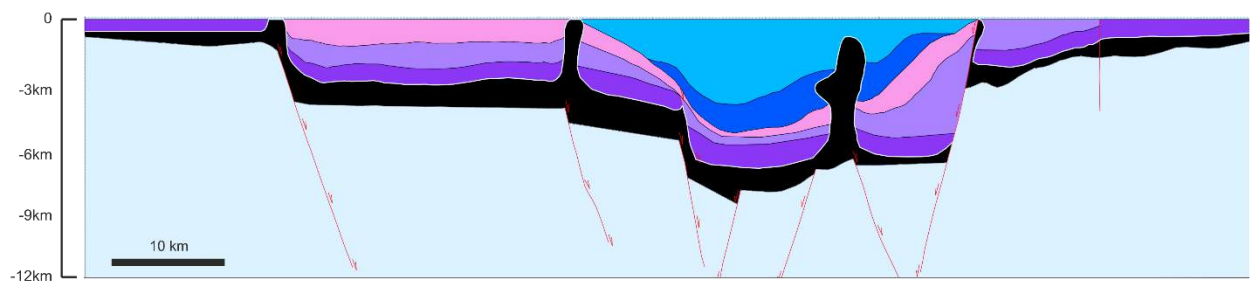
Figure 38: Resulting models of the structural restoration. These models are 2 times vertically exaggerated (2:1 depth-to-length ratio).



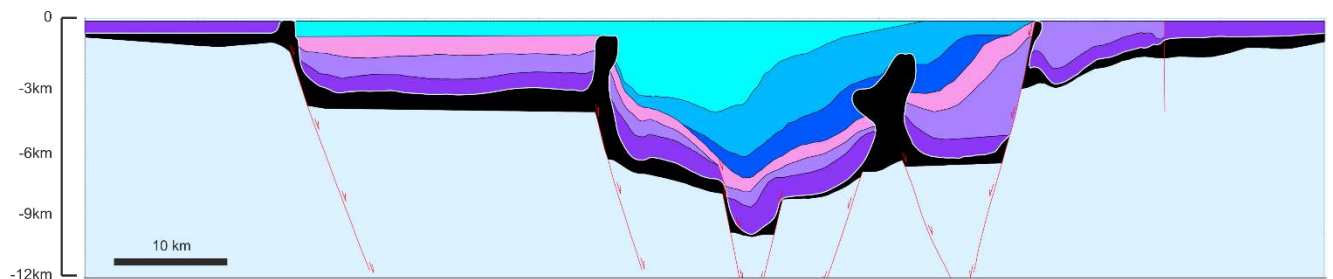
E: Early/Middle Jurassic (AT, 155 Ma)



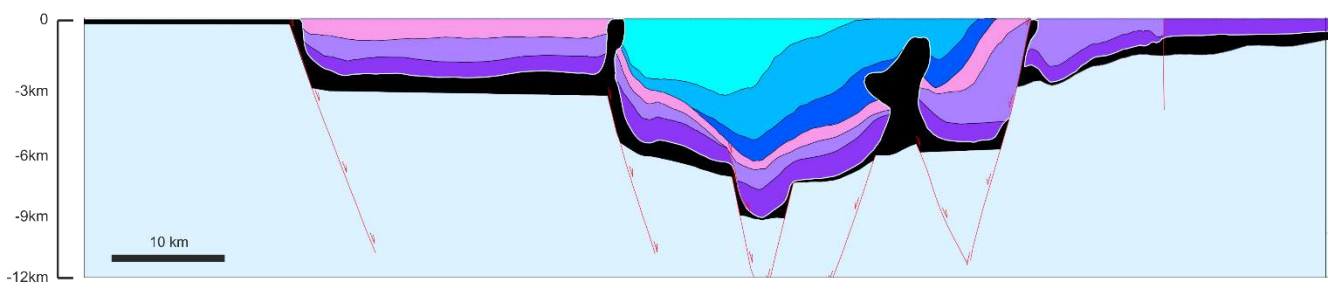
F: Late Jurassic (SL)



G: Late Jurassic/ Early Cretaceous (SL)

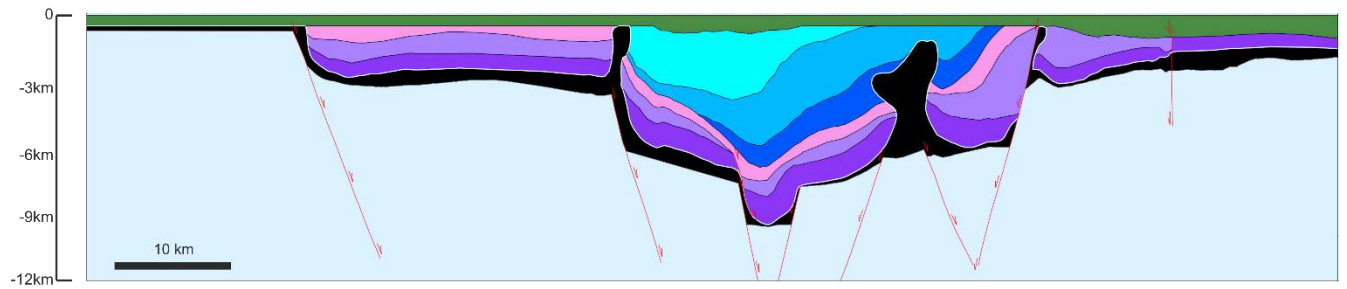


H: Early Cretaceous (134 Ma)

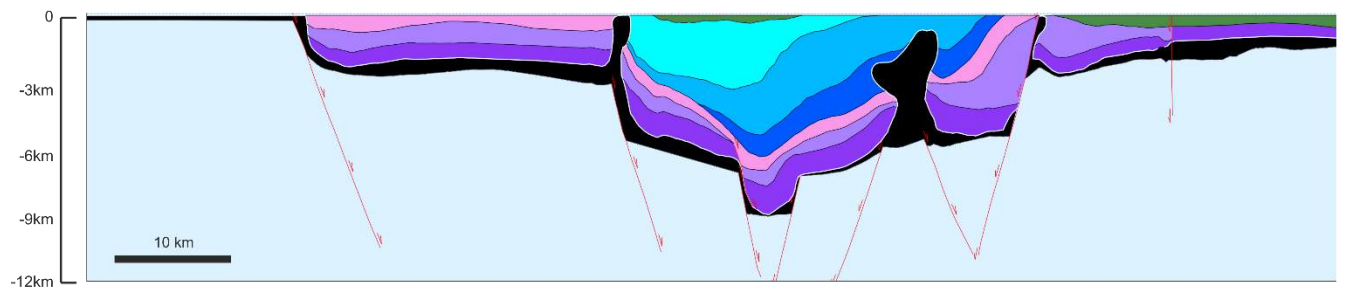




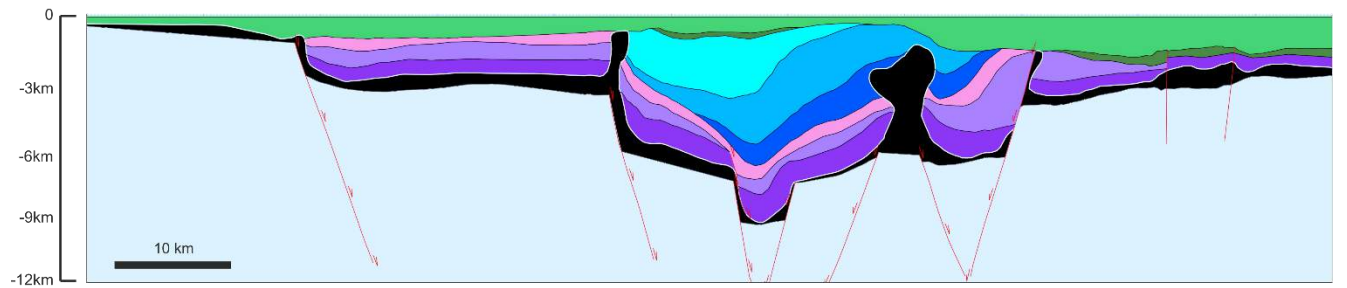
I: Early Cretaceous (KN)



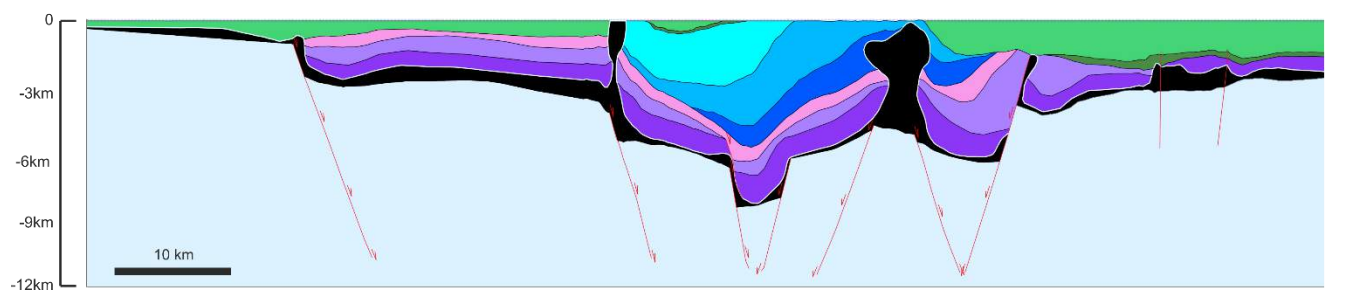
J: Early Cretaceous (KN, 97 Ma)



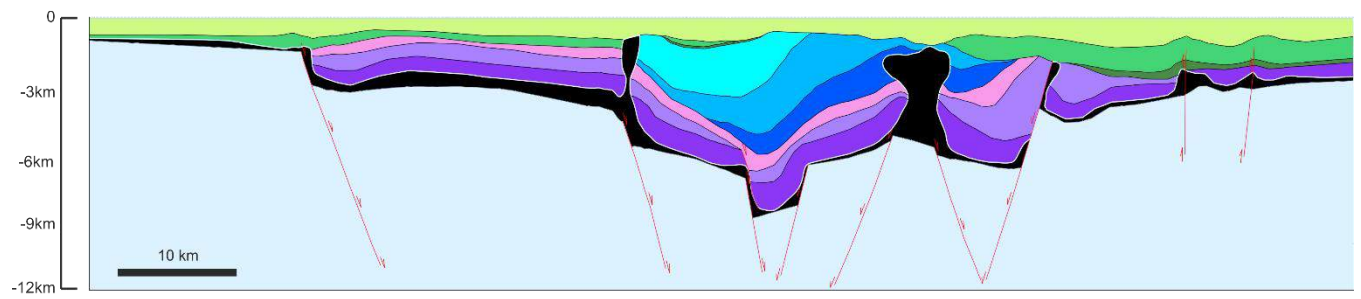
K: Late Cretaceous (CK)



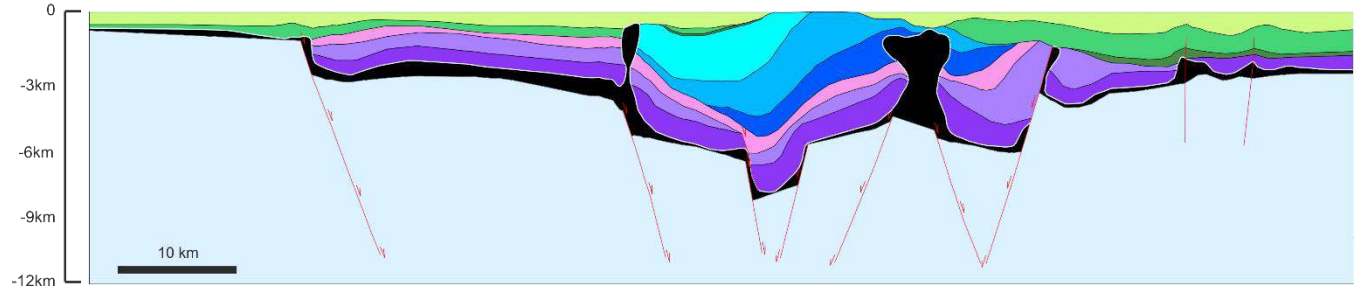
L: Late Cretaceous (CK)



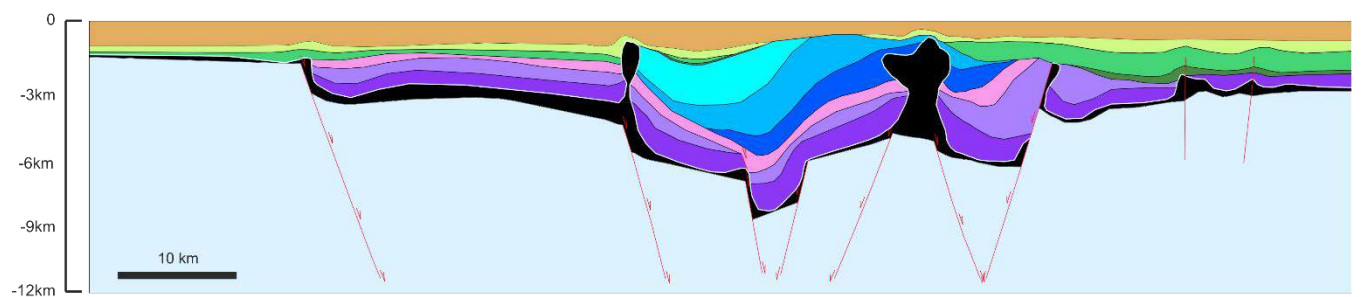
M: Late Cretaceous (CK)



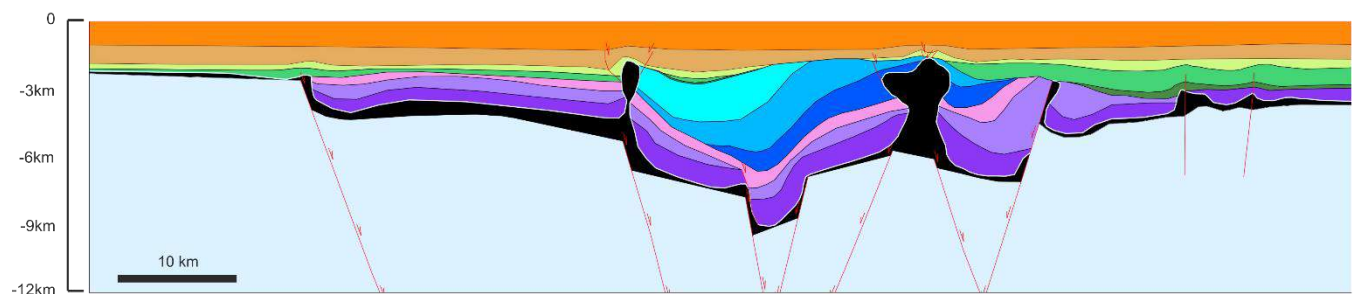
N: Late Cretaceous/Tertiary (CK, 60 Ma)



O: Tertiary (NS, 28 Ma)



P: Present



### Jurassic (Figure 38D-G)

**Figure 38D** shows the restored model after deposition of the Altena Group (AT). AT is characterized by a thickening towards the center of the DCG, where the interval has a secondary rim syncline geometry adjacent to salt structure Fo9-WEST<sub>1</sub> (see **Figure 41**). The rim syncline geometry implies that the salt structure pierced through the overburden at this point and was close the surface during deposition of AT in a peripheral sink. Towards the DCG boundary faults, AT is truncated and is absent on the platform areas and in the SG. Palaeo-geographic reconstructions (**Figure 40**) show AT was deposited in a widespread open marine setting. Therefore, the AT interval is restored in the entire section. AT is restored thinner outside of the DCG, since stratigraphic thinning is observed within the DCG towards the platform areas and the SG.

**Figure 38E** shows the restored model after a regional uplift, related to thermal doming in the Middle Jurassic (~155Ma), which induced deep erosion on the platform areas and minor erosion within the SG. This uplift event is clearly expressed in burial graphs from the Cleaver Bank Platform (**Figure 39B**). During the same period, the DCG continues to subside and is mostly unaffected by erosion (**Figure 39A**). All of the AT interval is eroded from outside of the DCG. On the platforms most of the Upper Triassic sediments are removed, while they are preserved in the SG and DCG. Salt structures Fo5Fo8-WEST<sub>1</sub> and Eo9Eo6Eo3-EAST<sub>1</sub> are interpreted to have been at the surface at this point.

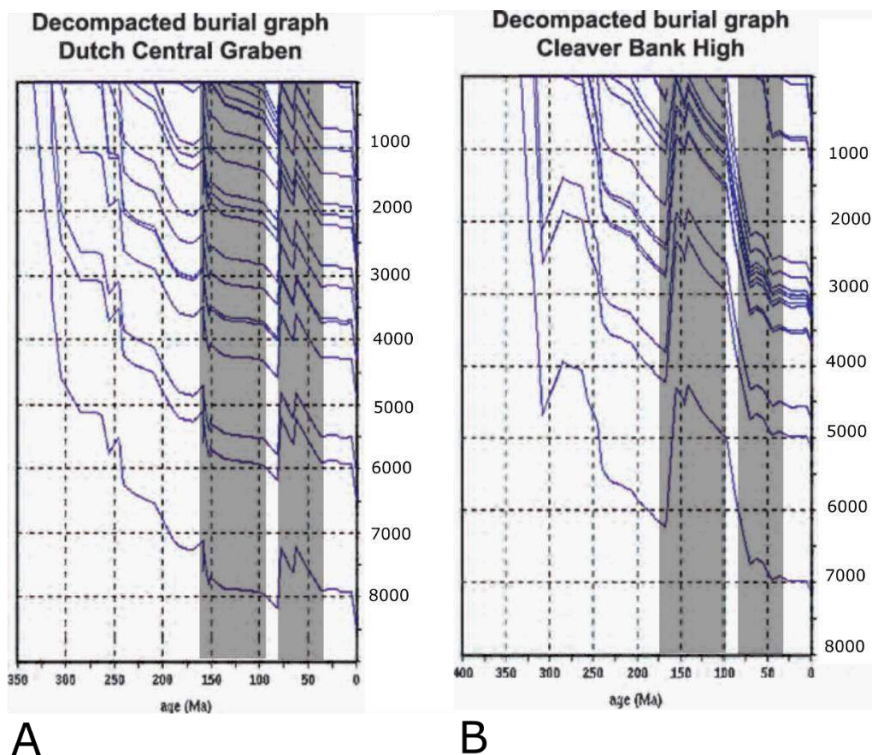


Figure 39: A: Burial Diagram of the Dutch Central Graben B). Burial diagram from the Cleaver Bank High, to the southwest of the study area (see **Figure 1**, CP). This figure illustrates continued subsidence during the Jurassic in the DCG, while platform areas are uplifted. Effects of inversion can be seen in the DCG, as several phases of uplift, while the platform area seems mostly unaffected (after De Jager, 2007).

The effects of the thermal doming also become evident in palaeo-geographic reconstructions during the Middle to Late Jurassic, which show a shift from widespread deposition during deposition of the AT interval, to restricted deposition within the DCG during the deposition of the SLo and SLi intervals (**Figure 40**).

**Figure 38F** shows the restored model after deposition of the SLo interval. During deposition of the SLo interval, a secondary rim syncline geometry adjacent to salt structure Fo9-WEST<sub>1</sub> persists, although a gradual shift of depocenter occurs towards the West (**Figure 35**). The shift of depocenter in the restored model is accommodated by basement block subsidence, related to active extension combined with increased salt withdrawal in the West of the DCG, although it is uncertain exactly what mechanisms controlled deposition. During this period the development of the SG as a separate structural element can be inferred, where the DCG develops as the deep, central part of the graben system and the Step Graben remains a marginal ('step') graben.

**Figure 38G** shows the restored model after deposition of the SLi interval. During the deposition of the SLi interval the shift of depocenter towards the West continues (**Figure 35**). Deposition of both SLo and SLi is restricted to the graben structures. More towards the North of this section, Late Jurassic sediments occur in rim synclines adjacent to salt structures within the SG (as is shown in **Figure 28**). This indicates some Late Jurassic deposition in the SG. In the restored models SL is interpreted to have been deposited within the SG, although it is unclear if this was a homogeneous deposition (as shown in **Figure 38G**), or deposition restricted to subsiding mini-basins, adjacent to salt structures. In this case, SLi is restored within the SG and DCG, with the main depocenter in the West of the DCG, thinning towards the eastern part of the DCG.



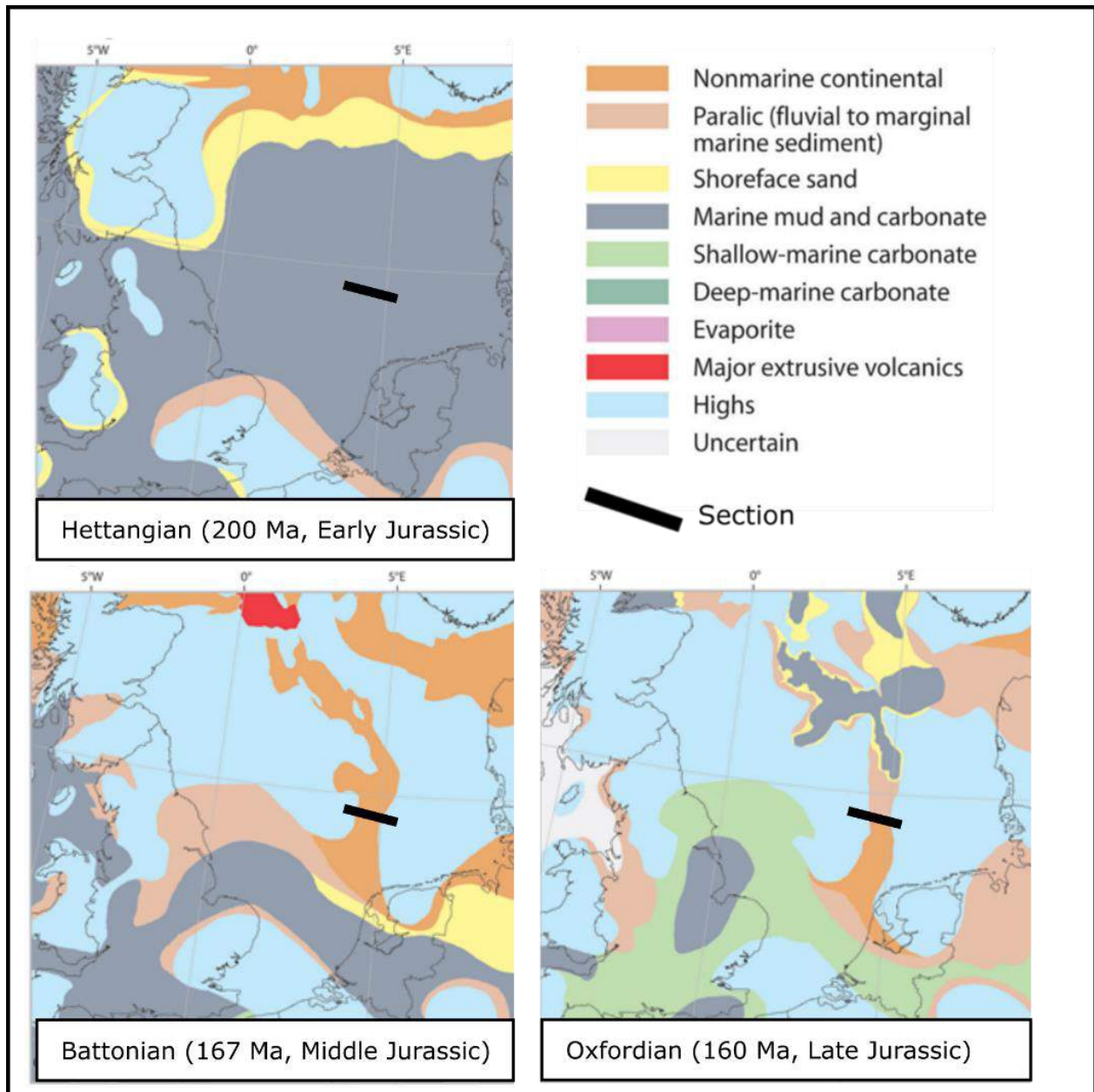


Figure 40: Palaeo-geography of the wider North Sea area throughout the Jurassic (Doornenbal et al, 2010; after Ziegler 1990; Cope et al 1992; Dadlez et al 1998; Ineson and Surlyk 2003; Feldman-Olszewska 2006). Note that deposition during the Middle and Late Jurassic is restricted, where deposition in the Early Jurassic is widespread.



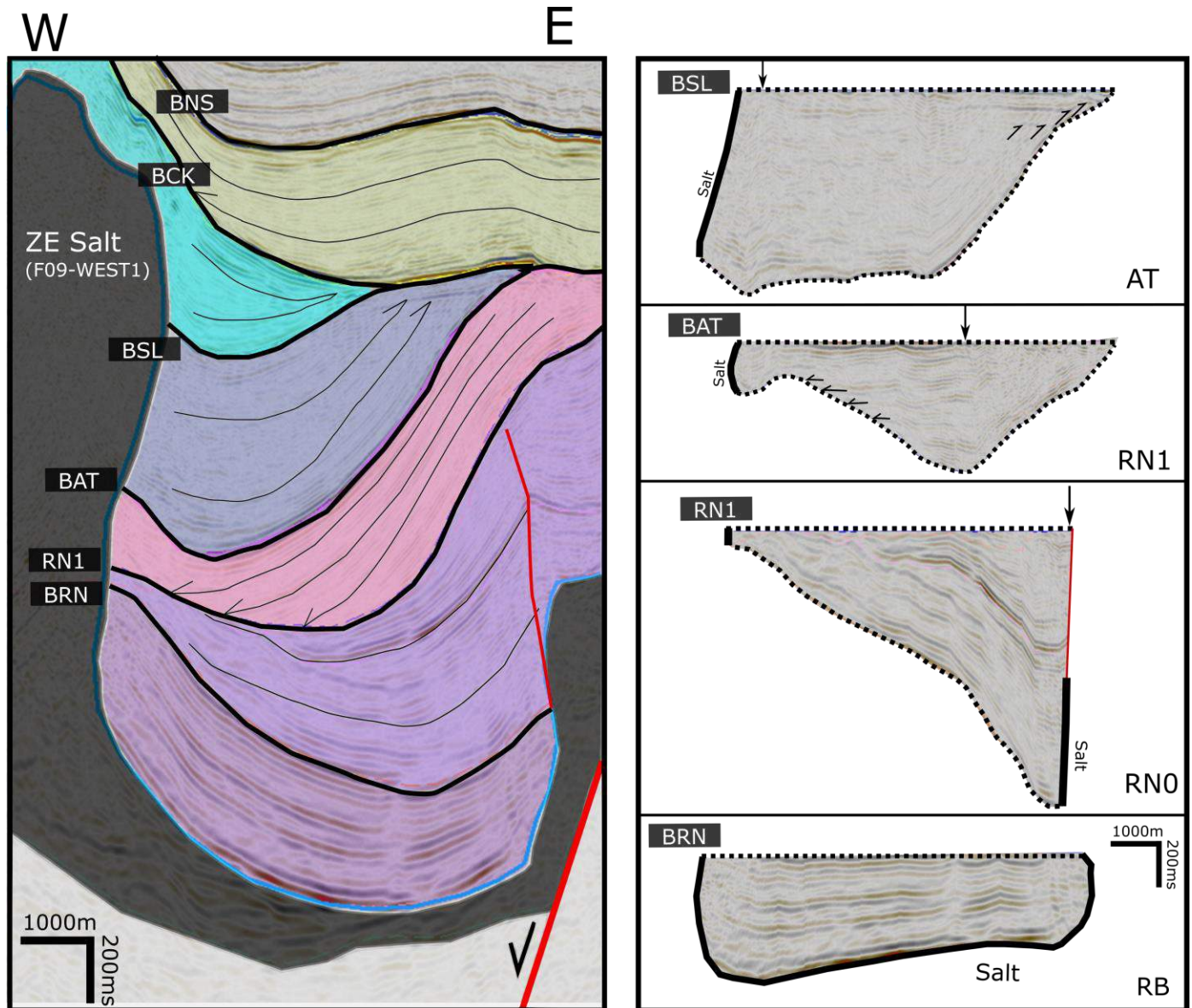


Figure 41: Detailed interpretation of the seismic section shown in **Figure 35**, showing salt structure F09-WEST1 and adjacent intervals to the East.. Four intervals are shown flattened on the corresponding top horizon: Lower Germanic Trias Group (RB), Upper Germanic Trias Group (RNo, RN1) and Altena Group (AT). The location of the palaeo-depocenter is interpreted (indicated by the black arrows; Seismic data courtesy Fugro).

### *Cretaceous and Tertiary (Figure 38H-P)*

**Figure 38H** shows the restored model after deposition of the Rijnland Group (KN). The base of the KN interval represents the major Base Cretaceous unconformity. Almost all Jurassic strata were eroded outside of the DCG. On the ESP erosion removed all sediments overlying the Zechstein salt and possibly partly eroded the Zechstein sediments themselves. Some erosion of Upper Triassic sediments occurred on the SGP and possibly within the SG. The Lower Cretaceous Rijnland Group (KN) is largely eroded above the DCG and SG. Locally KN strata can be seen being truncated by the base of the Chalk Group. The KN interval is interpreted to have been deposited regionally, thickening slightly in the basin center. During Late Cretaceous and Tertiary inversions the KN interval has then been eroded from most of the DCG and SG areas.

**Figure 38I** shows the restored model after deposition of the CKo interval. Within the Late Cretaceous Chalk Group (CK), the Late-Campanian unconformity is interpreted (Huijgen, 2014) separating the Chalk Group into two intervals (CKo, CK1). CKo can be seen onlapping towards the West on the eastern side of the DCG (**Figure 29**). Above the DCG almost no CKo can be found (**Figure 37**). The Late-Campanian unconformity coincides with the Base Cretaceous unconformity above most of the DCG (As seen in **Figure 37**, **Figure 35**, **Figure 41**). The CK that is present above the DCG is interpreted to be mainly CK1. These geometries are explained in the model with an initial deposition of CKo (**Figure 38K**), where thinning occurs above the DCG. Then inversion induces erosion of CKo above the DCG (**Figure 38L**) and subsequently CK1 is deposited (**Figure 38M**). During this Late-Campanian inversion Lower Cretaceous and Jurassic strata were also truncated. **Figure 42** shows the restored configuration of the section, where KN, SLo, SL1 and CKo are restored to their interpreted pre-inversion geometry and the interpreted eroded strata. After deposition of CK1, the central part of the DCG is inverted once more and CK1 is in turn eroded from this area (**Figure 38N**). These inversion are not instantaneous, and deposition will have continued during these inversions, therefore the CKo and CK1 intervals thin stratigraphically above the DCG. CK strata above salt structures is pushed upwards, due to reactivated growth of the salt after deposition. This configuration is seen in the CK1 interval, which has a marked anticlinal geometry above salt structure Fo5Fo8-WEST1 and Fo9-WEST1 (**Figure 35**) and to a lesser extent above salt structures Eo9Eo6Eo3-EAST1, Go7-WEST and Go7-EAST. Faults on the SGP are activated during these inversion and can be seen pushing CKo strata upwards (**Figure 43**). Indication for mass flow deposits associated with this inversion are present in the CK (for example near the eastern DCG boundary fault, block Fo9; as described by Huijgen, 2014, EBN). CK strata above the Late-Campanian unconformity appears less deformed, suggesting most inversion took place during the Late-Campanian inversion phase.

**Figure 38O** shows the restored model after deposition of the Tertiary North Sea Group (NS). NS shows a general thinning towards the axis of the DCG and thins above salt structures Fo5Fo8-WEST1 and Fo9-WEST1, indicating significant renewed vertical growth of these salt structures during this period, likely related to another phase of inversion. The thinning of NS indicates that the DCG was likely a structural high during deposition of most of the NS interval.

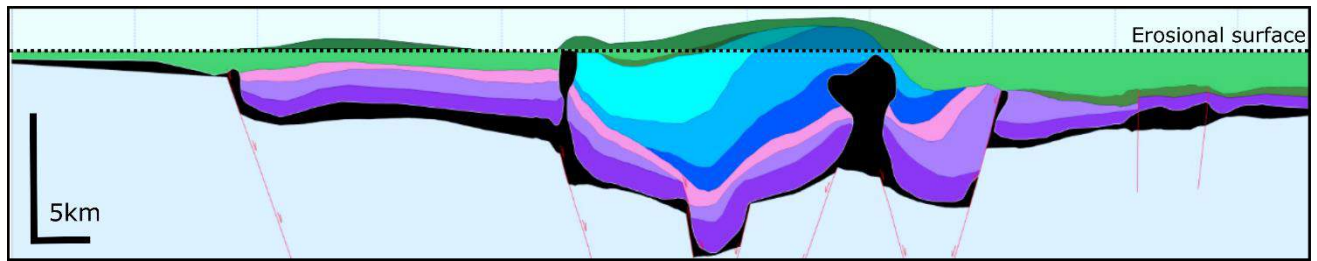


Figure 42: Restored configuration of SLo, SL1, KN and CK1 intervals above the SG and DCG. This section shows the total amount of interpreted erosion that is represented by the Late-Campanian unconformity. (2:1 Depth-to-length ratio)

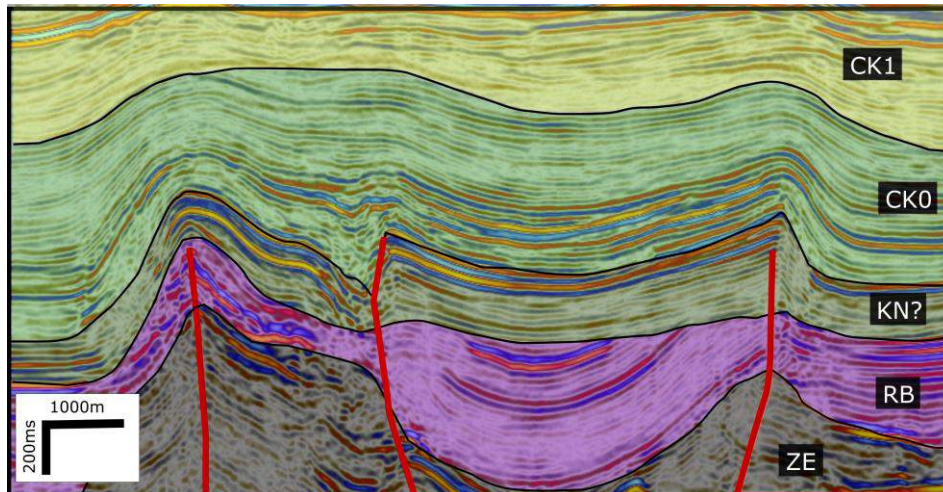


Figure 43: Interpreted seismic section showing ZE, RB, KN and CK intervals. Location is shown on the section in **Figure 35** (Seismic data courtesy Fugro).

## 6.3. Discussion

Below, some considerations for the restoration models are discussed, uncertainties and assumptions are outlined and alternative models suggested. Finally, a summary of the tectonic phases, which the restoration models represent, is given. For discussion on implications for prospectivity see chapter 8.

### 6.3.1. Restoration model considerations

While some indications for active tectonism are present towards the northern SG (e.g. near salt structure A12-EAST2) and along the eastern DCG boundary fault, nothing indicates active rifting and associated salt movement during the Early Triassic in this area. The first rifting phase to affect this area occurred in the Middle/Late Triassic. Although faults were mostly detached, they can be associated with active basement faults. Major fault movements are suggested at the eastern DCG boundary fault. It is unclear if this fault was detached in the Late Triassic, or already piercing through the salt cover as it does at present. The restoration model assumes a consistent structural style and therefore models the fault as a detached fault. It is likely that at this stage the location of salt structures was already determined and these Late Triassic salt pillows have a generic relationship to the salt structures within DCG we see today.

It appears Early Kimmerian rifting already focused in the DCG, while the SG was relatively undisturbed in this area. More active faults can be seen in the SG towards the north. Fault movements did occur along the faults that outline the DCG today. The shift of depocenter that can be observed within the Upper Triassic succession could be explained by intensified salt movement and possibly local initiation of salt structure piercing (Fo9-WEST1, Fo5Fo8-WEST1). However, this could also be due to also be due to the dying down of Early Kimmerian rifting at the end of the Late Triassic and a shift from fault controlled deposition to deposition controlled by salt movement.

The development of a secondary rim syncline during deposition of AT is interpreted in the restoration model as the piercing stage of the Fo9-WEST1 diapir (**Figure 38D**). However, the creation of accommodation space where AT was allowed to accumulate, could also be attributed to tectonic subsidence. The restoration model chooses to accommodate almost all of the AT sediments with the withdrawal of salt, because generally no active rifting is inferred during the Early Jurassic in this area and there is no indication of this in sedimentation patterns. Additionally, active salt movement during this period would be in agreement with the transition from Triassic pillowing to a fully pierced salt structure in the Late Jurassic.

The fact that AT is only preserved within the DCG, is explained in the restoration model by a continued subsidence of the DCG (see also **Figure 39**). However, this subsidence only occurs after the deposition of AT. The accommodation space needed to allow for the SLo and SLi intervals to be deposited can again be attributed to either salt withdrawal or tectonic subsidence. In this case

the restoration model incorporates active rifting, which then creates the accommodation space for SLo and SL<sub>1</sub> to be deposited. First of all, active rifting is known to have taken place during the Late Jurassic and therefore would be a plausible model. Secondly, the SLo and SL<sub>1</sub> intervals are most likely too thick to be only attributed to salt withdrawal (e.g. Wijker, 2014). Some salt withdrawal is incorporated in the restoration model during the deposition of SLo and SL<sub>1</sub>. So, where AT was mostly accommodated by salt withdrawal SLo and SL<sub>1</sub> are accommodated by both active rifting and salt withdrawal. A thickening of the AT interval into the DCG is modelled based on observations in seismic data, despite the fact that palaeo-geographic maps suggest a homogeneous depositional pattern (**Figure 40**).

The model proposed by Wijker (2014), in which deposition of Late Jurassic sediments is controlled by E-W running growth faults cannot be incorporated in the restoration of this section, since it runs almost perpendicular to this N-S oriented structuration.

In the restoration model, platform areas are eroded at the base Cretaceous unconformity to the depth where at present Cretaceous sediments are overlying Triassic and Permian rocks unconformably. Where KN was deposited exactly is uncertain due to the absence of the interval in most of the section. The restoration model restores the KN interval thickening onto the SGP and within the DCG, but otherwise mostly relatively homogeneous. Thickening of KN deposits in the DCG may be expected as palaeogeographic maps (Ziegler, 1982) show a transition towards deep marine deposition within the DCG during the Early Cretaceous, where in most of the area shallow marine deposition dominates.

In the restoration model most of KN is eroded before the deposition of CKo. This is a logical consequence of the fact that there was no KN underlying CKo in most of the section, as it was interpreted in its present day configuration (**Figure 35**). In reality KN was more likely gradually eroded from areas that became structural high during Late Cretaceous and Tertiary inversions. The restoration of CKo involves restoration of eroded Jurassic and Cretaceous strata associated with the Late Campanian unconformity. The restored geometry of these intervals is important, since this affects every older restoration step. The decision on how much strata to restore in this case is based on the most realistic geometry in the context of local geology and extrapolation of truncated reflectors above the late Campanian unconformity (flattened in seismic data). Additionally, basin modelling, constrained by vitrinite reflectance data, indicates this amount of uplift and erosion is in a realistic range (up to 700m; De Jager, 2003).

### **6.3.2. Uncertainties and assumptions**

The restoration models have to be regarded with the main assumptions and uncertainties in mind. First of all the model is limited by the fact that it is a 2D section. Therefore it does not take into account movements outside of the section plane. This has an impact on visualization of tectonic movements. Tectonic movements perpendicular to the plane of the section will not be modelled. Also strike-slip components will for example not be taken into account in these models, even though oblique components are suggested for several of the tectonic phases, e.g. during Late Jurassic rifting (Ziegler, 1991) and during the inversion pulses in the Late Cretaceous to Tertiary (De Jager, 2007).



Salt will also have moved outside and into the plane of the section. Major salt structure like Fo5Fo8-WEST<sub>1</sub> and Fo9-WEST<sub>1</sub> will have been sourced by salt from the surrounding areas and areas where deposition has focused will have been affected by salt withdrawal to adjacent areas, i.e. outside of the plane of the section. This effect can be assessed to a certain extent by assessing available 3D seismic data. Although this cannot be visualized directly in a 2D model, it will have to be included in the modelling of salt movement. The restoration model is based on a depth-converted seismic interpretation, but is often a simplification of the observed geometries. Due to poor deep well control the time-depth conversion is poorly constrained for the oldest intervals and top of the basement. Therefore the depth of the DCG in the deep part of the graben (up to 9km in the restoration model) has a large uncertainty and will locally be unrealistic.

Lithologies assigned to the interpreted intervals in the restoration model are not a precise representation. There is no lithological data from wells for deeper intervals in this area (**Figure 31**). The assigned lithologies are estimates based on information from adjacent areas. However, for the purpose of this restoration the decompaction factors, based on these lithologies will most likely be appropriate. In order to make better estimates for decompaction factors, lithological data from this area can be used in the future, if available. While vertical simple shear was applied in the restoration of faults and in unfolding, this may be unrealistic around salt structures, where strata dips steeply, because bed parallel extension will increase with increasing stratal dip. Therefore, in steeply dipping intervals, bed-length restoration algorithms might be more appropriate (Rowan, 2012). Additionally, effects of inversion were modelled using the same vertical simple shear algorithm, where this may have been more effective using bed-length restoration algorithms.

The parameters used to model the restoration may not always reflect the geological reality. Flexural loading and long-term thermal subsidence are not taken into account, while only Airy isostasy was applied. Applying a flexural isostasy algorithm in the model may have been suitable for this type of restoration (e.g. Rowan, 2012), since periods of rifting occur. This would be advisable for future restorations in this area. For this study this distinction does not have a significant effect on the restoration, since the section is flattened to a surface ( $z=0$ ) after every step.

### 6.3.3. *Alternative models*

At every step in the structural restoration, assumptions were made. This means that at multiple stages in the restoration process, alternative restoration models were possible, increasingly so moving back in geological time. Some examples of alternative restorations of the model are given below:

- Salt structure Fo9-WEST<sub>1</sub> fully pierces the overburden already in the Late Triassic (**Figure 38B-C**).
- The eastern DCG boundary fault already pierced the salt cover in the Late Triassic (**Figure 38B-C**)
- Deposition of the AT interval is more homogeneous and intense salt withdrawal does not occur until the Late Jurassic (**Figure 38D**)

- More Triassic strata is eroded from the platform areas during Jurassic doming (**Figure 38E**)
- Accommodation space is created during the Late Jurassic only by either salt tectonics or active rifting, not a combination of both (**Figure 38F-G**)
- Jurassic (AT, SL) sediments are not deposited homogeneously in the SG, but only locally in secondary rim synclines (**Figure 38D+G**)
- Thermal, post-rift subsidence was the most dominant mechanism for formation of accommodation space in the Jurassic.
- More Jurassic and Cretaceous strata were eroded during the Late-Campanian inversion, impacting decompaction of underlying strata (**Figure 42; Figure 38K-L**).

These alternative models may be tested in the future, when available data allows this, although some will likely remain subject to speculation. The restoration done in this study is one model for the structural development in this area, where decisions during restoration were made based on observations in available data, literature and generally accepted (salt) tectonic models.

#### **6.3.4. Summary of structural development**

A summary of the structural evolution resulting from the restoration models in **Figure 38** is given below.

- **Early Triassic:** Tectonic quiescence: this area is not affected by rifting.
- **Late Triassic:** Active rifting is accompanied by thin-skinned faulting and pillowing of salt. This phase of rifting is described as the Early Kimmerian rifting phase.
- **Early Jurassic:** Widespread deposition, locally controlled by diapiric salt structures.
- **Middle/Late Jurassic:** Regional thermal doming uplifts the platform and marginal areas, while rifting allows continued subsidence within the DCG, accompanied by piercing salt structures. The Step Graben and Dutch Central Graben are outlined during these Middle and Late Kimmerian rift events, although some structuration was already present, due to Early Kimmerian rifting.
- **Late Cretaceous and Tertiary:** Late Campanian and Laramide inversion pulses focused in the DCG, repeatedly forming a structural high above the DCG and subsequently eroding strata in this area. This process is accompanied by the deposition of the CK and NS intervals. The platforms and marginal areas are less affected by inversion and erosion, although some inverted faults are observed here.

## 7. Integration

The inventory of salt structures in this study resulted in an interpretation of the chronology of phases of salt movement in the study area (see chapter 5). Assessment of timing of salt structure growth and its effect on depositional patterns shows initiation of salt movement in the Triassic, salt tectonic climax in the Jurassic and renewed salt movement in the Cretaceous and Tertiary. By structurally restoring a cross section, salt tectonic evolution was modelled, taking into account the structural evolution of the Dutch Central Graben and Step Graben (see chapter 6). In order to obtain a comprehensive framework for salt tectonics in this area, observations from both exercises are to be compared and integrated:

*Is the salt tectonic evolution as modelled in the structural restoration representative for the whole study area? And are observations in the salt structure inventory compatible with the constraints of the structural restoration?*

**Figure 44** shows a simplified chart, in which the development of salt structure geometry is compared for three salt structures: F09-WEST<sub>1</sub>, B17-SOUTH<sub>1</sub> and A12-EAST<sub>1</sub>. These three salt structures are located in different locations within the study area (see also **Figure 15**). A12-EAST<sub>1</sub> is located in the North of the SG, B17-SOUTH<sub>1</sub> on the NW boundary of the DCG and F09-WEST<sub>1</sub> in the South of the study area, within the DCG. F09-WEST<sub>1</sub> is one of the salt structures that was restored in the structural restoration (chapter 6). The other salt structures are referenced to in the salt structure inventory (see also **Figure 24** and **Figure 30**).

Observations from both the salt structure inventory and the structural restoration indicate that the salt tectonic evolution of salt structures is not consistent for all salt structures in the study area and that the timing of salt movement can be different even for proximal salt structures. However, from the salt structure inventory a trend does become evident that timing of salt movement is closely linked to their location within the structural elements. Salt structures within the DCG (like F09-WEST<sub>1</sub>) appear to have been active more or less simultaneously. Salt structures associated with the western DCG boundary fault appear to differ more in their timing. Where B17-SOUTH<sub>1</sub> only pierces during the Late Cretaceous, other salt structures along the same boundary fault show Jurassic piercing. In the northern SG, active salt tectonics appears to have ceased relatively early (Late Triassic; e.g. A12-EAST<sub>1</sub>), with some reactivation in the Tertiary. Towards the South, salt walls within the SG are likely to have developed simultaneously, although this is difficult to test due to absence of most Jurassic strata.

Other salt structures from the salt structure inventory that were included in the structural restoration (chapter 6) are F05Fo8-WEST<sub>1</sub> and E09Eo6Eo3-EAST<sub>1</sub>. The restoration shows that salt structure F05Fo8-WEST<sub>1</sub> develops into a fully pierced structure in the Early/Middle Jurassic (**Figure 38E**). Observations from the salt structure inventory do suggest some salt movement in the Late Triassic, but does not show conclusive evidence for the timing of piercing of this structure. The location of this structure, on the margin of a rapidly subsiding DCG can explain the absence of rim syncline development near this structure during this period.

The structural restoration (chapter 6) shows that salt structure Eo9Eo6Eo3-EAST<sub>1</sub> is already present in the Late Triassic and reaches the surface in the Early/Middle Jurassic (**Figure 38C-E**). Observations from the salt structure inventory confirm that this structure moved during the Late Triassic, as local thinning is observed. Towards the north, Jurassic sediments occur locally near its eastern flank (see **appendix 3D-E**), which would concur with Jurassic salt movement of this structure. In the restoration model, some Late Jurassic deposition is interpreted to the East of this structure, despite the absence of Jurassic sediments at the location of the restored section. Movement of this structure was likely linked to movement along the western SG boundary fault. This is confirmed by the restoration, which shows simultaneous movement of this salt structure and the associated basement fault (**Figure 38E**).

As mentioned in chapter 5, the absence of Jurassic strata makes it difficult to constrain the salt movement in much of the SG and platform areas. Precisely this is one of the issues that the structural restoration (chapter 6) was able to provide a model for (see **Figure 38**). Despite the fact that this model also required major assumptions about these eroded intervals, it provides some constraints for the structural development, which are based on observations in seismic data, interpreted periods of regional tectonism and relevant literature. I.e. the structural model presented in chapter 6 allows for speculation about the timing of salt movement, in areas where direct information from stratigraphy is not available (i.e. SG, SGP, ESP).

The structural restoration is representative for most of the study area, for major tectonic events and the development of the main structural elements. However, timing of development of salt structures cannot always be extrapolated to adjacent areas. The structural restoration confirms how salt structures may develop differently in different structural elements, while salt structure growth within a structural domain is more consistent. For example, major periods of growth of salt structure Fo9-WEST<sub>1</sub> can be regarded as a template for growth of Central Graben salt structures. But it has to be noted that even within the same structural setting, local structural features and depositional patterns can cause a salt structure to develop differently. By making a diagram like **Figure 44** for a salt structure of interest, where major phases of salt tectonics are defined and linked to tectonic events, these aspects can be taken into account: 1). Observations from the salt structure inventory 2). The structural context of salt structure growth 3). Local geology affecting salt structure growth.

Especially in the case of the North Sea basin it is crucial that the discussion on salt tectonics takes into account these structural elements.

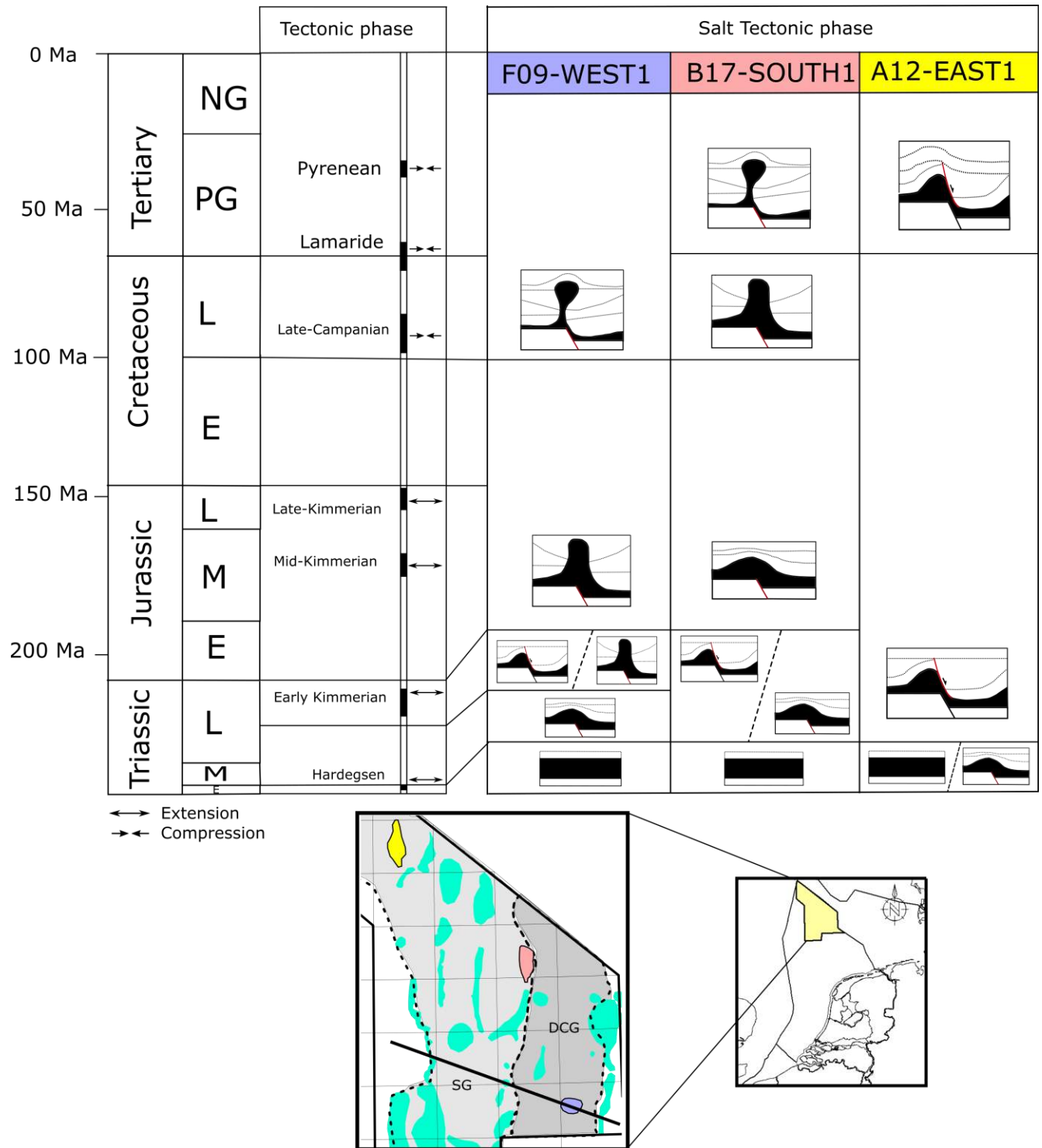


Figure 44: Simplified chart of interpreted salt structure geometry for salt structures F09-WEST1 (blue), B17-SOUTH1 (red), A12-EAST1 (yellow) and their location in the study area. Tectonic phases affecting the study area are shown.



## 8. Implications for prospectivity & Recommendations

Salt tectonics affects many aspects of prospectivity in the northern Dutch offshore. Several play concepts are influenced or completely controlled by salt movement. Some affected plays are described below, according to relevant petroleum play elements.

### 8.1. Chalk play

The Upper Cretaceous Chalk play is a proven petroleum play in the British, Danish and Norwegian North Sea and since the discovery of the Foz Hanze oilfield, the 'Chalk play' has also proven to be a working play in the northern Dutch offshore. The recent (2012) discovery of the F17 oil accumulation by Wintershall Noordzee has confirmed this. Play elements will be discussed below. The trap structure associated with salt structure F09-WEST1 will be discussed as an example of a Chalk lead, affected by salt movement.

**Source rock:** The oil-prone Lower Jurassic Posidonia shale fm. is the main source rock for the Foz Hanze oilfield. However, other source rocks in the area can potentially act as a source in the Chalk play as well, e.g. Upper Jurassic Kimmeridge fm., coal-bearing Dinantian strata and the Zechstein ZE2-Carbonate member (See **Figure 45A**). Analysis of the Foz Hanze oilfield suggests Late Tertiary to Early Quaternary hydrocarbon generation from this source rock favours success of the Chalk play (Guasti, 2010). Generally, in order to predict the potential of these source rocks a good understanding of their local burial history is important. In the study area, deposition and subsequent burial of sediments around salt structures is very much controlled by withdrawal of Zechstein salt and its accumulation in salt diapirs, walls and pillows. Formation of rim synclines in the Jurassic will have created accommodation space for the deposition of Jurassic source rocks and subsequently accelerated their burial, affecting their maturity. A good example is the burial of Posidonia shales sourcing the Mittelplatte oil-field (described by Grassman et al., 2006; see **Figure 12**). Therefore, the timing of movement as described in the salt structure inventory (chapter 5), is crucial. In order to get insight in the way salt withdrawal influenced source rock burial and heat flow, a basin modelling study analogous to the study on the Mittelplatte oilfield (Grassman et al., 2006) could be performed.

Another aspect affecting maturity of source rocks is the distribution of heat flow around salt structures. Strata adjacent to and above salt structures will have a significantly increased heat flow (**Figure 11**), which will accelerate maturation. Strata directly below salt structures will be exposed to reduced temperatures, retarding the maturation of e.g. pre-Zechstein Carboniferous source rocks (Verweij, 2009). Clearly, in order to predict the way in which salt structures affect heat flow

disturbance and thereby source rock maturation, it is important to understand the development of these salt structures through time.

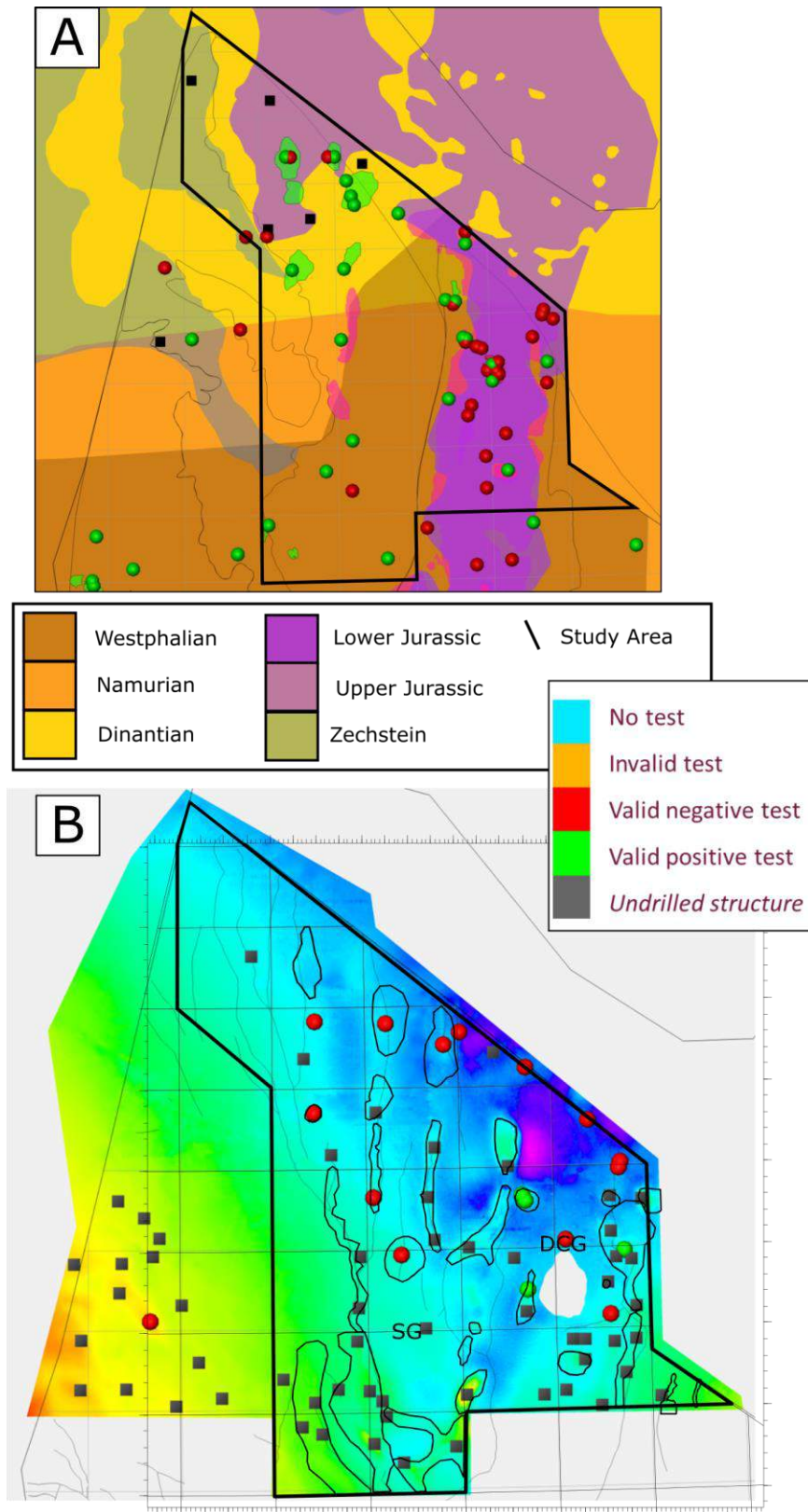


Figure 45 : (See previous page) A). Distribution of source rocks within the study area; tested structures shown B). Tested and undrilled structures for the Chalk play; Salt structure outlines shown (EBN, 2014). Note that many untested Chalk structures are identified, above or near salt structure, discussed in this study.

**Traps and seals:** Many successful Chalk field are associated with four-way dip-closures (e.g. Foz Hanze field, NL; Skjold field, DK) or faulted dip closures (e.g. Gorm field, DK) above salt diapirs and pillows (e.g. Harlingen field, NL; Kraka field, DK). Many potential traps above salt structures in the northern Dutch offshore are yet to be tested, many of which are associated with the salt structures described in this study (e.g. B16Fo1-WEST1, B17-SOUTH1, Fo9-WEST1 and many more). Stratigraphic traps within the Chalk have also been described (e.g. Halfdan field, DK; Calvert et al., 2014). The role of salt tectonics is evident in most of these cases. Formation of many structural traps is controlled by the timing of a vertical salt structure growth and subsequent pushing upwards of the overlying strata by the salt. **Figure 45B** shows identified trap structures (EBN, 2014) within the Chalk in the northern Dutch offshore.

The top seal is typically provided by the overlying Tertiary shales of the North Sea Group. Major faults transecting these intervals may cause failure of these seals.

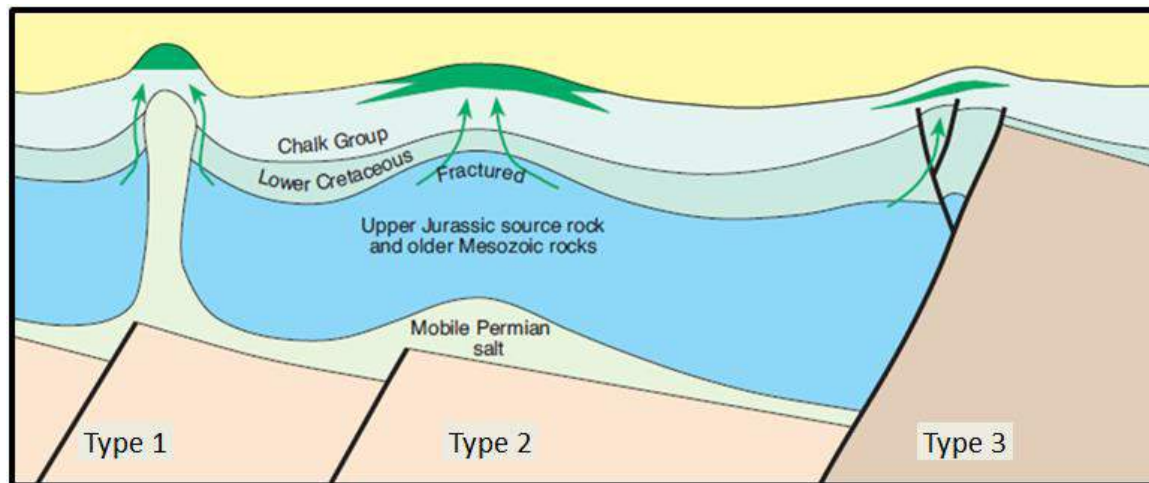


Figure 46: Most common traps in the Chalk play: Type 1 = Fractured chalk over salt diapir; Type 2 = High porosity basinal chalk over salt pillow; Type 3). Stratigraphic trap above inversion structure. (Surlyk et al, Millenium Atlas, 2003)

**Reservoir:** Reservoir quality of the Chalk reservoir varies depending on depositional environment, palaeo-topography, diagenesis and fracturing. Salt tectonics has an important role, here, since vertical growth of salt structures will change sea-bed topography during deposition. After deposition of the Chalk, further vertical salt structure growth will induce fracturing of the Chalk strata and possibly the younger overburden. This study shows it is likely this vertical growth can be associated with phases of inversion. These inversions are responsible for a regional differentiation of the sea-bed topography, where rising salt structures may have a more local, superimposed effect on the regional inversion. As a result of differentiated topography re-deposition of Chalk sediment occurred in the form of slides, slumps, debris flows and other secondary depositional processes (see **Figure 47**). These allocthonous Chalk deposits frequently occur around major salt structures (e.g. Salt structure B17-SOUTH1, studied by Lanting, 2013).

These secondary deposits have shown to be potentially of good reservoir quality. Results from this study could serve as a tool to predict the occurrence of these slope deposits.

This study shows active salt withdrawal occurred during the Late-Cretaceous in the northern DCG (See **Figure 22** and **Figure 30**) including around salt structures Fo2-NORTH<sub>1</sub> (Fo2 Hanze field) and B17-SOUTH<sub>1</sub> (B17-A field, see Lanting, 2013). This salt tectonic activity may have provided favorable circumstances for deposition of good quality Chalk reservoir facies in the study area. Unfortunately, not enough valid structure tests are available to date (as shown in **Figure 45**) to confirm this correlation. Provided enough wells are available, a facies analysis of Chalk reservoir around salt domes may provide a model for the interplay of Chalk deposition and vertical salt movement and its effect on reservoir quality.

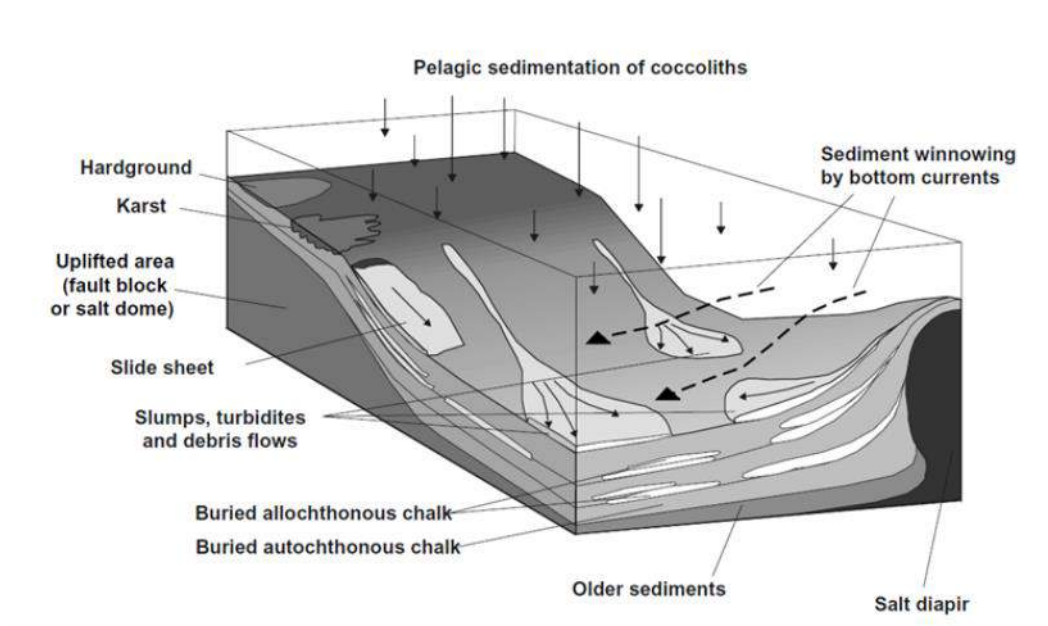


Figure 47: Different types of re-depositional processes, related to inversion and salt tectonics (Van Der Molen, 2004).

Within the Chalk Group high porosity sand bodies have also been observed above salt structures (e.g. well F17-4 found intra-Chalk sand; De Jager, 2003). This is likely the results of local vertical movement of salt, which exposed and subsequently eroded older sand-bearing intervals. E.g. during the Late Campanian inversion, Jurassic strata was likely eroded and locally re-deposited. No other nearby sources of clastic sediments were available during deposition of the Chalk Group, where the depositional environment was dominated by carbonate deposition in a large marine basin. The structural restoration performed in this study may provide a reference for where clastic sediments were possibly eroded and re-deposited during the Late Cretaceous (See **Figure 49**).

Another effect of salt tectonics on reservoir quality is the fracturing, caused by vertical movement of salt structures, after the deposition of the Chalk reservoir facies. This crestal fracturing can enhance permeability greatly (e.g. Skjold field, DK; Fo2 Hanze field, NL). However, since these fractures are below seismic resolution, their orientation and density can only be estimated prior to drilling. In order to predict fracture density in Chalk field above salt structures, geomechanical



models of the fracture patterns associated with crestal faults and with salt doming below the Chalk can be used (Freeman et al., 2015). Major crestal faults above salt structures can induce reservoir compartmentalization (e.g. Dan field and Gorm Field, DK).

Early diagenetic processes (up to 1000m burial) takes place from the time of deposition of the Chalk until the time when the pore waters from the sediment cease to be exchanged with the sea water, resulting in significantly reduced porosity and permeability. Firmgrounds and hardgrounds develop due to breaks in sedimentation. Due to their low porosity these hardgrounds may have a negative effect on reservoir quality. Hardgrounds are typically associated with structural highs, during deposition of the Chalk. These structural highs may be induced by vertically moving salt structures. Late-burial diagenesis may induce pressure solution features, which also negatively affects reservoir quality.

**Charge:** A key element controlling the success of the Chalk play is the charge. A trap structure and seal have to be in place in order to have successful charge of a reservoir, In the Chalk, absence of Lower Chalk has shown to be beneficial for successful charge (Guasti, 2010). This study has shown that Lower Chalk is mostly absent above the southern DCG due to inversion and erosion of the Lower Chalk (which becomes evident from models shown in **Figure 38**), which may favor charge in this area. This is supported by the fact that most Chalk fields in the Danish offshore are located within inverted areas, where Chalk is relatively thin and dominated by Upper Chalk sediments. This study may also provide insight in the timing of source rock burial adjacent to salt structures and the timing of hydrocarbon generation, which is crucial for successful charge. Observations by Huijgen (2014, EBN) suggest the Late-Campanian unconformity may act as an intra-reservoir seal, which may impact hydrocarbon migration and trapping mechanisms.

**Potential:** Salt structure F09-WEST1 (see **Figure 35**) will be discussed below to illustrate the potential impact of analysis of salt tectonics on the hydrocarbon potential of this structure. Note that there are other Chalk structures with larger prospective hydrocarbon volumes, for which this structure may serve as an analogue. Well F09-01 (Conoco, 1971) tested a four-way dip closure in the Chalk Group, on the northwestern crest of the salt structure (**Figure 48**). This well was drilled based on 2D seismic data and a detailed structure map was therefore most likely unavailable. The well log shows minor oil and gas shows, but was abandoned and shut in (by Conoco, 1971). **Figure 48** shows the well missed the top structure significantly (by up to 800m, up-dip potential: 3 km<sup>2</sup>, >100 m), where two other closures were not tested at all.

With high quality 3D seismic data available at present a re-evaluation of this structure is possible. The up-dip potential column of this structure may even be larger, since shallow gas pushdown might cause overestimation of crestal depth of the salt structure (EBN, 2014). The main elements of the Chalk play are present:

- The Posidonia Shale fm. can potentially serve as a **source rock** for this structure and is present in most of the area around the structure. A dedicated analysis of the burial of this source rock, including the effect of salt doming, is needed to assess the source rock maturity. Well F09-01 did have some oil and gas shows, which would indicate mature source rock.

- Structural restoration presented in this study shows formation of the **structural trap** most likely occurred in the Tertiary. Additionally the restoration shows Lower Chalk was most likely largely absent after the Late Campanian, which is possibly beneficial for **charge** after this time.
- In the **reservoir** interval 3 Cores have been taken in well F09-01, which show good porosity but low permeability.
- Tertiary strata could serve as a **seal** in this case. Some major crestal faults are present and may endanger sealing capacity. Indications of shallow gas are present above the crest of this structure.
- A first order **volumetric** calculation gives the following low, medium and high potential STOIP volumes in million barrels of oil equivalent (1 BOE = 0.159 m<sup>3</sup>) for the F09-WEST<sub>1</sub> structure:

STOIP LOW (MMBOE)	STOIP MED (MMBOE)	STOIP HIGH (MMBOE)
7	28	68

Table 5

Other structural closures, associated with salt structures that were assessed in the restored section (**Figure 35**) also show some up-dip potential or are untested (For example salt structures F05Fo8-WEST<sub>1</sub> and E09Eo6Eo3; see **Figure 45B**). Most play elements of the Chalk play are present around these structures (source, trap, reservoir and seal). To make more conclusive statements about prospectivity of the Chalk play above these salt structures, more research is needed.

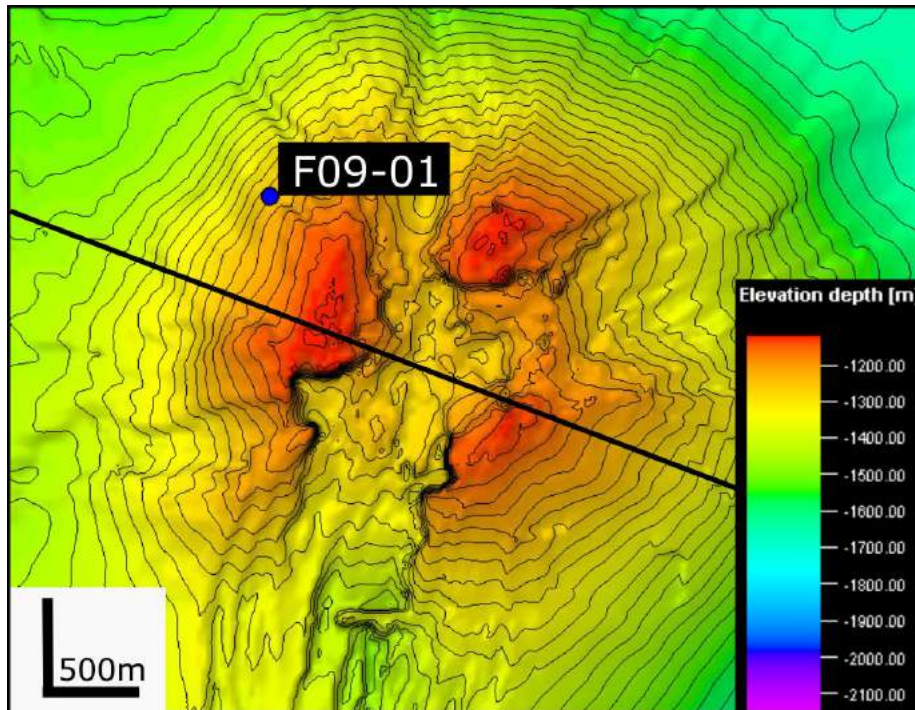


Figure 48: Structural closures above salt structure F09-WEST<sub>1</sub>. Well F09-01 has significant up-dip potential. Location of the section shown in **Figure 35** is included. Contour line interval = 20m.

## 8.2. Volpriehausen play

The Volpriehausen play is an established gas play with many fields in the Dutch offshore and counts as the second largest play in the Netherlands. F15-A, L2-FA, L5-FA, M1-A, G16-B and G17 are examples of fields in the Dutch offshore producing gas from Volpriehausen reservoirs. The Volpriehausen Sandstone fm. is part of the Lower Triassic Lower Germanic Trias Group.

**Source rock and charge:** Coal-bearing Carboniferous strata form the source rocks for all Volpriehausen fields. Maturity of these source rocks is uncertain, and varies between structural elements within the study area. Charge of the Volpriehausen reservoir requires conduits through the overlying Rotliegend and Zechstein strata which contain thick layers of salt and shales. Therefore it is relevant to assess how much salt was emplaced above the source rocks at the time of hydrocarbon generation, since hydrocarbon migration paths might develop by complete salt withdrawal and formation of a 'salt weld'. All-in-all charge forms the highest risk in this play (van Eijk, 2014, EBN). Restoration done in this study suggests salt windows may have formed as early as the Late Jurassic/ Early Cretaceous (See **Figure 38G-H**), after the most intense period of salt withdrawal.

**Traps and seals:** Traps include 3-way dip-closures against salt structures, 4-way dip closures above salt structures and fault associated traps. A seal is typically provide by the Volpriehausen Claystone Member (Van Eijk, 2014, EBN). Salt plugging of the reservoir, adjacent to salt structures, can also provide a seal.

**Reservoir:** Volpriehausen sandstone is typically a good reservoir (porosity =14-28%) and is present in most of the study area, apart from where salt pierces the interval. Reservoir quality decreases towards the North. The main threat for good reservoir quality is salt plugging (Van Eijk, 2014, EBN). Cementation of predominantly halite, anhydrite and dolomite within the reservoir can decrease porosity and permeability significantly. This is a secondary effect of the presence of Zechstein salt, typically seen around piercing salt structures. Salt plugging may be recognized on seismic data as an amplitude decrease and seismic phase change. When a reservoir is completely salt plugged a polarity reversal can occur. However it remains difficult to recognize a salt plugged reservoir without well-data, because seismic amplitude depends on reservoir quality and fluid fill at the same time (van Eijk, 2014, EBN).

**Potential:** A prospectivity review of this play in the northern Dutch offshore was done (Van Eijk, 2014, EBN). In this study leads were defined and reviewed, some of which associated with salt structures that are discussed in this study (e.g. F09-WEST1, 05-EAST1, G07-EAST1). Timing of salt tectonics is relevant here to assess when salt plugged seals were formed. For the charge it is crucial to know when salt welds formed, to allow for hydrocarbon migration through the Zechstein to the Volpriehausen reservoir.

Another effect of salt welds below Triassic strata is the occurrence of a so-called '*salt induced stress anomaly*'. Hoetz et al., (2011) presents this phenomenon as a model to explain velocity anomalies in the Triassic strata (variation of up to 18% within <1km). In areas where salt has withdrawn and a salt weld forms, stresses induced by overburden weight are focused, giving rise

to locally increased velocities in the overburden. This can also explain reduced porosities in underlying Rotliegend reservoirs.

### 8.3. Upper Jurassic plays

Several plays have been investigated and tested within Upper Jurassic intervals. Salt tectonics again plays a pivotal role in these plays. Prospective Jurassic reservoirs include the Heno Fm., Upper Graben Fm., Lola Fm. and Scruff Greensand Fm. These sandstones are typically hard to correlate laterally on a regional scale, due to localized deposition.

**Examples** of working Upper Jurassic plays are (Abbink et al., 2006):

- *Paralic/fluvial Sequence 1 play* (stratigraphic/truncation traps). Fields producing from the 'paralic/fluvial Sequence 1 play' include Lo6-A, Lo5-FA and Fo3-FB (Netherlands) and A6-A field (Germany).
- *Shallow marine Sequence 3, Spiculite play* (structural/truncation traps). The Fo3-FA field is an example of a field producing from the Shallow marine Sequence 3 spiculites.
- *'Mittelplatte play'*: The Mittelplatte oilfield in Germany produces from a Middle Jurassic reservoir directly above Posidonia source rock, deposited in a rim syncline, adjacent to a salt diapir (see Chapter 4).

**Source rock and charge:** For the generation of hydrocarbons from Jurassic source rocks, local burial depths are again controlled by salt withdrawal, as described above (chapter 8.1). Pre-Permian source rocks require windows in the Zechstein salt to migrate to the reservoirs (Chapter 8.2).

**Traps and seals:** Two types of Late Jurassic trap types can be identified 1). Stratigraphic/unconformity traps and 2). Structural traps. Closing structural traps have to be assessed locally, for instance using structure maps of Base Cretaceous. Traps may include: a four way dip closure with the reservoir truncated and sealed by the Vlieland Claystone on top of a salt structure or a truncation trap configuration on the flank of a salt structure. The timing of salt structure movement controls when these traps are formed. Seals may be provided by overlying shales, e.g. Kimmeridge Claystone or Vlieland Claystone (Abbink et al., 2006).

**Reservoir:** An important aspect of salt tectonics here, is the distributions of reservoir sands. During most of the Late Jurassic, this area was dominated by a marine depositional environment, without a proximal source for clastic sedimentation. The local occurrence of sands is an indication of the presence of palaeo-highs, which allowed local sand (re-)deposition. These highs are thought to have been induced by salt structures, moving vertically and creating a positive relief at the sea-floor. This possibly resulted in small islands with associated clastic sedimentation, which would explain the very much localized nature of many of the Upper Jurassic reservoir sands and explains why they are poorly correlatable. For example, the reservoir of the *spiculite* play comprises the sandstones of the Spiculite Member of the Late Jurassic Scruff Greensand Formation. For the deposition of these 'spiculites', salt structures were again a controlling factor.

Palaeo-highs created on the sea floor by vertically moving salt structures favored the development of sponge spicules, because of locally increased hydrodynamic energy. This is the reason spiculite reservoir is concentrated around palaeo-high areas. After reservoir deposition, continued growth of salt diapirs resulted in a sediment pile reduced in thickness (but sandy nevertheless) on the highs compared to off-high positions (Abbink et al., 2006).

## 8.4. Other affected plays

Other plays where salt plays an important role include the Tertiary Shallow Gas plays, Zechstein carbonate play, Zechstein Caprock play, Lower Cretaceous Vlieland sandstone play and the Triassic ‘fat sand’ play. **Table 6** shows an overview of the effects of salt tectonics for every play concept.

- Tertiary Shallow gas reservoirs are almost exclusively found above major salt structures. Gas in these reservoirs is suspected to be charged from underlying source rocks, biogenic gas generation, accelerated by increased temperatures above salt structures, or a combination of both.
- Zechstein reservoirs are found in marginal Zechstein platform carbonates. Although this play is not directly linked to salt movement, the location of these carbonate facies are an indication of the margins of the Zechstein salt basin.
- In areas where Zechstein salt was at the surface, ‘caprock’ reservoir may have developed. Where salt was exposed at the surface, large amounts of halite are thought to have been dissolved, leaving behind the less soluble lithologies like anhydrites, carbonates and dolomites. When Zechstein salt was at the surface is important here. The structural restoration performed in this study shows that Zechstein salt was at the surface at several locations during the Early/Middle Jurassic to Early Cretaceous (**Figure 38**).
- Erosion and dissolution of Zechstein strata may also have locally provided accommodation space for the Late Jurassic to Lower Cretaceous Scruff sandstone to be deposited. Again, the structural restoration performed in this study may provide a tool to predict the location of these reservoirs (**Figure 38**). An example of a working field in this play is the G16-A field. In this case the deposition of Jurassic shallow marine clastics, coastal plane and tidal flat sediments occurred in a basin controlled by dissolution of underlying Zechstein caprock.
- De Jager (2012) described the occurrence of the Triassic ‘fat sands’, where Middle Triassic sediments were deposited in a depocenter above a detached fault, soling out in the Zechstein salt cover on the flank of a salt pillow. The discovery of this play by well Log-7 lead to a producing field in Log. A similar geometry appears in several locations in the study area. A possible analogue is represented by the Middle to Late Triassic sediments forming a wedge against the eastern DCG boundary fault (see **Figure 41**). The structural restoration performed in this study shows the development of detached faults and associated depocenters, above a salt cover, at multiple locations in the restored section during Middle/Late Triassic times (see **Figure 38B**). These configurations may have been favourable for the deposition of (‘fat’) sands.



<i>Play concept/ Play Element, working fields</i>	<b>Chalk Play (chapter 8.1)</b>	<b>Volpriehausen Play (chapter 8.2)</b>	<b>Upper Jurassic plays (chapter 8.3)</b>	<b>Zechstein caprock play</b>	<b>Lower Cretaceous play</b>	<b>Shallow gas plays</b>	<b>Triassic Fat Sand Play</b>
<b>Source and Charge</b>	Controls source rock burial	Charge occurs through salt windows	Controls source rock burial/ Charge through salt windows	Controls source rock burial/ Charge through salt windows	Controls source rock burial/ Charge through salt windows	Controls location of charge, source rock burial/ Accelerates biogenic gas generation	Charge through salt windows
<b>Trap and seal</b>	Forms structural traps, affects intra-reservoir traps. Risk of breaking seal by vertical movement.	Forms structural traps, seals reservoirs (side, top seal, salt plugging)	Forms structural trap	Forms structural trap	Forms structural trap	Structural traps commonly above salt structures	Potential top/side-seals, potentially 3-way dip closure traps against salt structure
<b>Reservoir</b>	Controls reservoir facies, intra- reservoir boundaries, and reservoir fracturing	-	Controls reservoir sand facies distributions	Controls timing of reservoir rock formation;	Possibly controls sand (re-) distribution	-	Triassic 'fat sand' deposition is accommodated by salt withdrawal
<b>Fields</b>	F02-Hanze, F17	F15-A, L2-FA, L5-FA, M1-A, G16-B, G17	Lo6-A, Lo5- FA, Fo3-FA, Fo3-FB, Mittelplatte	G16-A	-	A12-FA, Fo2a-B, B13- FA	Log

Table 6: Overview of the effects of salt tectonics on play elements, and fields associated with these plays

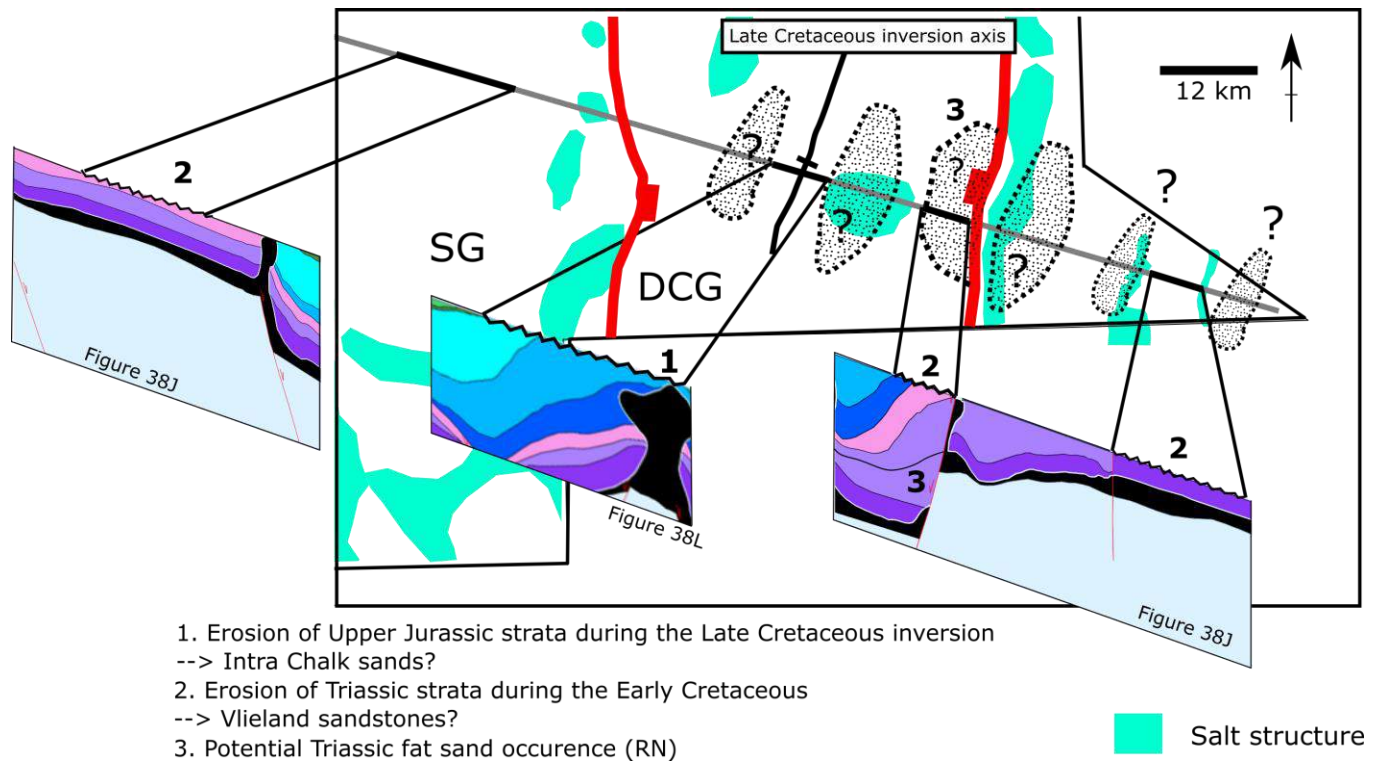


Figure 49: Locations of eroded Jurassic (location indicated with '1') and Triassic (locations indicated with '2') intervals: this might suggest proximal occurrence of reservoir sands, redeposited within Cretaceous intervals. '3' indicates the location for potential fat sand occurrence. For the full restored sections see also **Figure 38**.

## 8.5. Recommendations

- A better constrained time-depth conversion model will significantly reduce uncertainties in future studies, especially when interpreting the Jurassic and Triassic intervals of the northern Dutch offshore, particularly within the Dutch Central Graben. Better constrained depth-converted data will allow more precise interpretation and improve restoration models in future salt tectonic studies.
- The impacts of salt movement on prospectivity of the Chalk Group (see chapter 8.1: Chalk play) should be further investigated. A future study could include a high resolution structural restoration of a single salt structure, restoring its phases of vertical growth during the Late Cretaceous and Tertiary. This can provide detailed information on late salt tectonic movement, which could be essential for the Chalk reservoir quality, internal structure, trap formation and hydrocarbon charge. The structural restoration performed in this study can serve as an (lower resolution) analogue here.
- As more well data becomes available and more structural traps are tested, better correlations can be made between the timing of salt tectonics and positive tests of the Chalk play. This could provide a predictive tool for new Chalk prospects. The salt structure inventory presented in this study could be used as the starting point for these correlations. A similar approach may be applied to other play types.
- Salt tectonics affect many other aspects of prospectivity in the northern Dutch offshore (see chapter 8.1-8.4). In order to fully understand the effects of the presence of Zechstein salt and its movement on plays in this area, dedicated studies are to be done. Relevant studies may include:
  - o A study, modelling the effect of salt withdrawal on the local burial and maturation of Jurassic source rocks (e.g. Posidonia Shale fm. and Kimmeridge Claystone fm.).
  - o A study on the effects of salt movement on the distribution of reservoir sands in Jurassic and Cretaceous intervals.
  - o A study on the timing of formation of salt welds in the context of potential hydrocarbon migration paths for pre-Permian source rocks.
  - o A study, investigating the relationship between salt plugging of Lower Triassic reservoirs and timing of salt movement.
- This study can serve as the starting point of a complete and comprehensive salt structure inventory, which can be referenced to in exploration near salt structures. Such an inventory can be valuable tool and serve as a '*quick guide*' to the salt tectonic characteristics of any salt structure of interest to exploration.
- Discussion on the structural development of the area and specifically on the structural restoration done in this study, is encouraged. In the future, more available data in this area may reduce the uncertainties in the structural restoration, which would allow for better constrained assumptions.

## 9. Conclusion

**In this study the following results are presented:**

- An inventory of salt structures in the northern Dutch offshore, describing thirty (30) salt diapirs, walls and pillows, according to a set of salt structure characteristics.
- A structural restoration, based on a seismic section, transecting the Step Graben and the Dutch Central Graben is done, restoring it back to its Early Triassic configuration in twelve (12) steps.

**Conclusions that can be taken from this study are:**

- Widespread salt pillowing initiates in the Triassic in the northern Dutch offshore. During the Late Triassic, an interplay of active rifting and formation of elongated salt pillows results in elongated depocenters, adjacent to salt structures.
- During the Jurassic, Triassic salt structures developed into isolated, piercing salt diapirs in the Dutch Central Graben, while salt walls developed along graben boundaries and locally within the Step Graben. Depocenters are focused in areas where salt withdraws into adjacent salt structures.
- Reactivated vertical growth occurs in many salt structures during Late Cretaceous and Tertiary times. Locally Late Cretaceous piercing salt structures are observed.
- Timing of salt movement and types of salt structures are not consistent throughout the study area and may vary locally. Trends can be linked to the position within structural domains and the interplay with active fault movements, resulting in a specific structural style.
- Locations of salt structures in the northern Dutch offshore are controlled by active basement faults and were mostly already determined during Early Kimmerian rifting.
- The original depositional salt thickness is an important control on the dominant structural style. At the same time this is a major uncertainty, due to possible erosion, dissolution and salt migration, after deposition. It is likely depositional salt thickness increased from the Southern Permian Basin margin on the Elbow Spit Platform towards the Dutch Central Graben.
- All the classic stages of salt tectonic development (described by Trusheim, 1960) are observed within the study area, although many observations in depositional patterns cannot be explained without taking the structural development of the Step Graben and Dutch Central Graben into account.
- Results from the salt structure inventory and the structural restoration performed in this study, provide a salt tectonic framework in the context of the structural development of the Step Graben and Dutch Central Graben.

- Almost all elements of the post-Zechstein hydrocarbon systems in the northern Dutch offshore are affected, or completely controlled, by salt movement. The success of multiple play types is largely dependent on the way Zechstein salt behaves. Thorough understanding of salt tectonics through time is important for successful exploration of these petroleum plays.



# Acknowledgements

First of all I would like to thank everybody at the technical department of EBN and at the petroleum geology department of TNO for their valuable input and good company.

Specifically, I want to thank Bastiaan Jaarsma (EBN), Jan de Jager (UU) and Renaud Bouroullec (TNO) for spending their valuable time supervising me in this project. At EBN, I want to thank Eveline Roosendaal, Guido Hoetz, Maarten-Jan Brolsma, Marten ter Borgh and Walter Eikelenboom for their continued feedback. At TNO Utrecht I want to thank Abdul Rader Fattah, Hanneke Verweij and Johan Ten Veen for their help in this project. I also want to thank Armelle Kloppenburg for her advice on use of the MOVE software she helped to develop. I want to thank Fugro for possibility to use the seismic data of the DEF-survey.

I think it is hard to imagine a more informative and inspirational way to have spent my internship. I feel I am lucky to have had the opportunity to work with so many knowledgeable people and I think during my time at EBN and TNO I learned more about oil and gas, exploration geology and research than I could have imagined before I started.

# List of Figures

Figure 1: Location of the study area (black outline) indicated on a map showing the main structural elements in the northern Dutch offshore (after Kombrink et al. 2012) .....	8
Figure 2: Structural configuration in Northern Europe during the Carboniferous. Main suture zones are shown, where terranes amalgamate, forming the continent of Laurussia (Doornenbal et al., after Pharaoh et al., 2006). The study area of this study is indicated with the black box, where a 'proto-Dutch Central graben' is suggested. ....	10
Figure 3: Palaeogeographic maps, showing the plate configurations from the Late Ordovician to Early Tertiary. The position of the study area is indicated with the yellow star. (after De Jager, 2007) .....	12
Figure 4: Structural configuration of the southern North Sea. The study area is located in the Dutch sector and continues to the South. The study area of the analogue study of Rank-Friend and Elders (2004) is indicated with a black box. (after Wride, 1995) .....	14
Figure 5: The Late-Permian Southern Permian Basin (Modified after Geluk 1999); Note: Within the study area (blue box), the basin margin was modified based on recent EBN study of Zechstein carbonate platform facies occurrence (Tolsma, 2014). Towards the east, in the German offshore area, the location of the basin margin remains uncertain due to restricted availability of seismic and well data. ....	15
Figure 6: Zechstein Group Z1-Z5 formations: Zechstein Facies in the Netherlands, from South to North (Geluk, 1999) .....	16
Figure 7: Simplified stratigraphic chart of the Netherlands (Kombrink et al., 2012) .....	18
Figure 8: Development of a salt structure. Effects of successive tectonics events on salt structure development and associated cross-section shortening and extension (After Vendeville, 2002). ....	20
Figure 9: Linking of faults below and above a salt cover (after Ten Veen, 2012; 'Cartoon modified from Stewart (2007) and adapted to the Dutch North Sea'). 1). Non-Linked faulting 2). Soft-linked faulting 3). Hard-linked faulting. ....	21
Figure 10: Radial fault pattern in domed sediments above a salt diapir in the North Sea (Steward, 2006) .....	22
Figure 11: After Verweij 2009: 'Influence of salt structures on present-day temperature and heat flow distribution. High heat flows through salt structures (in red) are associated with increased temperatures in sediments close to the top of the salt structure and reduced temperatures below salt structures.' .....	25
Figure 12: Location of the Mittelplatte oil-field, the largest oilfield in Germany. The cross section shows four major salt structures and is used for a basin modelling study. The source rock here is the Late Jurassic Posidonia Shale (Grassman et al., 2005) .....	25
Figure 13: Coverage of 2D and 3D seismic data used in this study; The study area lies within the black outline. ....	26
Figure 14: Conversion from true vertical thickness (TVT) to true stratigraphic thickness (TST) of a dipping layer. ....	28
Figure 15: (Previous Page) TWT map of top Zechstein; All 30 salt structures are indicated and numbered with reference to the salt structure inventory ( <b>appendix 2</b> ) .....	30
Figure 16: Examples of the salt structure characteristics assessed in the salt structure inventory with numbers referring to the characteristics described in chapters 5.2.1.-5.2.4. A). Section view of a salt structure. B). Map view of the same salt structure. ....	30
Figure 17: Distribution of salt structure types as defined in Table 1 within the study area. ....	32
Figure 18: Distribution of salt structures; Salt structures where TZE is more than 4km above BZE are highlighted. ....	33
Figure 19: Distribution map of the dominant style of fault linking associated with each salt structure within the study area. ...	34
Figure 20: Distribution map of thinning of Stratigraphic intervals towards salt structures within the study area. ....	36
Figure 21: Distribution map of thickening of stratigraphic intervals towards salt structures within the study area. ....	37
Figure 22: Distribution map of salt structures around which a Late Cretaceous secondary rim syncline is observed. ....	39
Figure 23: Salt structure Fo6b-EAST2; BRB, BRN and BAT are interpreted. RB interval thins towards the east. (Location of the section is shown in <b>Figure 15</b> ) .....	41
Figure 24: Salt structure A12-EAST1; RB and RN intervals are interpreted above Zechstein salt and a faulted basement. (Section location is shown in <b>Figure 15</b> ) .....	42
Figure 25: Conceptual drawings showing the relationship between salt geometry and depocenter location: A). Salt-movement controls deposition, deposits thin above salt pillows. B). Thin-skinned faulting induces a thickening of sediments towards the fault, above the salt structure. C). Thick-skinned faulting induces thickening towards the fault. D). Map view: The depocenter moves away from the salt pillow, as shown in A. E). Map view: Depocenter moves towards fault and associated salt pillow, as shown in B and C. ....	43
Figure 26: A). Time thickness map of RN (TWT) near the eastern DCG boundary fault and salt structures Fo5-EAST1 and Fog-WEST1. B). Seismic time-slice at -3333ms from DEF-survey in the same location (Fog block) .....	45

Figure 27: A). Jurassic depocenters around the salt structure Fo5-EAST <sub>1</sub> ; A seismic Z-line is shown at -3168ms together with the Base Schieland Group (BSL) TWT map; B). Seismic section with relevant intervals indicated; the location of the section (B) is shown in figure A. ....	49
Figure 28: An interpreted seismic section of salt structure Bi6Fo1-EAST <sub>1</sub> and surrounding strata, above a structured basement; Jurassic sediments can be observed in secondary rim synclines, east of the structure (Location of the section is shown in Figure 15).....	49
Figure 29: Interpretation of Late-Campanian unconformity East of Fo9-WEST <sub>1</sub> (after Huijgen, 2014; Section location is shown in Figure 15). Note that the Late-Campanian unconformity runs close to Top CK in this area. ....	51
Figure 30: A). Seismic section, with relevant intervals interpreted. 1= Jurassic depocenter 2= Cretaceous depocenter B). Seismic Z-line @-2792ms; Cretaceous depocenter is indicated (black line) C). Seismic Z-line @-3816ms; Jurassic depocenter (black line) and shifting depocenter (red arrow) are indicated D). Thickness map in TWT of the Cretaceous Chalk Group (CK) E). Thickness map in TWT of the Jurassic Altena Group (AT).....	52
Figure 31: Wells in the vicinity of the restored section; Well name, deepest penetrated stratigraphic interval and final TVD of the well are plotted. NS= North Sea Group, CK= Chalk Group, AT=Altena Group, RB= Lower Germanic Trias Group, RO= Rotliegend Group. Location of this section is shown in Figure 15.....	55
Figure 32: Illustration of vertical simple shear in fault movements (modified from Dula, 1991).....	57
Figure 33: Thickness distribution of original ZE salt thickness (Z <sub>2</sub> , Z <sub>3</sub> and Z <sub>4</sub> cycles) based on smoothing restoration (Ten Veen, 2012). Note that salt dissolution and erosion, which could be as much as 50% of the original salt volume, is not taken into account here and this map only shows the result of smoothing of existing salt volume. ....	59
Figure 34: Restoration model stratigraphy including lithologies and decompaction factors: .....	60
Figure 35: (Previous page) The interpreted seismic section described in Table 4. This interpretation was used for building the restoration model shown in Figure 37.. The location of this section is shown in Figure 15; Locations of Figure 36 and Figure 43 are indicated (black boxes). ....	65
Figure 36: Interpreted seismic section showing ZE, RB, RNo and RN <sub>i</sub> intervals. Location is shown on the section in Figure 35. ....	66
Figure 37: Restoration model at its present day configuration. This model has no vertical exaggeration (1:1 depth-to-length ratio). Main structural elements and salt structures (in black) are indicated. All interpreted stratigraphic intervals with associated colors are shown again. (see also Figure 34).....	68
Figure 38: Resulting models of the structural restoration. These models are 2 times vertically exaggerated (2:1 depth-to-length ratio).....	69
Figure 39: A: Burial Diagram of the Dutch Central Graben B). Burial diagram from the Cleaver Bank High, to the southwest of the study area (see Figure 1, CP). This figure illustrates continued subsidence during the Jurassic in the DCG, while platform areas are uplifted. Effects of inversion can be seen in the DCG, as several phases of uplift, while the platform area seems mostly unaffected (after De Jager, 2007). ....	73
Figure 40: Palaeo-geography of the wider North Sea area throughout the Jurassic (Doornenbal et al, 2010; after Ziegler 1990; Cope et al 1992; Dadlez et al 1998; Ineson and Surlyk 2003; Feldman-Olszewska 2006). Note that deposition during the Middle and Late Jurassic is restricted, where deposition in the Early Jurassic is widespread. ....	75
Figure 41: Detailed interpretation of the seismic section shown in Figure 35, showing salt structure Fo9-WEST <sub>1</sub> and adjacent intervals to the East.. Four intervals are shown flattened on the corresponding top horizon: Lower Germanic Trias Group (RB), Upper Germanic Trias Group (RNo, RN <sub>i</sub> ) and Altena Group (AT). The location of the palaeo-depocenter is interpreted (indicated by the black arrows). ....	76
Figure 42: Restored configuration of SLo, SL <sub>i</sub> , KN and CK <sub>i</sub> intervals above the SG and DCG. This section shows the total amount of interpreted erosion that is represented by the Late-Campanian unconformity. (2:1 Depth-to-length ratio) .....	78
Figure 43: Interpreted seismic section showing ZE, RB, KN and CK intervals. Location is shown on the section in Figure 35..	78
Figure 44: Simplified chart of interpreted salt structure geometry for salt structures Fo9-WEST <sub>1</sub> (blue), Bi7-SOUTH <sub>1</sub> (red), A12-EAST <sub>1</sub> (yellow) and their location in the study area. Tectonic phases, affecting the study area are shown. ....	85
Figure 45 : (See previous page) A). Distribution of source rocks within the study area; tested structures shown B). Tested and undrilled structures for the Chalk play; Salt structure outlines shown (EBN, 2014). Note that many untested Chalk structures are identified, above or near salt structure, discussed in this study. ....	89
Figure 46: Most common traps in the Chalk play: Type 1 = Fractured chalk over salt diapir; Type 2 = High porosity basinal chalk over salt pillow; Type 3). Stratigraphic trap above inversion structure. (Surlyk et al, Millenium Atlas, 2003) .....	89
Figure 47: Different types of re-depositional processes, related to inversion and salt tectonics (Van Der Molen, 2004). ....	90
Figure 48: Structural closures above salt structure Fo9-WEST <sub>1</sub> . Well Fo9-01 has significant up-dip potential. Location of the section shown in Figure 35 is included. Contour line interval = 20m. ....	92

Figure 49: Locations of eroded Jurassic (location indicated with ‘1’) and Triassic (locations indicated with ‘2’) intervals: this might suggest proximal occurrence of reservoir sands, redeposited within Cretaceous intervals. ‘3’ indicates the location for potential fat sand occurrence. For the full restored sections see also **Figure 38**..... 97

# References

- Abbink, O.A., Mijnlief, H.F., Munsterman, D.K., Verreussel, R.M.C.H.,** 2006 - New stratigraphic insights in the 'Late Jurassic' of the Southern Central North Sea Graben and Terschelling Basin (Dutch Offshore) and related exploration potential  
Netherlands Journal of Geosciences 85-3, 221 - 238
- Back, S., van Gent, H., Reuning, L., Grötsch, J., Niederau, J., Kukla, P.,** 2011 - 3D seismic geomorphology and sedimentology of the Chalk Group, southern Danish North Sea  
Journal of the Geological society, London, Vol. 168, 393-405
- Baldwin, B., Butler, C.O.,** 1985 - Compaction curves  
AAPG Bulletin, 69, 622-626.
- Baykulov, M., Brink, H-J., Gajewski, D., Yoon, M-K.,** 2009 - Revisiting the structural setting of the Glueckstadt Graben salt stock family, North German Basin  
Tectonophysics, 470, 162-172
- Calvert, M.A., Roende, H.H., Herbert, I.H., Zaske, J., Hickman, P., Miksch, U.,** 2014 - The impact of a quick 4D seismic survey and processing over the Halfdan Field, Danish North Sea First Break, 32, 43-50
- Carruthers, D., Cartwright, J., Jackson, M.P.A., Schutjens, P.,** 2013 - Origin and timing of layer-bound radial faulting around North Sea salt stocks: New insights into the evolving stress state around rising diapirs  
Marine and petroleum geology, 48, 130-148
- Clausen, O.R., Nielsen, S.B., Ejolm, D.L., Goleadowski, B.,** 2012 - Cenozoic structures in the eastern North Sea Basin — A case for salt tectonics  
Tectonophysics 513-517, 156-167
- De Jager, J.,** 2012 - The discovery of the Fat Sand Play (Solling Formation, Triassic), Northern Dutch offshore – a case of serendipity  
Netherlands Journal of Geosciences, 91-4, 609-619
- De Jager, J.,** 2007 – Geological development  
Geology of the Netherlands, 5-26
- De Jager, J.,** 2003 – Inverted basins in the Netherlands, similarities and differences  
Netherlands Journal of Geosciences, 92, 355-366
- Doornenbal, H., Stevenson, A.,** 2010 – Southern Permian Basin Atlas



**Dronkers, A.J. & Mrozek, F.J.**, 1991 - Inverted basins of The Netherlands.  
First Break 9: 409-425.

**Duffy, O.B., Gawthorpe, R.L., Docherty, M., Broncklehorst, S.H.**, 2013 - Mobile evaporite controls on the structural style and evolution of rift basins: Danish Central Graben, North Sea Basin Research, 25, 310-330

**Duin, E.J.T., Doornenbal, J.C., Rijkers, R.H.B., Verbeek, J.W. & Wong, Th.E.**, 2006 - Subsurface structure of the Netherlands –results of recent onshore and offshore mapping. Netherlands Journal of Geosciences / Geologie en Mijnbouw 85: 245-276.

**Dula, W.F.**, 1991 - Geometric models of listric normal faults and rollover folds  
AAPG Bulletin, 75, 1609-1625

**Fattah, R.A., Verweij, J.M., Witmans, N.**, 2012 - Reconstruction of burial history, temperature, source rock maturity and hydrocarbon generation for the NCP-2D area, Dutch Offshore  
TNO report - TNO-034-UT-2010-0223

**Geluk, M.C., Paar, W.A., Fokker, P.A.**, 2007 - Salt  
Geology of the Netherlands, 283-294

**Geluk, M.C.**, 2005 - Stratigraphy and tectonics of Permo-Triassic basins in the Netherlands and surrounding areas  
Utrecht University, Faculty of Geosciences, PhD-Thesis

**Geluk, M.C.**, 2000 - Late Permian (Zechstein) carbonate-facies maps, the Netherlands  
Geologie en Mijnbouw / Netherlands Journal of Geosciences 79 (1): 17-27 (2000)

**Geluk, M.C.**, 1999 - Late Permian (Zechstein) rifting in the Netherlands: models and implications for petroleum geology  
Petroleum Geoscience, 5, 189-199

**Grassmann, S., Cramer, B., Delisle, G., Messner, J., Winsemann, J.**, 2005 - Geological history and petroleum system of the Mittelplate oil field, Northern Germany  
International Journal of Earth Sciences, 94, 979-989

**Harding, R., Huuse, M.**, 2015 - Salt on the move: Multi stage evolution of salt diapirs in the Netherlands North Sea  
Marine and Petroleum geology, 61, 39-55

**Hoetz, G., Steenbrink, J., Bekkers, N., Vogelaar, A., Luthi, S.**, 2011 - Salt-induced stress anomalies: an explanation for variations in seismic velocity and reservoir quality  
Petroleum Geoscience, 17, 385-396

**Hudec, M.R. and Jackson, M.P.A.**, 2006 - Terra infirma: Understanding salt tectonics  
Earth-Science Reviews 82, 1-28

**Jackson, C.A-L., Kane, K.E., Larsen, E.,** 2010, Structural evolution of minibasins on the Utsira High, northern North Sea; implications for Jurassic sediment dispersal and reservoir distribution  
*Petroleum Geoscience*, 16, 105-120

**Kane, K.E., Jackson, C.A-L., Larsen, E.,** 2010 - Normal fault growth and fault-related folding in a salt-influenced rift basin: South Viking Graben, offshore Norway  
*Journal of Structural Geology*, 32, 490-506

**Kombrink, H., Doornenbal, J.C., Duin, E.J.T., den Dulk, M., ten Veen, J.H., Witmans, N.,** 2012 - New insights into the geological structure of the Netherlands; results of a detailed mapping project  
*Netherlands Journal of Geosciences*, 91-4, 419-446

**Maystrenko, Y.P., Bayer, U., Scheck-Wenderoth, M.,** 2013 - Salt as a 3D element in structural modeling — Example from the Central European Basin System  
*Tectonophysics*, 591, 62-82

**Rank-Friend, M., Elders, C.F.,** 2004 - The evolution and growth of Central Graben salt structures, Salt Dome Province, Danish North Sea  
*Geological Society, London, Memoirs*, 29, 149-163

**Rowan, M.G. and Ratliff, R.A.,** 2012 - Cross-section restoration of salt-related deformation: Best practices and potential pitfalls  
*Journal of Structural Geology* 41 (2012) 24-37

**Scheck, M., Bayer, U., Lewerenz, B.,** 2003. Salt movements in the Northeast German Basin and its relation to major post-Permian tectonic phases—results from 3D structural modelling, backstripping and reflection seismic data  
*Tectonophysics* 361 (2003) 277– 299

**Schultz-Ela, D.D., Jackson, M.P.A., Vendeville, B.C.,** 1993 – Mechanisms of active salt diapirism  
*Tectonophysics*, 228, 275-312

**Sclater, J.G., and Christie, P.A.F.,** 1980, Continental stretching: An explanation of post-mid-Cretaceous subsidence of the central North Sea basin  
*Journal of Geophysical Research*, 85, 3711-3939.

**Stewart, S.A.,** 2007 – Salt tectonics in the North Sea Basin: a structural template for seismic interpreters  
*The Geological Society, London, Special Publications*, 272, 361-396

**Surlyk, F., Dons, T., Koch Clausen, C., Higham, J.,** 2003 - Upper Cretaceous  
Millenium atlas

**Ten Veen, J.H., van Gessel, S.F., den Dulk, M.,** 2012 - Thin- and thick-skinned salt tectonics in the Netherlands; a quantitative approach

Netherlands Journal of Geosciences, 91-4, 447-464

**Tolsma, S.**, 2014 – Seismic characterization of the Zechstein carbonates in the Dutch northern offshore

Utrecht University, faculty of geosciences, EBN B.V., MSc.-Thesis

**Trusheim, F.**, 1960, Mechanisms of salt migration in northern Germany.

Association of Petroleum Geologists Bulletin, 44, 1519-1540

**Van Dalfsen, W., Doornenbal, J.C., Dortland, S., Gunnink, J.L.**, 2006 – A Comprehensive seismic velocity model for the Netherlands based on lithostratigraphic layers

Netherlands Journal of Geosciences, 85-4, 277-292

**Van Gent, H., Urai, J., de Keijzer, M.**, 2011 – The internal geometry of salt structures e A first look using 3D seismic data from the Zechstein of the Netherlands

Journal of Structural Geology, 33, 292-311

**Van der Molen, A.S., Dudok, H.W., Wong, T.E.**, 2005 – The influence of tectonic regime on chalk deposition: examples of the sedimentary development and 3D stratigraphy of the chalk Group in the Netherlands offshore area

Basin research, 17, 63-81

**Van Wijhe, D.H.**, 1987 - Structural evolution of inverted basins in the Dutch offshore.

Tectonophysics 137: 171-219.

**Vendeville, B.C. and Jackson, M.P.A.**, 1992; The rise of diapirs during thin-skinned extension.

Marine and Petroleum geology, 9, 331-353

**Vendeville, B.C.**, 2002 – A new interpretation of Trusheim's Classic Model of Salt Diapir growth

Gulf Coast Association of Geological Societies Transactions, 52, 943

**Verweij, J.M., Souto Carneiro Echternach, M., Witmans, N.**, 2009 - Terschelling Basin and southern Dutch Central Graben Burial history, temperature, source rock maturity and hydrocarbon generation - Area 2A

TNO report - TNO-034-UT-2009-02065

**Weijermars, R., Jackson, M.P.A., Vendeville, B.C.**, 1993, Rheological and tectonic modelling of salt provinces.

Tectonophysics, 217, 143-174

**Wijker, D.**, 2014 - Fault Mapping and Reconstruction of the Structural History of the Dutch Central Graben

Vrije Universiteit Amsterdam, EBN, MSc-Thesis

**Wride, V.C.**, 1995 - Structural features and structural styles from the Five Countries Area of the North Sea Central Graben

First break, Vol. 13, No 10, 395

**Ziegler, P.A.**, 1992 – North Sea rift system  
Tectonophysics, 208, 55-75

**Ziegler, P.A.**, 1990 - Tectonic and palaeogeographic development of the North Sea Rift system. In:  
Blundell, D.J. & Gibbs, A.D. (eds): Tectonic Evolution of the North Sea Rifts.  
Oxford Science Publications (Oxford): 1-36.

**Ziegler, P.A.**, 1977 - Geology and hydrocarbon provinces of the north sea.  
Geo-Journal, 1, 7-32

***Relevant Links***

[Link to structural restoration video](#)

[Link to author profile](#)

## **10. Appendices**